270
7/3/68

Ldr 364

364

AI-AEC-12680

COPY

MASTER

QUARTERLY TECHNICAL PROGRESS REPORT
AEC UNCLASSIFIED PROGRAMS
JANUARY–MARCH 1968

AEC Research and Development Report

ATOMICS INTERNATIONAL

A DIVISION OF NORTH AMERICAN ROCKWELL CORPORATION

DISTRIBUTION OF THIS DOCUMENT IS UNLIMITED

DISCLAIMER

This report was prepared as an account of work sponsored by an agency of the United States Government. Neither the United States Government nor any agency Thereof, nor any of their employees, makes any warranty, express or implied, or assumes any legal liability or responsibility for the accuracy, completeness, or usefulness of any information, apparatus, product, or process disclosed, or represents that its use would not infringe privately owned rights. Reference herein to any specific commercial product, process, or service by trade name, trademark, manufacturer, or otherwise does not necessarily constitute or imply its endorsement, recommendation, or favoring by the United States Government or any agency thereof. The views and opinions of authors expressed herein do not necessarily state or reflect those of the United States Government or any agency thereof.

DISCLAIMER

Portions of this document may be illegible in electronic image products. Images are produced from the best available original document.

LEGAL NOTICE

This report was prepared as an account of Government sponsored work. Neither the United States, nor the Commission, nor any person acting on behalf of the Commission:

A. Makes any warranty or representation, express or implied, with respect to the accuracy, completeness, or usefulness of the information contained in this report, or that the use of any information, apparatus, method, or process disclosed in this report may not infringe privately owned rights; or

B. Assumes any liabilities with respect to the use of, or for damages resulting from the use of information, apparatus, method, or process disclosed in this report.

As used in the above, "person acting on behalf of the Commission" includes any employee or contractor of the Commission, or employee of such contractor, to the extent that such employee or contractor of the Commission, or employee of such contractor prepares, disseminates, or provides access to, any information pursuant to his employment or contract with the Commission, or his employment with such contractor.

Printed in the United States of America
Available from
Clearinghouse for Federal Scientific and Technical Information
National Bureau of Standards, U.S. Department of Commerce
Springfield, Virginia 22151
Price: Printed Copy $3.00; Microfiche $0.65

AI–AEC–12680
GENERAL, MISCELLANEOUS,
AND PROGRESS REPORTS

QUARTERLY TECHNICAL PROGRESS REPORT
AEC UNCLASSIFIED PROGRAMS
JANUARY–MARCH 1968

The preceding Quarterly Progress Report
was
AI–AEC–12638

LEGAL NOTICE

This report was prepared as an account of Government sponsored work. Neither the United States, nor the Commission, nor any person acting on behalf of the Commission:

A. Makes any warranty or representation, expressed or implied, with respect to the accuracy, completeness, or usefulness of the information contained in this report, or that the use of any information, apparatus, method, or process disclosed in this report may not infringe privately owned rights; or

B. Assumes any liabilities with respect to the use of, or for damages resulting from the use of any information, apparatus, method, or process disclosed in this report.

As used in the above, "person acting on behalf of the Commission" includes any employee or contractor of the Commission, or employee of such contractor, to the extent that such employee or contractor of the Commission, or employee of such contractor prepares, disseminates, or provides access to, any information pursuant to his employment or contract with the Commission, or his employment with such contractor.

ATOMICS INTERNATIONAL

A DIVISION OF NORTH AMERICAN ROCKWELL CORPORATION

CONTRACT: AT(04–3)–701
ISSUED:

DISTRIBUTION OF THIS DOCUMENT IS UNLIMITED

DISTRIBUTION

This report has been distributed according to the category "General, Miscellaneous and Progress Reports" as given in the Standard Distribution for Unclassified Scientific and Technical Reports, TID-4500.

CONTENTS

AEC TASK	PROJECT	PAGE
5-A	Cross-Section Analysis	5
5-B	Fast-Spectrum Doppler Measurements	11
5-C	Basic-Theory Calculation — Region Dependent Flux Spectra	19
5-D	Integral Reactor-Physics Measurements	21
5-E	Basic-Theory Calculation — Monte Carlo Methods	27
6-A	Reactor Dynamics Simulator Development	31
6-C	Fission-Product Contamination and Control Studies	33
6-D & E	Sodium Fire Fission Product Release	43
6-G	Boiling-Studies for Sodium-Reactor Safety	59
8	Sodium-Reactor Experiment Operation	69
10-A	Coolant Management	73
10-B	Materials Management	77
10-C	Mechanical Properties in Sodium	79
10-D-1	Dynamic Loop Operation	93
10-D-2	Dynamic Loop Testing (Mechanical Properties)	97
10-D-3	Dynamic Loop Testing (Mass Transfer)	113
10-E	Modes-of-Failure and Helium Degradation	123
11-A	Mixed Carbide Fuels (Basic Properties)	141
11-B	Mixed Carbide Fuels (Irradiation Studies)	143
11-C	Mixed Carbide Fuels (Casting Studies)	151
12	Sodium Chemistry	155
13	HNPF Retirement	165
15	High Temperature Chemistry	171
16	Radiation Chemistry	177
17	Electronic Structure of Metals and Alloys	181
18	Radiation Damage in Crystalline Solids	187
22	Radiation Chemistry of Chromosomes	197
25	Noise Analysis Instrumentation	203

UNCLASSIFIED TOPICAL REPORTS
PUBLISHED JANUARY-MARCH 1968

AEC		NAA-SR No.	Title	Author(s)
Task	Distr			
5-A	UC-34	12533	Legendre Expansion Coefficients for Theoretical Angular Distributions of Elastically Scattered Neutrons	Campbell, Alter, and Berland
6-G	UC-34	12503	TRANSFUGE-IIa A Digital Code for Transient Two-Phase Flow in Single Heated Channels	J. A. Landoni
7	UC-25	12549	Final Report Fission Effects in Metal Fuels	Anderman, Gehman, and Holmes
10-A	UC-4	12616	Sampling Blanks for the LMFBR Cladding Program	E. W. Murbach

Program: Reactor Physics
AEC Task: 5-A, Cross Section Analysis
Project Manager: H. A. Morewitz
Reporting Period: January-March 1968
General Order: 7701 Subaccount: 13130 AEC Category: 04-40-01-03.1

Principal Scientists: H. Alter, C. L. Dunford

I. PROJECT OBJECTIVES

The objectives of this project include the evaluation, production, and maintenance of an up-to-date set of basic nuclear data; production and evaluation of multigroup constants; and the improvement of present day methods of neutronic calculations as related to microscopic and macroscopic nuclear data.

To accomplish these objectives, existing experimental and theoretical information on nuclear data will be surveyed, analyzed, and compiled. Automated methods will be developed for manipulating and evaluating large amounts of available nuclear data, and for the periodic updating of compiled data. Nuclear model calculations will be developed, extended, and used to help fill gaps in the data. The optical model analyses have two prime goals: to develop and test improved nuclear optical models for energy regions of interest to the fast reactor program, and to develop sufficient confidence in the results of theoretical calculations so that they may be used confidently to predict neutron cross section data where no experimental data are available. An automated system will be developed and maintained for the ready production of multigroup constants, and spectra generating techniques for production of realistic multigroup constants will be developed and incorporated into the system.

II. MAJOR ACCOMPLISHMENTS IN FISCAL YEAR 1968

Angular data obtained from theoretical nuclear model calculations performed at Los Alamos, were analyzed in terms of Legendre expansions. Expansion coefficients for 36 isotopes and for an energy range of 0.5 to 16.0 Mev were calculated, the results evaluated, and a report was issued. The large amount of angular distribution data in the form of Legendre coefficients was appropriately "formatted" and submitted to the National Neutron Cross Section Center at Brookhaven for inclusion in ENDF/A.

Significant progress in the development of the interactive computer graphics program SCORE was made in a number of areas. These include data storage and retrieval, partitioned memory operation, data correction procedures, spline fitting methods, multilevel analysis of resonance cross sections, and the overlay of ENDF/B evaluated data with the experimental information from the SCISRS file.

III. PROGRESS DURING REPORT PERIOD

A. AUTOMATED (INTERACTIVE) NEUTRON CROSS SECTION EVALUATION SYSTEM, SCORE

A preliminary resonance parameter analysis of resonance cross sections with SCORE was completed. A version of the COMBCO program, supplied by Idaho Nuclear, was modified to be compatible with SCORE. This code contains both a two-fission channel Reich-Moore multilevel, and a Breit-Wigner single-level formula with procedures for resolution and Doppler broadening. Mechanisms which will add, modify, or delete resonances and/or parameters and recalculate a new curve were developed. A chi is calculated for each case and thereby the "goodness" of the fit can be compared. The previously displayed curve may be overlayed for a point-by-point comparison. Multilevel and single level effects are compared by using the single level option.

Investigations of automated procedures for choosing the initial spline nodes continue. Preliminary tests on an automatic cubic spline fitting routine developed at Purdue University show that it works very well on smooth input data, Figure 1; however, if the code is allowed to choose its own knots (x coordinates which correspond to where the cubics are joined) for scattered experimental data, unacceptable results, Figure 2 [(n, α) reaction for Na^{23} between 6 and 21 Mev)] occur. If instead, the evaluator chooses the knots, better results, Figure 3, are obtained. The present version of the code does not presently make use of reported experimental uncertainties in the data.

A detailed comparison of this code and the Powell code from Aldermaston is being carried out in order to evaluate the best way to automate our current cubic spline fitting technique. The simple spline technique used in SCORE is quite fast, but the goodness of the fit depends on the ability of the evaluator using the graphic input device to select the nodes (x and y coordinates where

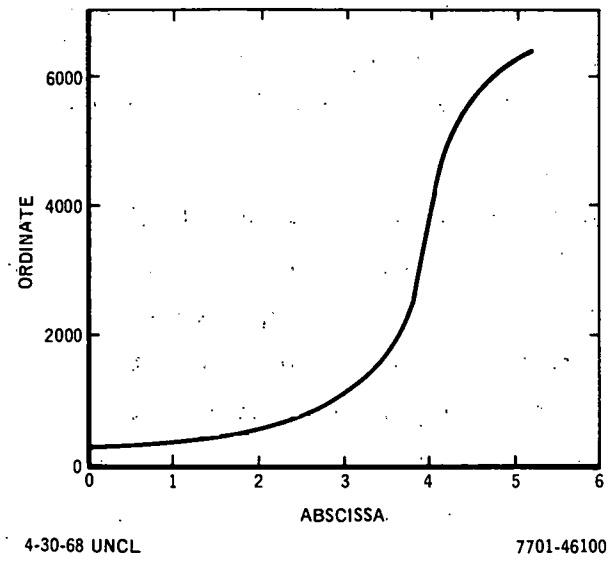

Figure 1. Nonlinear Spline Approximation

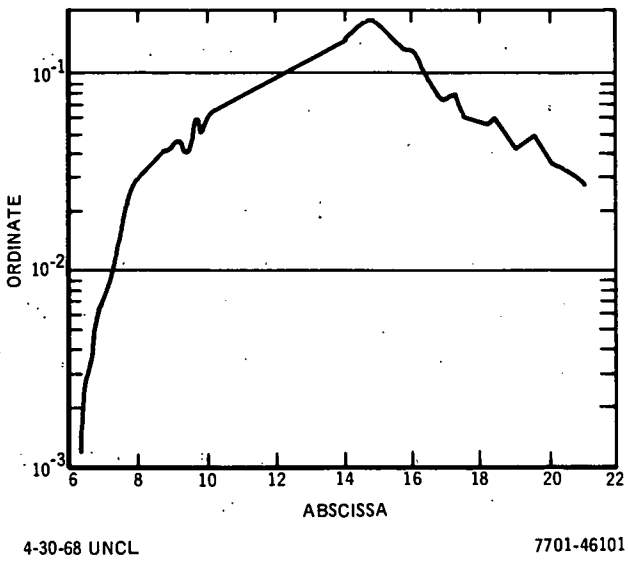

Figure 2. Nonlinear Spline Approximation

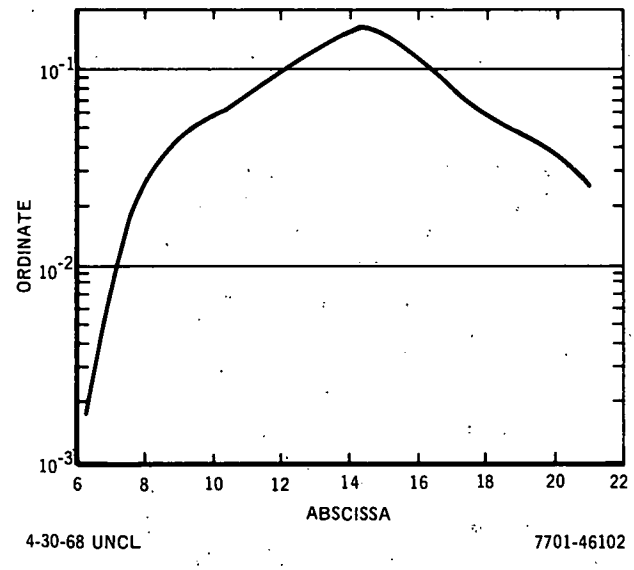

Figure 3. Nonlinear Spline Approximation

the cubics are joined) through which the cubic spline curve is fit. At present, the most promising technique appears to be one in which a graphic input device is used to position the knots and a least squares method is used to compute the corresponding ordinate values. Knowledge gained from studying these methods will aid in providing the proper curve fitting techniques in the SCORE program and in making the system suitable available for general application elsewhere.

The computer program SCOFF was completed, compiled, and executed. The code was written to reformat ENDF/B data tapes for the

convenience of SCORE, so that evaluated data from ENDF/B and experimental data from SCISRS may be displayed simultaneously. Work on the programming of subroutines to read and plot data obtained as output of SCOFF was successfully completed.

A generalized data conversion routine has been completed and checked out, as has been a generalized sorting routine. These routines will be introduced in SCORE as soon as the Fortran graphics package has been incorporated and debugged. Work continues on the ENDF/B overlay module. A survey of the structure of SCORE was completed and it was decided that with an overlay structure and additional reprogramming, SCORE can be fit into 125,000 bytes of memory; ie., approximately 25,000 words of core storage.

The SCORE document, NAA-SR-MEMO-12529, describing Version 1 of the system has been published. A demonstration of SCORE was held in Washington for the benefit of personnel from the Atomic Energy Commission, the National Bureau of Standards, and several local universities. The response was enthusiastic with considerable interest generated by several spectators who wish to adapt the methods employed by SCORE to the solution of their particular problems.

A paper entitled, "Automated Evaluation of Experimental Data," was presented at the Second Conference on Neutron Cross Sections and Technology, March 4-7, 1968. The abstract is as follows:

> A large fraction of the time required to produce an evaluated cross section library may be classified as nonproductive. A considerable portion of any evaluation is concerned with purely mechanical operations; consequently, not only is there often insufficient time for extensive data evaluation, but there are also long delays between the reporting of measured data and its availability for use in neutronic calculations. To help alleviate some of the problems associated with current data evaluation methods, a comprehensive automated data evaluation system is being developed which will encompass all the operations from the generation of theoretical data to the final evaluated cross section libraries. Such an extensive undertaking has been made possible by major technological advances in the new generation of computers. In particular, these advances are represented by new devices which permit on-line communication between man and a high-speed digital computer.

The full text of the paper is to be published in the Proceedings of the Conference.

B. ENDF/B DATA EVALUATION AND CODE DEVELOPMENT

The benchmark calculations for the ZPR-3-48 critical assembly using the AI processed ENDF/B cross sections were completed. A value of 0.953 was obtained for k; whereas, the corresponding value obtained by using the AIENDF 1967 cross sections is 1.017. The results from the ENDF/B calculation were submitted to the Cross Section Evaluation Working Group.

The central reactivity worths of various isotopes in ZPR-3-48 were calculated by several laboratories using the ENDF/B cross sections. There is a wide variation in the relative calculated worth of sodium; the relative calculated worths of U^{235} and iron show reasonably good agreement with experiment results. These comparisons indicate that the methods of processing the data were being tested, rather than the basic data itself; thus, the processing mechanisms need reexamination.

MC**2 was compiled and executed on the CDC 6600. The test problem for MC**2 was successfully run and requires less than 6 minutes on the CDC 6600. This compares to a running time of 27 minutes on the CDC 3600. The CDC 3600 is believed to be 2 to 4 times faster in execution than the IBM 360/50. The MC**2 test problem was kept simple and included only five nuclides.

A special purpose program, MERGB3, was written to merge selected materials from up to 4 ENDF/B mode-3 tapes. A considerable savings in machine time was realized when using this program instead of DAMMET for the merging of the data tapes. Preparations to merge data from a series of four ENDF/B cross section tapes into a single working tape were completed. A version of the ETOE program which prepares ENDF/B cross section data for use in MC**2 has been received from Bob Dannels, Westinghouse APD, and will be compared with the Brookhaven version of ETOE.

In compliance with a request from the AEC, the document NAA-SR-12533, "Legendre Expansion Coefficients for Theoretical Angular Distributions of Elastically Scattered Neutrons," was reduced in overall length, appropriate portions were rewritten, and the report was published. The large amount of

angular distribution data in the form of Legendre coefficients which was to have been included in this report has been appropriately formatted and submitted to the National Neutron Cross Section Center at Brookhaven for inclusion in ENDF/A.

IV. EVALUATION OF EFFORT TO DATE

The introduction of interactive computer graphics has opened a new dimension to the data evaluator. Man-computer interaction during the execution of a data evaluation problem can now be economically accomplished by the use of a graphic display console as a high-speed input-output device. The economy of this mode of operation is based on its time-sharing capability and its convenient output form (namely, graphic displays). The data evaluator, using the input device on a display console, can direct the processing and evaluating of experimental data by monitoring intermediate results. Errors may be corrected easily, before a large amount of computer time is consumed. In addition, the evaluator may inject his analysis of partial results (which otherwise might be very difficult or expensive to approximate, by the computer program) during execution of the program. This interaction can save computer time and turnaround time, and provides insight into the problem being solved.

V. NEXT REPORT PERIOD ACTIVITIES

Implementation of the SCORE program will continue with emphasis on:

Semiautomated spline fitting techniques for data evaluation,
Modularization of core to fit smaller computer core partition size, and the
Overlay feature for comparison of experimental and evaluated data.

Analysis of the copper isotopes and ENDF/B data testing will continue as funding permits.

Program: Civilian Power, LMFBR
AEC Task: 5-B-Reactor Physics, Fast Spectrum Doppler Measurements
Project Manager: H. A. Morewitz
Reporting Period: January-March 1968
General Order: 7701 Subaccount: 14610 AEC Category: 04-01-61-02.1

Principal Investigators: R. J. Tuttle and T. H. Springer

I. PROJECT OBJECTIVES

The objectives of this project are to (a) refine further the techniques originally developed at this laboratory for measuring Doppler reactivity coefficients, (b) investigate the Doppler coefficients of various fuel and fertile materials in a variety of fast spectra, (c) provide better understanding of temperature-induced reactivity changes by analytically and experimentally investigating these changes at cryogenic as well as very high temperatures, and (d) investigate resonance-overlap and interference effects, and the effect of varying the surface-to-mass ratio.

II. MAJOR ACCOMPLISHMENTS IN FISCAL YEAR 1968

The experimental program in Core 14, which has a very soft-spectrum test region, has been completed. Measurements in this core showed a significant interaction between a U^{238} sample and a surrounding, heated blanket.

The spectrum in the test region was made slightly harder by replacing part of the carbon with low-density aluminum to establish Core 15. Spectrum measurements (when using proton-recoil and fission counters), Doppler-effect measurements and reactivity measurements have been made in the latter core. The Doppler effect of U^{235} was determined to be positive, and that of a $Pu^{239}O_2$ sample was negative. Further, more extensive measurements with heated blankets have shown the effect of resonance interference in both U^{238} and Th.

A new test region designated Core 16 was constructed. This test region simulates a sodium-cooled, oxide-fueled, fast, breeder reactor. Spectrum measurements by use of proton-recoil counters and activation analysis have been made. Reactivity measurements have been made with selected materials.

Previously obtained data have been analyzed in an effort to obtain information on the effective capture-to-fission ratio α^{49}, of Pu^{239}.

III. PROGRESS DURING REPORT PERIOD

The test region was changed to provide simulation of a large fast breeder reactor. The composition (and atom ratios) of this test region, identified as Core 16, are: U^{235}(1.0), U^{238}(6.3), C(13.8), Al(12.2), and stainless steel (15.0). The materials were loaded in the drawers in the usual manner; that is, transverse to the drawer axis and with the front of each drawer continuing the loading cycle from the rear of the preceding drawer, so that no slabs or strips of constant composition exist and the heterogeneity approaches that due to the plate geometry alone.

Since this test region contains U^{235} and U^{238} as the fissionable material, the calculated median fission energy of 66 kev cannot be directly compared with that of FBR's. The calculated median flux energy is 150 kev which indicates that the spectrum is slightly harder than that of FBR's which have median flux energies around 140 kev.

A 35-group library was prepared for this core by using AILMOE to provide an ultra-fine group spectrum and GRISM to account for the resonance depression of the flux and to provide group-averaged cross sections. Cross sections for use in the decoupler, driver, and reflector regions had been prepared previously. Adjustments to some of the group cross sections in this latter set, and the proper division of the decoupler between two thorium cross section sets, had been made on the basis of Core 14; these were used unchanged for Core 16 and produced a criticality constant (k_{eff}) of 1.0014 compared to the experimental value of 1.0008.

The criticality constant is very sensitive to the division of the decoupler between the two thorium cross section sets, varying from 0.986 at one extreme to 1.0076 at the other, but the central flux spectrum is very insensitive to these changes. The central flux spectrum is shown in Figure 1.

The operating parameters of this core, regulating rod and safety rod worths, and table separation worth, have been measured. The power instruments have been calibrated in terms of the neutron production rate of the reactor

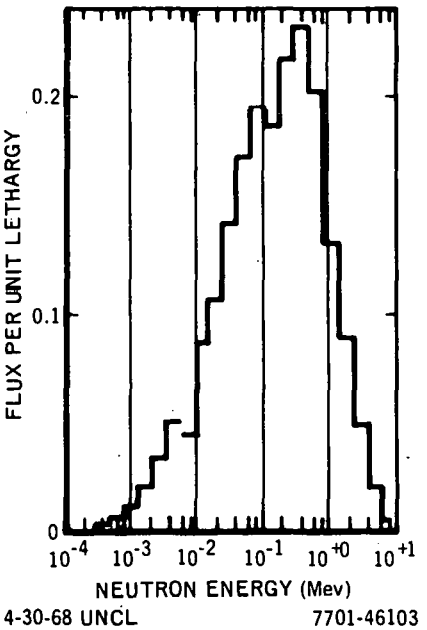

Figure 1. Core 16 8-plate Cycle

Spectrum measurements have been made in Core 16 by two methods: the proton-recoil proportional counter and the foil activation method used successfully in Core 14. Proton-recoil counters filled with hydrogen and with methane at various pressures were used to cover the spectrum from 30 kev to 1.6 mev. Analysis of the data has not yet been completed.

The foil activation method is based on an iterative modification of the calculated spectrum to produce agreement between the calculated activity and observed activity of a large number of various activation materials. Thermal, resonance, and threshold reactions in these materials provide energy coverage from the thermal to the mev region.

Like the measurements in Core 14, these measurements involved several laboratories in a cooperative effort planned and coordinated by W. N. McElroy, now at Battelle Northwest Laboratories. Cross checks between different laboratories were provided by redundancy in foil materials and in counting induced activities. In order to provide four irradiation locations, the foil materials were located in four symmetrical positions in the stationary half, approximately 4 in. from the center. To increase the apparent homogeneity

around the foil locations, the test region plates immediately in front and behind were rearranged so that all six faces of the cubical irradiation cavities were composed of plate edges. Because of the greatly different sensitivities of some of the activation materials, three irradiations were performed, from a short low power run, to one at full power (150 watts) lasting 22 hours.

The temperature coefficients of reactivity of several materials were measured in Core 16. These included samples of U^{235}, U^{239}, and Th metal, and Pu^{241} oxide. The Pu^{241} sample has been prepared for shipment to Oak Ridge National Laboratory for cross section measurements.

In addition, reactivity measurements were made with a wide variety of materials. The results are being analyzed. These materials included: NaF, Al_2O_3, glass, and quartz (for possible use in providing sodium, and providing oxygen while still maintaining the flexibility of metallic fuel); plutonium samples 2 through 8 (to determine the expansion effect of standard plutonium and to measure the reactivity of the higher isotopes); various stacks of U^{235} plates (for comparison with calculations of the heterogeneity effect); and samples of uranium of 10, 22, and 93% enrichment.

Some differences in the temperature coefficients and expansion coefficients of fissile isotopes in Core 16 compared to Core 13 (which had a similar spectrum but contained thorium instead of natural uranium) have been observed. Definite conclusions must wait, until a more detailed analysis of the results and spectra in the two cores has been made.

In view of the recent integral and differential measurements on the effective capture-to-fission ratio for Pu^{239}, $\bar{\alpha}^{49}$, and the serious implications for fast breeder reactors of the large values obtained, an analysis of previously obtained data was undertaken. The cores studied in this analysis were No. 5, built for the AETR program supported by the Southwest Atomic Energy Associates; and No. 15, built for the current AEC-supported Fast Spectrum Doppler program. Core 5 was a Th/U^{233} system with a spectrum similar to that of fast breeder reactors; Core 15 had a relatively soft spectrum. Methods such as those used by Redman at Argonne and Andersson in Sweden involve differences between terms of nearly the same size. Thus, these methods are very sensitive to errors in any of the terms involved.

By using one variation of these methods, and assuming that the calculated value of $\bar{\alpha}$ for U^{235} is correct, values of α^{49} were determined from fission ratios and small-sample reactivity measurements. For Core 5 (63-mev median fission energy) $\bar{\alpha}^{49} = 0.12 \pm 0.08$. In Core 15 (18-kev median fission energy), the corresponding value is 0.05. There are indications, however, that the experimental Pu^{239}/U^{235} fission ratio, the resulting value of α^{49} is 0.316 which is more reasonable and is consistent with the calculated value of 0.306. (Analysis of data obtained in other cores will continue, both to obtain information on the variation of α (of various fissile isotopes) with the spectrum, and to gain a better insight into the experimental requirements for successful measurements.)

These methods avoid direct determination of the so-called "denominator" (importance-weighted neutron production rate) of perturbation theory, by elimination with various ratio techniques. This quantity can be determined directly, however, from detailed neutron-importance measurements by using mock fission neutron sources. In Core 5, some such measurements were made. Two of them were used together with measured reactivities and fission rates to determine an $\bar{\alpha}^{49}$ value of 0.40 ± 0.13. Although this result is markedly different from that quoted previously, probably because of use of too few sources and insufficiently accurate source traverses, the method has great promise in that the sensitivity of $\bar{\alpha}$ to errors in $\bar{\nu}$ and the ratio of fission importance to absorbed-neutron importance is about a factor of two less; furthermore, boron measurements and thermal-flux normalizations are avoided entirely. The experimental techniques for neutron-importance measurements made by using numerous types of isotopic neutron sources routinely, have already been demonstrated. Analysis of the results from other cores to determine $\bar{\alpha}$ in other spectra is under way.

An estimate of the effect of differences in the cross sections used to calculate several terms in the Swedish method was made. Calculations of adjoint fluxes averaged over constant 1/v and 1/E cross sections in the spectrum of ZPR-III-48, determined from each of three cross section libraries, were made to aid quantitative evaluations of the uncertainty in $\bar{\alpha}$ due to spectrum and cross-section uncertainties. It was concluded that the determination of α^{49} by the Swedish method has a minimum uncertainty of about 33% due to uncertainties in calculated factors.

A review of the methodology used for calculating the prompt fuel-temperature coefficient of samples in the ECEL was made. The validity of using the CAESAR, TRIX-PERT, CALHET combination was affirmed, but several areas where further sophistication in details might significantly reduce the uncertainty in the result were noted.

Calculations of the specific reactivities, as a function of sample size, have been made for U^{235}, U^{238}, Pu^{239}, Pu^{240}, Pu^{241}, and Pu^{242} in Core 14 (4-kev median fission energy). These calculations were made by using first-order perturbation theory and cross sections modified on the basis of escape probability. The agreement between the calculated values and measured values is not as good as those that had been observed for Core 13, which had a harder spectrum (63-kev median fission energy). This is probably due to the fact that group cross section adjustments based on escape probability in the resonance region are too large. Use of combination of escape probability and explicit resonance shielding accomplished by the TRIX program is expected to produce superior results.

Modifications are being made to TRIX to permit varying the group potential scattering cross sections. In addition, the code is being changed so that the contribution to the resonances of neutrons with different values of angular momenta may be calculated at one time rather than requiring separate calculations with subsequent combination of the cross sections.

A topical report covering measurements made in Core 15 is being prepared. This report will include discussions of reactivity measurements; temperature, expansion, and Doppler coefficients; self-shielding effects; measurements with heated blankets; and data relating to $\bar{\alpha}^{49}$.

Approximately 300 cans of metallic sodium have been prepared for studies of sodium-loaded test regions.

A paper has been submitted to the American Nuclear Society and has been accepted for presentation at the annual meeting in June. This paper discusses the results of the Core 15 experiments dealing with the change in the Doppler coefficients of Th and U^{238} as a function of the type and temperature of the environment.

Preliminary designs for the fuel-pin lattice assembly have been refined. Calandria-type sodium boxes, to fit in the present matrix, will contain fuel tubes in a 7x7 array. These boxes will then be used to construct a pin fuel test region. A prototype box is being assembled for testing.

IV. EVALUATION OF EFFORT TO DATE

The construction of Core 16 provides a test region with real and adjoint fluxes that closely simulate those in current designs for the LMFBR. The flux spectrum has been well determined by more extensive calculations than used previously, and by proton-recoil and foil-activation measurements. The first measurements of the reactivity of Pu^{241} in a fast breeder reactor spectrum have been made.

Analyses of past data and current measurement methods for determination of the effective capture-to-fission ratio have been conducted. An improved measurement method has been developed.

Temperature coefficient and reactivity measurements of selected materials have been made prior to modifying the test region by adding sodium. Further progress has been made in developing analytical techniques for interpreting small sample reactivity measurements.

V. NEXT REPORT PERIOD ACTIVITIES

The central part of the test region (approximately 3/4 of the radius) will be reloaded, and canned sodium will be substituted for most of the aluminum, some carbon, and some stainless steel in the present loading. Measurements will be made in this core and in a modification produced by replacing the canned sodium with empty cans. These measurements will include fission ratios, proton-recoil spectrometry, neutron importance, Doppler measurements in heated blankets, and reactivity associated with changes of state.

THIS PAGE

WAS INTENTIONALLY

LEFT BLANK

Program: Reactor Physics
AEC Task: 5-C-Basic Theory Calculation, Region Dependent Flux Spectra
Project Manager: H. A. Morewitz
Reporting Period: January-March 1968
General Order: 7701 Subaccount: 13310 AEC Category:

Principal Scientist: F. L. Fillmore

I. PROJECT OBJECTIVES

The general objective of this project is to develop and extend fast reactor physics analysis methods which are efficient, and of adequate accuracy and sufficient scope to meet fast breeder reactor nuclear design and safety requirements. This objective is to be realized by development and extension of methods for accurately determining the energy and spatial distribution of direct and adjoint spectra required for realistic evaluation of the safety and economic characteristics of fast reactors and the development and extension of physics methods to provide accurate information with regard to fast reactor fuel cycle requirements, safety design requirements, and accident conditions.

II. MAJOR ACCOMPLISHMENTS IN FISCAL YEAR 1968

The required computer code development to enable an entire region dependent weighting spectrum calculation to be performed in a single computer operation has been completed and checked out.

III. PROGRESS DURING REPORT PERIOD

A 25-group, one-iteration calculation was made for the ZPR-3-48 assembly. The results of this calculation, and of those from the 5-group ZPR-3-48 calculation, were analyzed. In both cases, there were small differences between the zeroth and first iterations results. However, these differences were usually less than the corresponding differences due to the variation in group structure of the 25-group and the 5-group calculations. The conclusion drawn is that, in assessing criticality for critical assemblies of the ZPR-3-48 type, it is more important to use an adequate number of groups than to employ region-dependent weighting spectra. This conclusion has not been verified for large fast reactors and for quantities such as the sodium void coefficient, the Doppler coefficient, and the breeding ratio. The analyses of the results from

the 25-group zeroth and first iterations for the ZPR-3-34 calculation were continued. Only small differences were found between the corresponding results from these calculations.

IV. EVALUATION OF EFFORT TO DATE

The code development work to enable an entire region-dependent weighting spectrum calculation to be made in a single computer run was completed. The process of linking the AILMOE, GRISM, CAESAR and PERT computer codes proved to be more involved than initially estimated. By using the newly linked system of computer codes, calculations were made for the two critical assemblies, ZPR-3-34 and ZPR-3-48, whose blanket regions are similar. Both of these assemblies were analyzed in the previous fiscal year by using the various individual links of the computer code. The reanalysis was used as the basis for verifying that the linked code calculation did indeed give the same results as the unlinked calculation; this was the case. The differences in K_{eff} obtained with the fundamental weighting spectrum and the region-dependent weighting spectra for these assemblies do not appear to be significant; however, the effect of spatial weighting on Doppler, sodium void, and reactivity coefficients have yet to be determined.

V. NEXT REPORT PERIOD ACTIVITIES

The effort for FY 1968 was completed with the checkout of the computer code development required to perform the necessary calculation in a single pass through the computer.

In FY 1969, the region-dependent weighting spectra calculations will be made for (1) a soft core spectrum assembly, (2) a high leakage assembly, (3) a reflected assembly where the reflector is a light or medium mass material, and (4) a typical 3,000 liter prototype system. Particular emphasis will be placed on the effect of region-dependent weighting spectra on the sodium void and the Dopper coefficients for a typical prototype fast breeder reactor.

Program: General Reactor Technology
AEC Task: 5-D-Reactor Physics, Integral Experiments
Project Manager: H. A. Morewitz
Reporting Period: January-March 1968
General Order: 7701 Subaccount: 13210 AEC Category: 04-40-01-02.1

Principal Investigator: R. K. Paschall

I. PROJECT OBJECTIVES

The purpose of the fast reactor physics program is to supply data pertinent to both the safe and economic design and operation of fast power reactors. Safety and economics often compete in good reactor design and very conservative estimates are usually made in the area of safety because of the paucity of precise physics data. This program is designed to study these specific areas and confirm the nuclear parameters and calculational methods used on conceptual evaluation and preliminary design.

The large volume of coolant (50%) and structural material (15%) in current fast reactor designs make increasingly important the accurate knowledge of light element scattering cross sections which affect the magnitude of both the Doppler and sodium-void effects. Also of concern is the resonance shielding for various mixtures of the light elements.

A series of integral experiments are being performed by use of coolant material (sodium) and the predominant structural material (iron). The measurements seek to determine the differential neutron spectrum in large volumes of sodium, in a large quantity of pure iron, and in appropriate mixtures of these materials for both isotopic and reactor neutron sources. The resulting neutron spectra will be compared to predictions based on Monte Carlo calculations, in order to check the scattering cross sections presently being used. The use of a reactor as a neutron source will allow, in addition, reactivity measurements of the sodium void as well as direct studies of spectral changes occurring during this voiding.

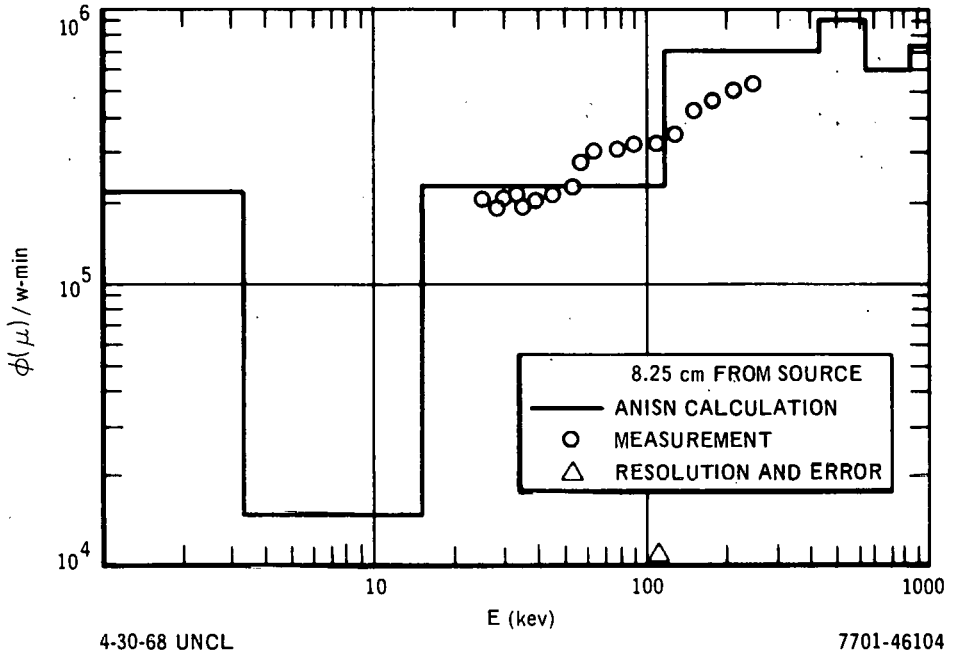

Figure 1. Neutron Spectrum in Sodium

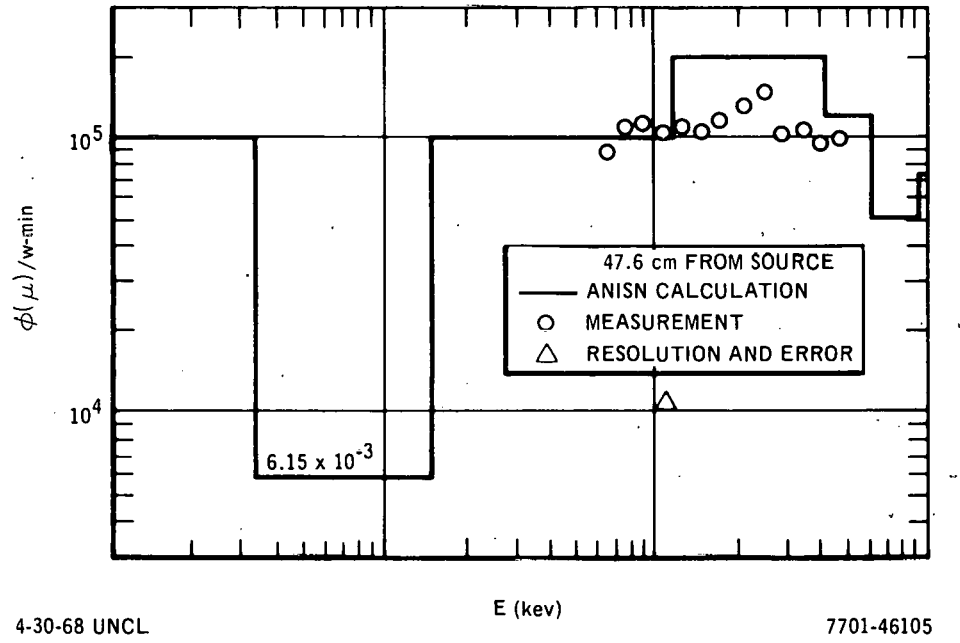

Figure 2. Neutron Spectrum in Sodium

II. MAJOR ACCOMPLISHMENTS IN FISCAL YEAR 1968

The neutron energy distribution from 25 to 200 kev has been measured in a large volume of sodium metal (5 ft x 5 ft x 10 ft) at a distance of about 8 cm from a fission spectrum source. A similar measurement at approximately 48 cm from the source has also been made.

III. PROGRESS DURING REPORT PERIOD

The analysis was completed on preliminary neutron spectrum measurements performed in a large volume of sodium at the STIR facility. Results of measurements and calculations are shown in Figure 1 (at 8.25 cm from the source) and in Figure 2 (at 47.6 cm from the source). Experimental and calculated spectra are compared directly in the following manner. Absolute flux per unit lethargy at a particular detector location is determined by the data-analysis code from counts per unit energy (collected by the pulse-height analyzer), data-collection time, number of hydrogen atoms in the detector, detector volume, and the (n,p) cross section for hydrogen.

To calculate the flux at that location, the reactor power level (determined by a calibrated ionization chamber) is recorded. For any reactor power level, the fission-neutron flux from the fission plate is known from previous intercalibration measurements made by the staff at the STIR facility. The calculated flux distribution throughout the sodium volume is then based upon a known initial fission-neutron flux from the fission plate. Therefore, at any reactor power level and any location within the sodium, the flux per unit lethargy can be calculated and directly compared with the measured results. To maintain a high counting rate, the reactor power is increased as the distance between the fission plate and detectors is increased; the measured and calculated fluxes are then divided by the reactor power to compare the results at all locations.

In preparation for a more extensive set of measurements, both in energy and location in the large volume of sodium, system electronics were further improved. Also, by use of a well-thermalized neutron origination from an isotopic source located in a four foot graphite cube, more detailed proton-recoil counter calibrations were carried out. The calibration techniques consisted of measuring the energy channel location of the proton peak produced by the He^3 (n, p)H^3 reaction. A He^3 calibrations gas is added to some of the counters

at a pressure of about 1 mm of Hg for this purpose. The general characteristics of the pulses were in agreement with expectation as far as the energy distribution for the major proton and triton peaks are concerned; however, some other, as yet unexplained peaks, were also observed.

Some spectrum measurements were made in the ECEL Core 16 reactor. Most of the data were taken with a 1-in. lead shield around the detector. The lead was removed for one running and the resulting data showed that no measurable effect could be attributed to the gamma shield. Also, one run was made with the detector located outside the reactor but looking down the empty central drawer to the core center. The results generated with the detector outside of the reactor showed that the initial shielding configuration was not sufficient to screen out the neutrons coming from all other parts of the reactor; consequently, those neutrons coming from the core center could not readily be distinguished. A new, more efficient shield has been designed and constructed to provide better collimation.

The ECEL measurements and the preliminary measurements in the sodium showed that the base-line was shifting in the pulse shaper electronics at moderate count rates. This problem was investigated and it was shown that modifications to the pulse shaper to improve the dynamic range and count rate capabilities were required. The pulse shaper was completely reconstructed in a NIM module. The diode pump to the sample capacitor was direct coupled. (Previously a 10-sec RC time constant was included in the circuit at this point.) The nuvistor vacuum tube diode was replaced with a thin film silicon diode which has just recently been made available. This diode [Isolfilm (1BB13)] has a very low reverse leakage, a forward voltage drop of 0.2 volt at 1.0 ma forward current, and a reverse recovery time of 2 nanoseconds. A gain-of-2 amplifier was then added before the diode pump in order to increase the peak voltage to the sample-and-hold circuit to 20 volts. The increased gain also enabled integration and a much faster secondary clip at the output so that the pulse shape was more compatible with the ADC of the Nuclear Data pulse height analyzer. The forward voltage drop of the silicon diode is now only 1% of full scale and the dynamic range of the instrument is now better than 100 to 1. A diode limiter was placed before the trigger amplifier to prevent it from going into saturation. This improved the bias stability of the Schmitt trigger. In the

original set-up, overload pulses in the trigger amplifier became numerous when the system gain was increased to observe low energy pulses. In the modified pulse shaper, this effect was eliminated and tests with very active gamma sources showed that essentially no base-line shift occurred even at very high counting rates. The photopeaks from Co^{60} and Na^{22} gamma sources shifted less than 2% with counting rates of approximately 50,000 counts per second (approximately 50% dead time on the analyzer).

IV. EVALUATION OF EFFORT TO DATE

The preliminary neutron spectra data in the large sodium volume were analyzed. Good agreement was obtained with calculated spectra. A problem was detected with one of the electronic components and corrected. The problem did not affect the data but did make it necessary to count for a long time at low reactor powers. Now adequate statistics can be achieved with one hour runs at relatively high powers. This also improves the neutron to gamma ratio.

V. NEXT REPORT PERIOD ACTIVITIES

A more complete series of spectrum measurements will be made in the large volume of sodium.

THIS PAGE

WAS INTENTIONALLY

LEFT BLANK

Program: Reactor Physics
AEC Task: 5-E — Fast Reactor Monte Carlo Methods
Project Manager: H. A. Morewitz
Reporting Period: January-March 1968
General Order: 7701 Subaccount: 13320 AEC Category: 04-01-61-02.1

Principal Scientist: L. B. Levitt

I. PROJECT OBJECTIVES

The basic objective of this project is to advance the state-of-the-art of Monte Carlo applications to the analysis of fast reactors and fast critical assemblies. This development is needed so that experimental programs and design studies may be optimized through the use of computer programs capable of describing complicated geometric configurations while calculating the effects of localized perturbations. Attainment of these objectives will be manifest by the development of fast reactor criticality codes and specialized codes to treat perturbations due to changes in temperature, density, and material composition.

II. MAJOR ACCOMPLISHMENTS IN FISCAL YEAR 1968

Direct and adjoint versions of the code (STRIFE) which calculates the resonance escape probability for a two slab lattice were written.

III. PROGRESS DURING REPORT PERIOD

In an adjoint simulation of elastic scattering, a statistical weight factor arises because the scattering kernel is unnormalized. Transformations have been developed to help reduce the spread of the statistical weight factors thereby leading to a considerable reduction in the variance of the estimate.

Two transformations of the adjoint Boltzmann equation have been developed for reduction of the variance in adjoint Monte Carlo calculations. One of these will be most useful when the scattering cross sections are smooth in the energy range of interest. The other will be more useful when the masses of the isotopes in a given medium are similar. A code (STRIFE) has been written to test these transformations and compare results with a direct Monte Carlo calculation. The problem chosen is one in which the efficiency of the adjoint mode

calculation is approximately that of the direct mode calculation. Thus, one can obtain, with reasonable cost, a well converged normal mode result to serve as the standard against which the various adjoint calculations will be compared.

Direct mode calculations are being compared with various adjoint formulations in order to determine which adjoint sampling techniques result in estimates of lowest variance. The normalization factors and methods of sampling required by the transformed adjoint equation are different from those used in conventional multigroup adjoint representations. The STRIFE code is being used as an experimental tool to develop proper methods both for source weighting and final tallying, and for comparison of variance in the estimates.

The investigations performed to date with STRIFE have revealed fundamental difficulties in sampling from the equations adjoint to the collision density or flux. This difficulty applies to both the actual adjoint equation and to the above mentioned transformations. The difficulty manifests itself in the inherent inability to straightforwardly sample from the space and energy parts of the transition kernel in the proper order.

As a result, the equation adjoint to the one describing the density of particles emerging from collision was tried as a basis for particle simulation. The above mentioned transformations are equally applicable to this equation. The STRIFE code was therefore modified to investigate the test problem using this equation.

While the collision-to-collision particle history simulation remains essentially unchanged, a more complex source function arises from which initial phase space coordinates of the adjoint particles must be chosen. A procedure to correctly account for this has now been developed for use in STRIFE, and preliminary results indicate agreement between the direct mode and the current version of both the regular and transformed adjoint simulation procedures.

In addition, importance sampling schemes are being investigated for the purpose of simplifying the selection of scattering angles in those energy regions where the elastic scattering is anisotropic. Simplification will be useful in the techniques mentioned above when applied to fast reactor problems where the angular distributions may change with energy. While the motivation for this investigation was the improvement in efficiency of adjoint selection procedures,

this particular simplification will also serve the same purpose on direct mode fast reactor criticality calculations.

An invited talk titled, "Some Applications of Monte Carlo to Particle Transport," was prepared for the SHARE 30 meeting in Houston on February 29, 1968. An abstract was prepared for an invited talk titled, "Applications of Monte Carlo to Problems In Reactor Design and Experimental Analysis," to be presented at the Toronto ANS Meeting, June 9-13, 1968.

IV. EVALUATION OF EFFORT TO DATE

The simulation procedure needed for sampling from a Boltzmann equation adjoint to the one describing the density of particles emerging from collisions has been developed and is now undergoing careful testing and refinement. Results from the simple test problem being investigated in STRIFE indicate that — in addition to anticipated reduction in variance for appropriate problems — the computation time is actually shorter than for comparable direct mode computations because of the lower number of collisions per history. It is clear that the development and subsequent refinement of the non-multigroup adjoint Monte Carlo techniques will greatly broaden the scope of experiments which can be subjected to detailed analysis using the Monte Carlo method.

V. NEXT REPORT PERIOD ACTIVITIES

During the next report period, the checkout of the various adjoint procedures in the STRIFE code will be completed. These include several methods of final tallying as well as the use of importance sampling in the source energy selection. As soon as the adjoint techniques presently under investigation have proven completely workable in every detail, they will be combined with various forms of correlated sampling on a suitable test problem, first in STRIFE and then in the cylindrical geometry code TRAFE. Dimensional and temperature perturbations will be investigated using this combination, both in the total estimate and the spectral components, so that problem areas where additional importance sampling may be needed can be detected and given proper attention.

The invited talk titled, "Applications of Monte Carlo to Problems in Reactor Design and Experimental Analysis," will be prepared and presented at the Toronto ANS Meeting, June 9-13, 1968.

THIS PAGE

WAS INTENTIONALLY

LEFT BLANK

Program: Nuclear Safety
AEC Task: 6A — Reactor Dynamics Simulator Development
Project Manager: H. A. Morewitz
Reporting Period: January-March 1968
General Order: 7702 Subaccount: 29110 AEC Category: 04-60-01-09.1

Principal Scientist: E. U. Vaughan

I. PROJECT OBJECTIVES

The basic objective of this project is to improve the present state of kinetics codes for use in fast reactor safety calculations. Improved codes and methods to study the kinetics of fast breeder reactors are needed to remove some of the existing uncertainties in conceivable FBR accidents. These improvements will produce a space-dependent calculational scheme able to give a reasonably accurate picture of the complexities of space-time-energy dependent fluxes at computation costs lower than those obtained by the "exact" solution.

II. MAJOR ACCOMPLISHMENTS IN FISCAL YEAR 1968

Not applicable.

III. PROGRESS DURING REPORT PERIOD

Considerable work was done on the formulation of the problem. The original idea was to use a multigroup representation of the neutron spectrum in order to ensure the spectral detail needed in treating fast reactors. As a result of further study it appeared more advantageous to apply to the energy distribution the same "synthesis" technique originally proposed for treating the spatial distribution.

This decision was based on the development at AI of an energy synthesis approximation to the time-independent neutron transport problem.* It was shown that the consistent P-1 equations can be synthesized through the use of

* P. Rose, B. D. O'Reilly, and E. U. Vaughan, "Energy Synthesis in the Consistent P-1 Approximation," AI-68-TDR-22 (February 20, 1968).

trial functions which consist of linear combinations of known energy spectra. The energy synthesis approach makes possible the inclusion of considerable spectral detail in the neutron distribution description without having to overtly introduce many energy groups. Further detailed work will be required to show that, in the practical application of this technique, substantial improvement is obtained in the machine running time of the problem.

IV. EVALUATION OF EFFORT TO DATE

During the report period the original plans were modified in the following ways:

1) Spectral synthesis is now preferred to the multigroup method.

2) The former preference for spatial synthesis rather than the multi-node method has been weakened, as the use of spectral synthesis may reduce the dependence of coupling constants on flux shape that previously made the multi-node method less desirable.

3) The choice of a proper form of synthesis method was enlarged by adding the group (or region) balance method to the variational and Galerkin methods previously considered. The variational method is probably eliminated, however, by its requiring adjoint calculations.

4) The effect of using the consistent P-1 approximation as an alternative to diffusion theory is being explored, though completely effective implementation of this alternative in preliminary computer programming is not likely.

V. NEXT REPORT PERIOD ACTIVITIES

Preliminary programming will be evolved for the purpose of comparing the amount of computing effort involved in spectral synthesis with that in a multigroup treatment of the spectrum. The adequacy of a synthesis representation of the spectrum in terms of a limited number of basic spectra will be explored; this will entail some work with the codes that average physical data over spectra.

A number of improved feedback mechanisms will be studied prior to being incorporated into AIROS II-A.

Program: Reactor Development
AEC Task: 6-C – Nuclear Safety, Fission Product Contamination and Control Studies
Project Manager: S. C. Carniglia
Reporting Period: January-March 1968
General Order: 7702 Subaccount: 29410 AEC Category: 04-60-10-01.1

Principal Investigator: M. Silberberg

I. PROJECT OBJECTIVES

The objective of this program is to elucidate the behavior of fission products released to the coolant in a fast, sodium-cooled, LMFBR reactor during normal operation, in order to provide information necessary for the development of fission product trapping techniques in such systems. The disposition of fission products during normal operation must also be known in order to assess the consequences of potential accidents. Information is required on the extent of fission product retention in sodium coolant, the rate and extent of release to the cover gas, and the rate and extent of plate-out on surfaces.

II. MAJOR ACCOMPLISHMENTS IN FISCAL YEAR 1968

A paper entitled "Fission Product Deposition in a Fast Breeder Reactor System Containing Failed Fuel Elements," by W. P. Kunkel and S. Berger, was presented at the 1967 ANS Winter Meeting.

Fundamental vaporization experiments have been conducted which show that cesium behaves according to Henry's Law in the concentration range 60 to 550 ppm ($X_{cs} = 8 \times 10^{-5}$) at temperatures approximating 700 to 900°K.

A series of cold-trapping runs was completed in which the cold-trapping characteristics of cesium in sodium were studied over a temperature range of approximately 425 to 750°K, and at oxygen concentrations in the sodium ranging from 5 to 155 ppm. These studies indicate a definite trend in which the amount of cesium removed appears to be related to both the cold-trap temperature and the oxygen concentration in the sodium. The low oxygen concentration run also shows a tendency to remove cesium, even at temperatures above which the oxygen is theoretically in solution.

TABLE 1

RADIATION INDEX

Assumptions: One-year operation at 2120 Mwt fractional fission product release of 10^{-5}; two-week shutdown period.

Isotope	Radiation Hazard Relative to Na-22	Total Concentration (Radioactive and Stable isotopes)* (ppb)
La-140	1.1	5.9†
Na-22	1.0	
Nb-95	0.7	0.6
Zr-95	0.6	2.4
Ru-103	0.5	2.0
Ba-140	0.09	2.3
I-131	0.09	0.02
Cs-137	0.08	3.3
Ce-141	0.07	
Nd-147	0.03	
Sb-125	0.02	0.011
Ce-144 (Pr-144)	0.02	
Te-132	0.01	0.4
Mo-99	0.006	0.2
Te-129	0.006	
Y-91	0.003	0.5
Te-125	0.003	
Ag-111	0.001	0.5
Ce-143	0.0007	

* Assuming uniform dispersion in sodium
† Total rare earth

The detailed design of the new Fission Product Behavior Loop and the fabrication of loop components were completed. Loop assembly is in progress.

Fundamental vaporization experiments were conducted for the sodium iodide - sodium system at temperatures of 695, 754, and 863°K, with a sodium iodide concentration of ~6 ppm or 10^{-6} mol fraction.

III. PROGRESS DURING REPORT PERIOD

A. PUBLICATIONS

The preparation of a topical report on the status of the project was initiated. Drafts of the various sections of the report were completed and are now being integrated for initial editorial review.

B. SOURCE TERM EVALUATION

To compare the relative importance of various fission products which could contribute to the after shutdown radiation levels during maintenance or repair, a new radiation index was computed for the case of clad-failed fuel in a LMFBR. A previous radiation index compilation had been prepared for a vented fuel situation.[1] For the purpose of this study, it was assumed that 1% of the fuel pins in a 1000 Mwe (2120 Mwt) LMFBR fail after one year of operation and 0.1% of the fission products are released from the failed pins. This constitutes a fractional release of 10^{-5} of the total fission product inventory. The released fission products are assumed to be uniformly dispersed in the coolant. The gamma dose rate from 1 curie of each isotope at one foot was computed and multiplied by the inventory of the isotope in the coolant to obtain the contribution of each fission product to the radiation level. The relative radiation hazard, or radiation index, of the various fission products was then compiled by normalizing to the anticipated dose rate from Na-22, since the radiation level from this isotope will be present after the normal time interval to allow for Na-24 decay, prior to system maintenance, thus providing a convenient basis for comparing fission product dose rates. The radiation index after a two-week, pre-maintenance shutdown period to allow Na-24 decay, is shown in Table 1. The radiation index for each isotope as a function of time beyond the initial two-week shutdown is presented in Figure 1.

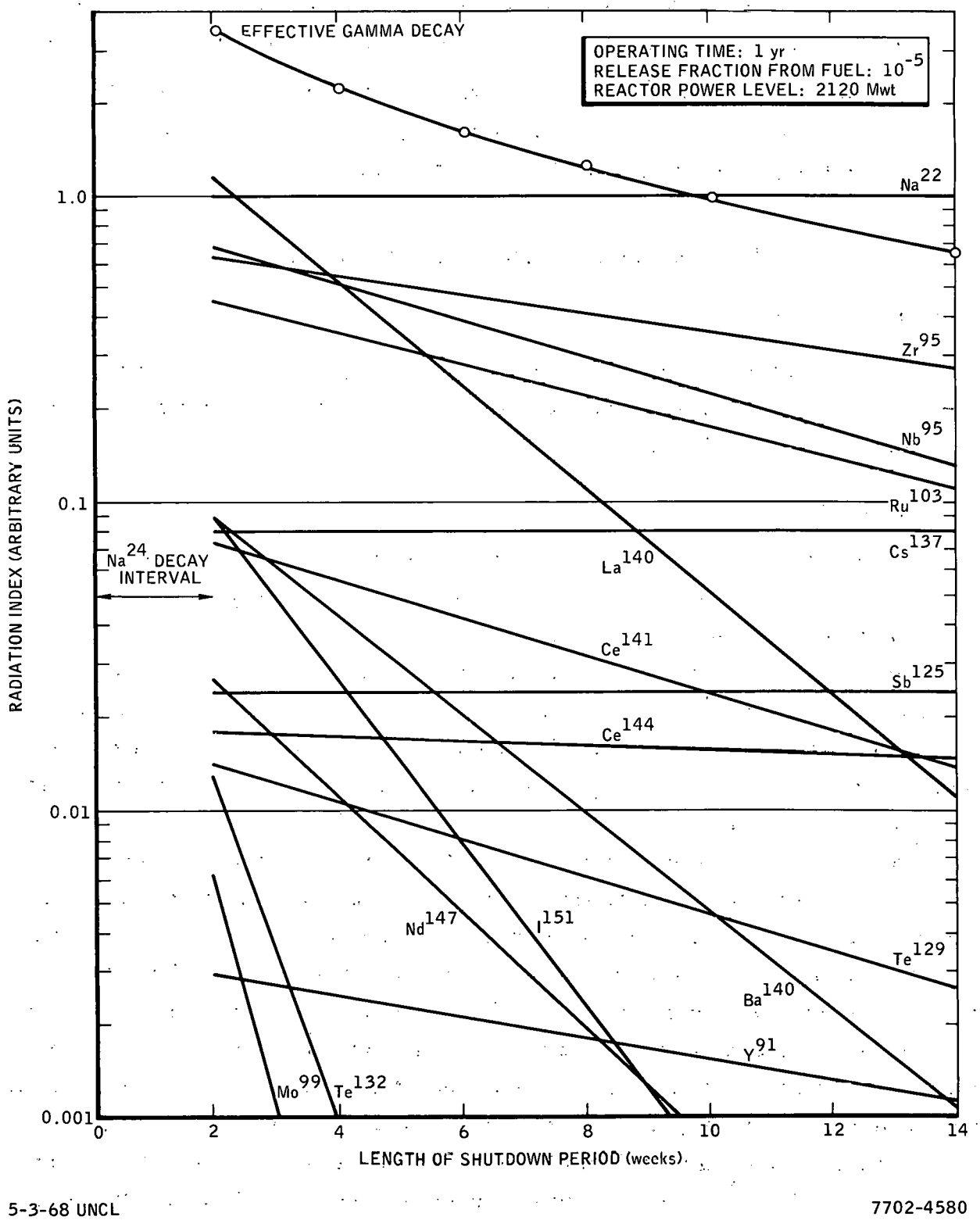

Figure 1. Radiation Index

Typical arrangements of sodium system components in the primary and purification portions of conceptual fast reactor designs were studied to obtain a reference system for the development of a detailed source term model. A simplified reference system was selected and will be used as the basis for preparation of a series of analytical expressions to describe the spatial and temporal disposition of fission- and corrosion-products released to the coolant. The relationships which will be derived to describe the various assumed depletion processes for all system components will be integrated (next fiscal year) into a computer program to provide complete accounting of all system contamination as a function of time and the conditions imposed.

C. FUNDAMENTAL STUDIES

1. Vaporization Experiments

A series of runs were successfully conducted in the modified transpiration apparatus to obtain data on the relative volatily of sodium iodide in sodium. Thc runs were made with sodium (~25 ppm oxygen) containing 6 ppm NaI (10^{-6} mol fraction) with NaI-131 tracer at temperatures of 695, 754, and 863°K. The results are shown in Figure 2, which is a plot of the distribution coefficient, K_d^* vs the reciprical of absolute temperatures. A best-fit line through the experimental data gives the following expression:

$$\log K_d = \frac{1836}{T} - 2.336$$

For comparison, the analytical expression derived previously for NaI vaporization,[2] having a somewhat greater slope than the experimental correlation, is also shown in Figure 2. The NaI vaporization results are further compared, in Figure 3, with data reported at other laboratories.[3, 4, 5] Figure 3 shows that the AI experimental correlation is in general agreement with data from

---

* $K_d = \frac{\gamma P^o_{NaI}}{P^o Na}$; where γ is the activity coefficient for NaI in Na solution; and P^o_{Na} and P^o_{NAI} are the vapor pressure of pure sodium and pure sodium iodide, respectively.

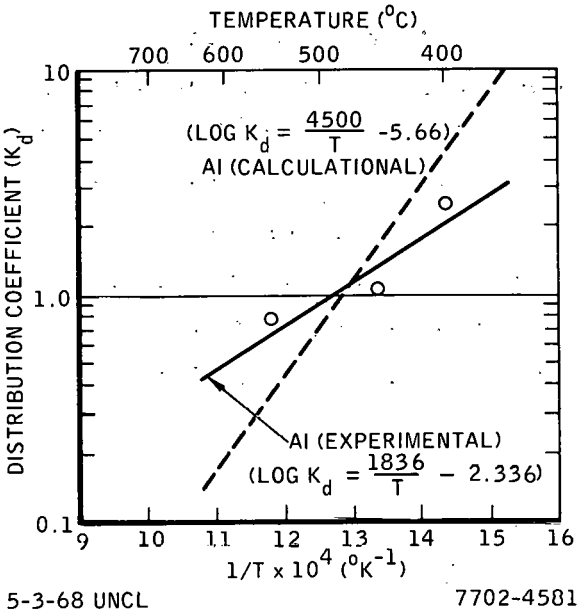

Figure 2. Relative Volatility NaI-Na System AI Data

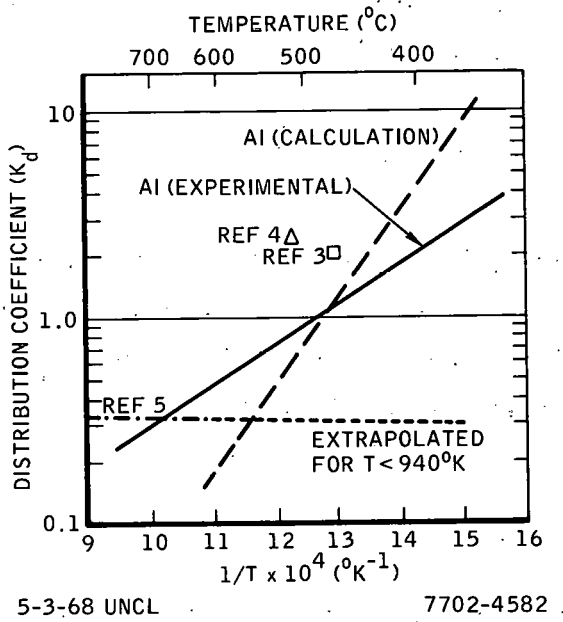

Figure 3. Relative Volatility NaI-Na System Comparison With Other Labs

References 3 and 4, but that the expression reported in Reference 5 shows a considerably different temperature dependence for the distribution coefficient such that agreement with our work is evident only in the region of about 1000°K, with increasing departure at lower temperatures.

2. Fission Product Behavior Loop (FPBL)

Fabrication of all components for the FPBL has been completed. Integration, by welding, of spools has started. Prior to assembly of spools into loop configuration, all parts will be cleaned. Thermocouples for the loop have been prepared and calibrated. The control console is complete. Preparation of the laboratory in which the loop will operate is proceeding. Control and power cables to interconnect the loop and instrumentation are being installed. Two gamma counting systems, to be used to follow fission product activity, have been repaired by the vendor and are currently under test.

Test planning has been initiated for the FPBL. Based on the free energies of formation of the oxides, relative volatilities, and the ability to form intermetallic compounds with the major constituents of stainless steel, the various fission products have been divided into analog groups (Table 2). Since gamma counting techniques will be used to follow the fission product distribution, a survey has been made of possible isotopes suitable for use in the program. Table 2 lists the selected isotope for each analog group. As estimate of the cost of production of an adequate quantity of these isotopes has not been made.

IV. EVALUATION OF EFFORT TO DATE

The revised radiation index compiled for fission products released from clad failed fuel shows approximately the same order for the important isotopes as the previous compilation for the vented fuel case, but with several additional isotopes which are of secondary interest.

The difference between the observed vaporization behavior of the NaI - Na system and the behavior predicted previously by AI is not exceptionally large or unreasonable. The predicted values were obtained by assuming Henry's Law behavior for the solute and computing activity coefficients from experimental solubility data for NaI in sodium. The solubility data employed were for the

TABLE 2

ANALOG GROUPING AND EXPECTED FATE
OF VARIOUS FISSION PRODUCTS

Analog Grouping	Expected Fate in Stainless Steel System	Radioisotope to be Used (at least initially) in FPBL Studies			
		Isotope	Reaction	T1/2	γ energy (Mev)
Cs	Volatilization or deposition as complex oxide	Cs-134	(n, γ)	2.1y	0.6
Ba, Sr	Deposition as oxide	Ba-133	(n, γ)	7.2y	0.36
Mo, Ru, Sb, Ag*	Diffusion into S.S.	Ru-103	(n, γ)	40d	0.5
Ce, La, Nd, Y, Zr	Deposition as oxide or diffusion into S.S.	Ce-141 (or Y-88) (or Zr-95)	(n, γ)	32-1/2d	0.14
Nb	Deposition as oxide or diffusion into S.S.	Ta-182	(n, γ)	115d	1.2
H^3, I, Te	Vaporization or diffusion into S.S.	Se-75	(n, γ)	120d	0.4

* May not be a successful analog grouping

lowest experimental temperatures and could be subject to considerable error. The discrepancy between the AI data and the work reported in Reference 5 is of some concern. If the latter relationship (obtained for the region of 940 to 1200°K) is extrapolated to 750°K, the disagreement between the two studies is as large as a factor of 10. The reasons for these differences are not immediately apparent.

The preparation of the FPBL is progressing satisfactorily and no problems have thus far been encountered in fabrication or integration of the loop components.

V. NEXT REPORT PERIOD ACTIVITIES

The topical report on project status will be published. Effort will be initiated on the derivation of analytical expressions which describe contamination depletion processes and source term in the LMFBR.

Assembly of the FPBL will be completed in preparation for initial checkout of the loop with sodium. Estimates of the quantity and cost of preparation of radioisotopes for the loop studies will be made.

References

1. "Quarterly Technical Progress Report - AEC Unclassified Programs, July-September 1966," NAA-SR-12175.

2. "Quarterly Technical Progress Report - AEC Unclassified Programs, January-March 1966," NAA-SR-11900.

3. W. S. Clough in "A Summary of Research and Development Work Carried Out in 1966 in Health and Safety Departments of UKAEA," AHSB (RP) M 46 (September 1967).

4. J. Saroul, "Investigation of the Behavior of Fission Products in Sodium and Argon – PIRANA Experiments," Int. Conf. on the Safety of Fast Reactors, at Aix-en-Provence, September 1967.

5. A. W. Castleman, Jr. and I. N. Tang, "Thermodynamics of Fission Product - Sodium Solutions," BNL-11611 (November 1967).

THIS PAGE

WAS INTENTIONALLY

LEFT BLANK

Program: Reactor Development
AEC Task: 6D and E – Nuclear Safety, Gaseous Effluents, Sodium Fires
Project Manager: H. A. Morewitz
Reporting Period: January-March 1968
General Order: 7702 Subaccount: 31111 AEC Category: 04-60-40-04.1

I. PROJECT OBJECTIVES

The general objective of this project is to develop experimental information and analytical methods which characterize the release and transport of effluents and energy generated during a primary-coolant-sodium accident. The source of energy generation may be from the escaping coolant by rapid thermal energy transfer and/or by combustion of the sodium coolant. The effluents are sodium (as Na 24) or its oxide, in particulate form, and selected fission products available as potentially serious dispersions of radioactivity. The information to be developed is required for the design and safeguards analysis of economical, sodium-cooled fast reactors.

II. MAJOR ACCOMPLISHMENTS IN FISCAL YEAR 1968

Three papers, listed below, were presented at the 1967 ANS Winter Meeting on November 5-9, 1967.

1) D. F. Hausknecht and M. A. Greenfield, "A Model Describing the Behavior of the Aerosol Produced by a Sodium Fire."

2) R. L. Koontz, C. T. Nelson, and L. Baurmash, "Characteristics of Aerosols Generated During Sodium Fires."

3) C. T. Nelson, R. L. Koontz, and L. Baurmash, "Characteristics of Vaporizing UO_2 in Air."

Two papers* were presented at the International Conference on the Safety of Fast Reactors at Aix-en-Provence, France in September 1967.

* See Task 6D and E of "Annual Technical Progress Report Fiscal Year 1967," NAA-SR-12492.

Five sodium fire experiments were conducted successfully in the Phase I, Large Fundamental Fires Apparatus. Four experiments were performed with an inlet gas mixture oxygen concentration of 4 vol % and bulk sodium temperatures ranging from 600 to 1300°F. The data obtained show a distinct increase in the sodium burning rate with bulk sodium temperature. Satisfactory data were also obtained during the fires on the distribution of energy between the gas and liquid phases and the structural surroundings. A fifth experiment was conducted with an oxygen concentration of 10 vol % and bulk sodium temperatures varied from 950 to 1300°F.

Site construction of the Phase II large modeling fires test installation (2500 ft^2 chamber) was completed and preparations for the first test were initiated.

An empirical model has been developed relating the laboratory scale experiments on aerosol agglomeration and fallout to full-size containment volumes.

III. PROGRESS DURING REPORT PERIOD

A. PUBLICATIONS

A draft was prepared for a topical report which describes the operational characteristics of the Phase I Large Fundamental Fires Apparatus.

A draft was initiated for a topical report which describes the application of aerosol agglomeration characteristics to fast reactor safeguards evaluation.

Abstracts of four papers were prepared and submitted for the IAEA Symposium on Operating and Developmental Experience in the Treatment of Airborne Radioactive Wastes to be held in New York City, August 26-30, 1968.

B. FUNDAMENTAL EXPERIMENTS

1. Laboratory Test Chamber (LTC) Studies - Na_2O Aerosol Characterization

Test 15 was conducted in the LTC using a 6-in. diameter pot containing 150 gm of sodium and a chamber atmosphere of 3 vol % oxygen. The purpose of the test was to oxidize all of the sodium in a longer time than in previous runs. The oxygen concentration was monitored and was observed to decrease

exponentially with an initial half-time of about 45 min. The initial sodium temperature was 1100°F, but a rapid decrease occurred when the lid was removed from the liquid sodium. For some unknown reason a peak concentration occurred at 9 min even though the oxygen decreased (and hence sodium burned) for 75 min before leveling off at 1% O_2 to a slower rate of decrease. The final oxygen level was about 0.6% and indicated that 113 grams of sodium was oxidized. Only 12.8 gm of the oxidized sodium was found on the walls and floor, representing a release fraction of only 11%. This value is inconsistent with the 20 to 40% previously observed. The rapid drop of the sodium temperature to a level of nearly 600°F may have caused this decrease of the release fraction.

One major accomplishment of Test 15 was that the air concentrations were measured for 115 hr. The final air concentration measured was in the range of 10^{-15} μg/cc, and the removal half time was 15 hours. Eighty-seven percent of this mass had a particle size less than 0.9-μ diameter.

2. Particle Deposition and Transport Studies in the LTC

Observed mass deposition rates on the walls of the LTC can be understood only by defining the several mechanisms which contribute to the deposition rate. When a temperature gradient is present between the gas and collecting surface in a chamber, the particles move toward the collecting surface; this mechanism is known as thermophoresis. A second removal mechanisms occurs when particles are impacted due to turbulent conditions which may exist in the LTC during a sodium fire. Another mechanism for deposition is due to the diffusion of particles brought about by collisions with the gas molecules. In a confined volume where particles are allowed to grow, gravitational settling becomes important and may be the prime mechanism for deposition.

Since all these deposition mechanisms determine the removal of particles from an environment, and since their importance will vary as conditions of the environment change, a simple formulation cannot be used to explain the measured values. Figure 1 shows some theoretical estimates of the relative importance of thermal and diffusional wall plating rates compared to gravitational settling in the LTC. The velocities shown in Figure 1 are divined as follows:

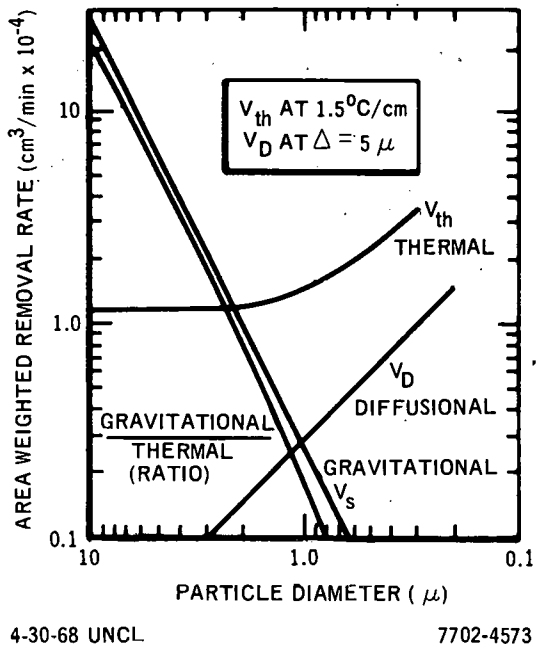

Figure 1. Area Weighted Removal Rates for LTC

$$V_{th} = \frac{F_{th}}{6\pi\nu_r} \times 10^4 \ , \ V_D = \frac{D}{\Delta} \ , \ V_s = 0.012 \ pr^2$$

where

F_{th} = thermo phoretic force, (dynes/cm^2)

ν = viscosity of gas, (gm/cm-sec)

r = particle radius, μ

Δ = wall plating distance, cm

D = diffusion coefficient, cm^2/sec

p = density, gm/cm^3

C = Cummingham correction factor for small values of r

3. Sodium Spray Aerosol Characterization

The first sodium spray fire was generated in the 31.5 ft^3 (2-ft diameter by 10-ft high) spray test vessel filled with a 5% oxygen atmosphere. The spray injection system consisted of a heated sodium supply pot connected to a full

cone 15° spray nozzle through which 142 gm of 700°F liquid sodium was driven with 40-psig nitrogen gas pressure. Of the 142 gm sprayed, 65 gm were found on the floor, walls, and ceiling.

During the test, observations were made of the rate of decrease of oxygen and of changes in temperature and pressure. In addition, the mass of sodium which was airborne, and that which settled on the floor, walls and ceiling, were monitored as a function of time. After the sodium injection was terminated, round jet impactors were used to measure the airborne particle size distribution by mass as a function of time.

The 4 psig initial pressure in the vessel increased to 7 psig during the release of sodium spray. From the decrease in oxygen concentration, it was calculated that approximately 35 gm of sodium were oxidized to form Na_2O.

During the first minute, 29 gm of sodium (as Na_2O) fell to the floor. During the injection period of approximately 2 sec, 15 gm deposited on the ceiling and 10 gm on the walls. After 2 minutes, the air concentration was 5.4 μg/cc of Na_2O. The initial (2-min) median aerodynamic diameter was 5.1 μ and persisted for 30 min.

The initial measured air concentration decreased at a 5-min half-time. This increased to a 26-min half-time after 30 min. These half-times are not interpretable in terms of particle sizes in the same manner as previously reported for the stirred settling LTC experiments because the air concentrations were higher at the sampling stations in the lower half of the vessel, thus indicating a "tranquil" rather than "stirred" environment. A simple model assuming tranquil settling of the initially measured distribution showed that agglomeration must have been occurring in the chamber during the life of the aerosol.

4. Phase I, Large Fundamental Fires

The effort on the Phase I program during the report period included primarily the reactivation of the test facility following the Phase II installation, the preparation, performance and data reduction of Test IG. Work near the end of the quarter involved cleanup of Test IB and preparations for Test IH. This test will be the last of the current series prior to the Phase II activation.

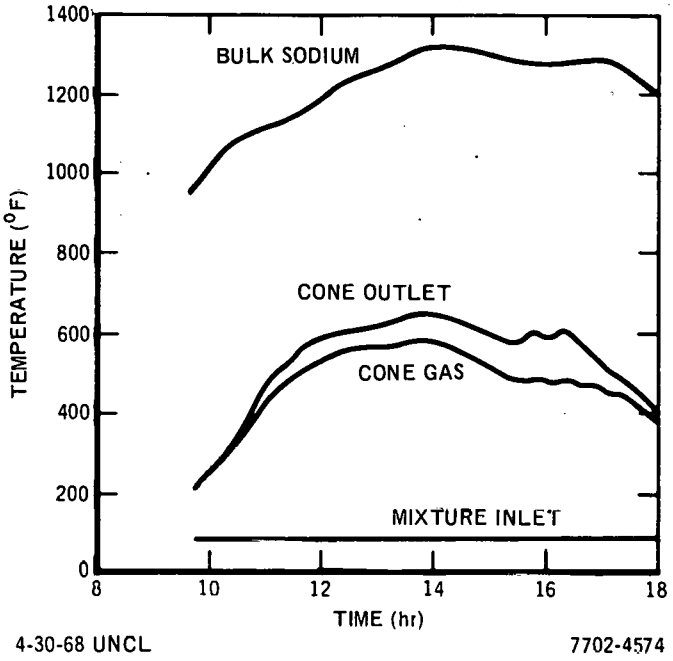

Figure 2. Temperature Averages
Test IG

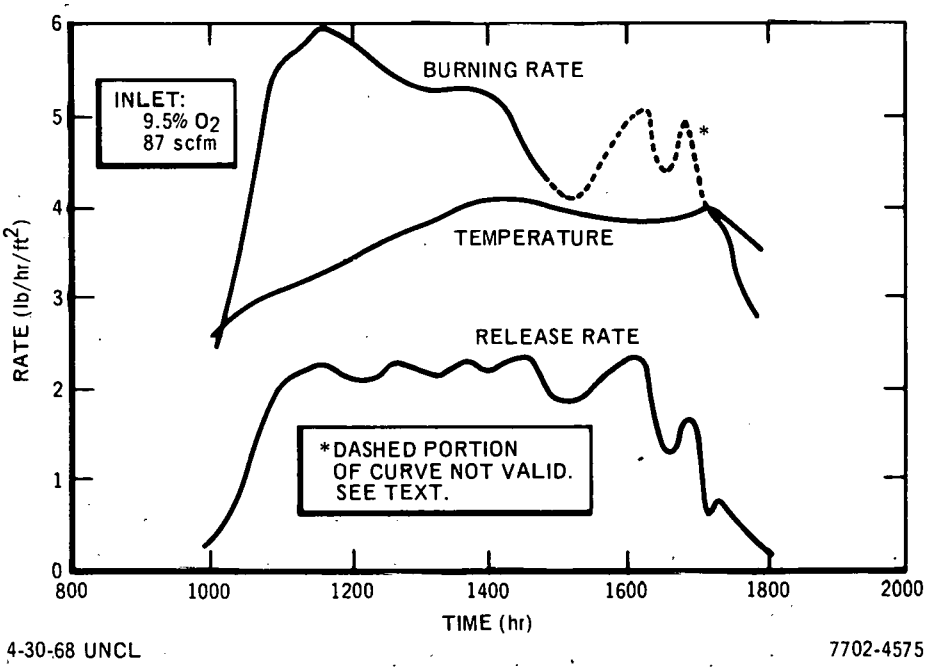

Figure 3. Burning and Release History
Test IG

Test IG was conducted on February 20. The inlet gas mixture flow rate was held constant at 87 scfm and the inlet oxygen concentration was a constant 9.5 vol %. The initial sodium weight was 110 lb (as in previous tests) at a temperature of 950°F. The combustion heat was supplemented with the electrical heaters, and the sodium temperature was brought to a maximum of 1311°F in 4 hr and 20 min. At that point, the electrical power was turned off and in the next 4 hr the temperature cooled to about 1200°F. At this time more than 90% of the sodium had been consumed. The behavior of the system temperature average is shown in Figure 2. For comparison, the burning rate, release rate, and temperature histories are shown in Figure 3.

Several rather interesting effects were noted in analyzing the data from this test. In Figure 4 that the burning rate-temperature plot establishes a burning rate "plateau" near 1120°F. This burning rate plateau varied between 5.2 and 5.9 lb/hr/ft while the temperature steadily increased to 1311°F (in 4 hr). At this point the electrical heat was removed and the sodium temperature slowly decreased. The burning rate, however, dropped rapidly thus indicating a considerable "hysteresis" effect. These data are shown in Figure 4. (The loss of oxygen data between 15:10 and 17:10 hr is a result of some mechanical difficulties that we encountered in the course of the test.) At 14:00, the time at which the peak sodium temperature occurred, 45% of the initial charge of sodium remained in the pot. In Test IB, on empirical determination of the contribution of each of the two sodium burning reactions was made. The two reactions are:

(1) $4\ Na + O_2 \rightarrow 2\ Na_2O$

(2) $2\ Na + O_2 \rightarrow Na_2O_2$

We note that if reaction (1), the oxide reaction were involved alone, twice as much Na would be consumed than the case would be if reaction (2), the peroxide reaction, were exclusive. Thus, with a knowledge of the total sodium and total oxygen consumption, an average ratio of the contribution of one reaction to the other was determined. For Test IG, as an average over the entire test, approximately 70% of the sodium was consumed by the oxide reaction and 30% by the peroxide reaction.

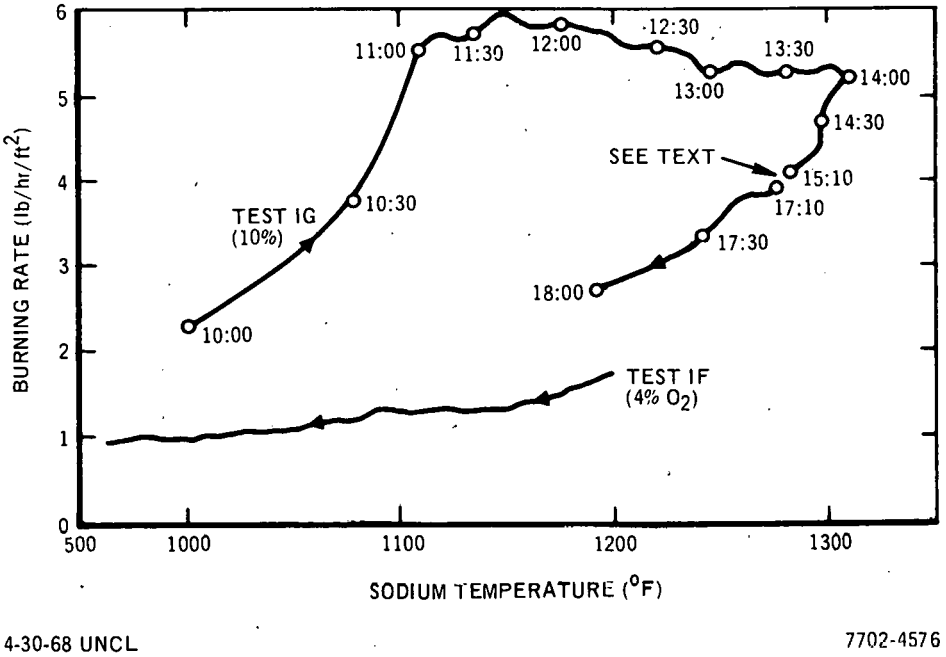

Figure 4. Sodium Temperature Effect on Burning Rate

The effect of the peroxide reaction was incorporated into the Phase I Heat Balance code with a resultant improvement in energy accountability. For the greater portion of Test IG, both the system and surface region energy accountability was of the order of 95%.

C. PHASE II, LARGE MODEL FIRES TEST

Installation of the Phase II test chamber was completed by the contractor and the system turned over to project. Figure 5 shows the Phase II system in the cell of the Sodium Fires Test Installation after completion of construction. Preparation of the test chamber for the initial test is in progress. This includes installation of instrumentation sensors, inter-connection of instrumentation leadwires from the contractor-installed junction panels to the readout instruments and to the instrumentation sensors, and the design and fabrication of other test hardware.

The geometry of the first Phase II sodium fire has been selected and will model a sodium spill which occurs within a closed cell containing a normal air atmosphere. The spill will involve a small amount of sodium, (25 lb at 1000°F) and will cover an area of 6 ft^2. Measurements will be made as a function of

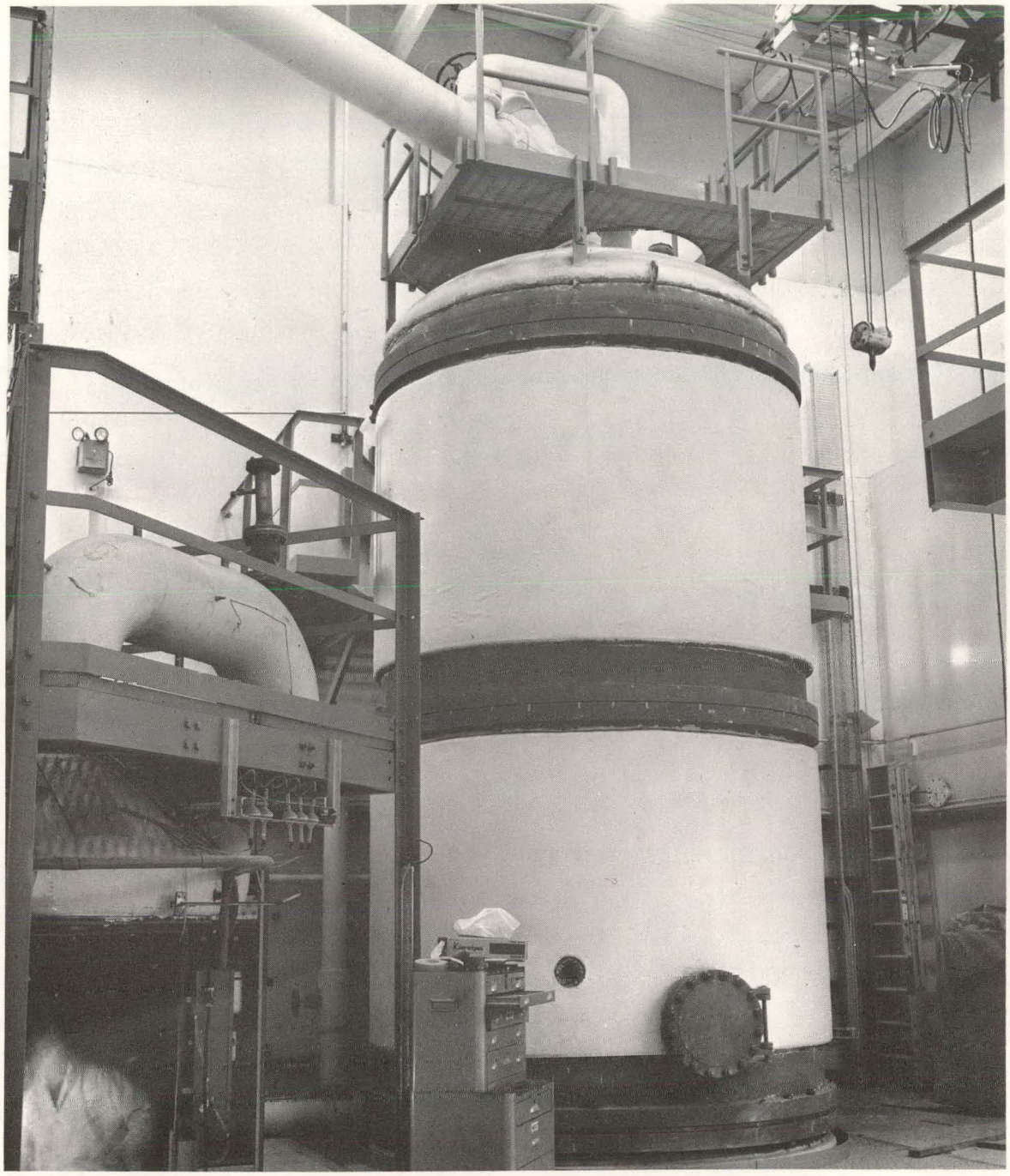

1-18-68 UNCL

00-102207

Figure 5. Task 6D and E

time of temperature; pressure; oxygen concentration; radiant heat flux; distribution of released sodium oxide between the air, floor and wall; deposition rates; and particle size distribution.

D. ANALYTICAL DEVELOPMENT

1. Phase II Data Reduction Code

The data conversion code for the Phase II tests has been written and checked-out. This code provides the fundamental conversion from the sensor output, usually in mv, to engineering units. These data are then tabulated and plotted. The visual temporal plots are provided in addition to axial and radial profiles throughout the test chamber. The converted data, as appropriate, will then be input to the Phase II heat balance code. This code utilizes standard heat transfer equations to account for the heat losses occurring in the Phase II test chamber during a test. Volume and area weighted enthalpy change and conduction equations (similar to those used in the Phase I Heat Balance code) calculate the respective heat loss terms as a function of time. A summation of the weighted heat loss terms is compared with the heat generated by the sodium fire to determine a continuous heat balance accountability. Development and checkout of the heat balance code will be completed prior to the initial test.

2. Transient Sodium Burning Model

In programming the equations for the transient sodium burning code, difficulties were encountered in obtaining convergence for sodium temperatures around 1000°F. Below this temperature, the results were satisfactory. Results to date, therefore, were obtained for sodium temperatures below 1300°F. Figure 6 shows the dependence of burning rate and flame temperature as a function of time and sodium spill temperature for the case of fully ventilated secondary volume. For these calculations the initial oxygen concentration of the cell was taken to be zero. Thus the results reflect only the limiting case when the burning rate is limited by the rate at which oxygen can be drawn through the cell opening. It should be noted that this rate of burning is considerably smaller (0.3 lb/hr-ft^2 at 940°F and 21 vol % oxygen in the primary cell) as compared to Phase I experiments where the burning rate at this sodium temperature was (0.9 to 1.5) lb/hr-ft^2 but with only 4 vol % oxygen. This is due essentially to the small cell opening (9 ft^2) used in the calculation.

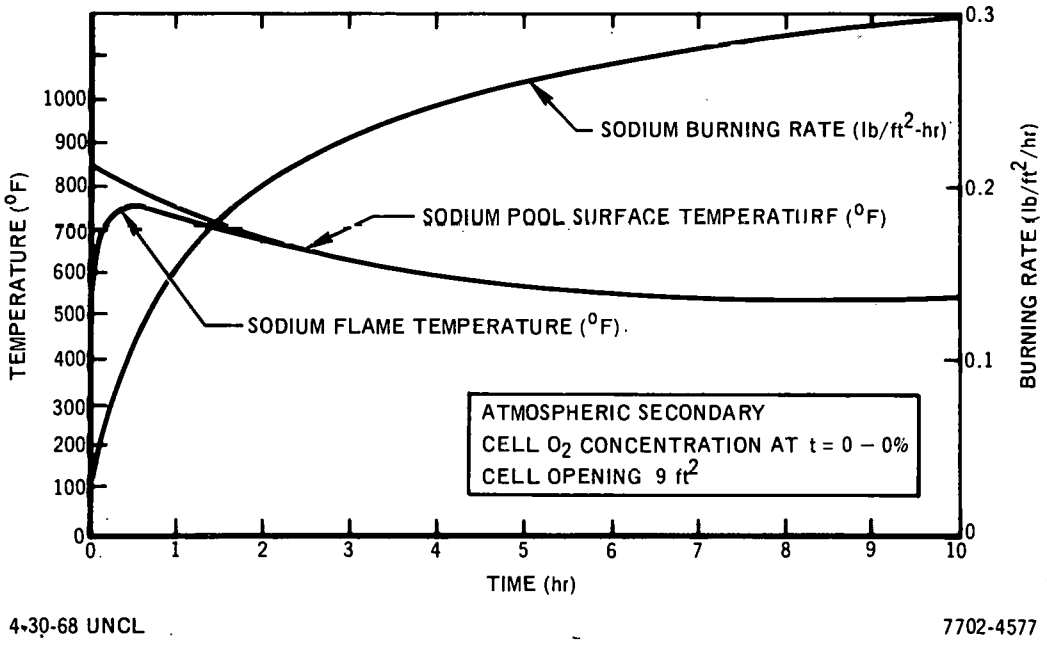

Figure 6. Transient Sodium Burning Code

3. Empirical Aerosol Modeling

An empirical mass model (EMM) has been developed on the basis of prior LTC studies. The model has been programmed on the IBM 360/50, and good agreement with the laboratory test results has been obtained. The model equations are based on two empirically observed relations between (M_R/V), the toal mass, M_R, released into the LTC column, V and the plating and settling rates. The general equation relating the air concentration and the removal rates is,

$$\frac{d\rho}{dt} = S_m - \alpha\rho - \beta\rho \qquad \ldots(1)$$

where

α = removal rate due to fallout on floor (sec^{-1})

β = removal rate due to wall deposition (sec^{-1})

S_m = source term $\frac{M_{R\tau}}{V}$ ($\mu g/cm^3$-sec)

τ = source time or burning time (sec)

ρ = air concentration (μg/cc) .

However,

$$\alpha = \frac{v_s}{H} \text{ and}$$

$$\beta f = v_p \frac{Aw}{V}$$

where

H = height of the chamber (cm)

A_w = wall surface area of the chamber (cm^2)

v_s = settling velocity (cm/sec)

v_p = plating velocity (cm/sec)

From experiments on sodium oxide aerosols $v_s = 0.029\rho^{0.8}$ and $v_p = 1.67 \times 10^{-3}\rho^{0.6}$. Substituting the above expressions into Equation 1 yields the following relationship which is solved by the computer:

$$\frac{d\rho}{dt} = S_m - \frac{0.029\rho^{1.8}}{H} - 1.67 \times 10^{-3}\rho^{1.6} \qquad \ldots(2)$$

4. Analysis of Phase I Experiments

The results of the Phase I experiments with 4 vol % oxygen showed that the burning rate increased rapidly with the increase in sodium surface temperature. Since the theoretical models developed to date are based on the assumption that the burning rate is controlled by the rate at which oxygen can arrive to the reaction zone, it is important to examine if this assumption is consistent with the experimental observations.

The observed temperature dependence of the burning rate could be a result of one or more of the following factors.

(1) Burning rate is reaction-rate controlled.

(2) Burning rate is controlled by the rate at which sodium vapor diffuses to the reaction zone.

(3) The flow-geometry combination causes increase in oxygen arrival rate to the reaction zone with increase in sodium surface temperature.

The mass transfer coefficient for the transfer of oxygen from the bulk to the reaction zone should exhibit the same dependence on system parameters as the convective component of the heat flux leaving the reaction zone; therefore, as a first step for the analysis information about the heat transfer characteristics of the system is needed.

From the heat balance runs (no sodium burning) the total heat leaving the pot was obtained. Assuming values for the emissivity of the surface as 0.1 and 0.79, the corresponding convective component could be deduced by subtracting the radiation term from this heat flux. The driving force for the heat flux is the difference between surface temperature and bulk gas temperature, where conditions are constant.

For the present geometry the bulk gas temperature is not a constant but varies with the flow rate. Therefore a more suitable reference temperature would be the temperature at which the gas enters the chamber, approximately room temperature. Figure 7 is a plot of the heat transfer coefficient, h, vs the difference between the pot and the room temperatures. It is seen that h depends both on the flowrate and $(t_{pot}-t_{room})$.

As shown in Figure 8, if, instead of choosing the initial gas temperature as a reference, the cone temperature is used, the heat transfer coefficient exhibits the same behavior as previously but with a more pronounced dependence of h or ΔT. It is also noted that the value chosen for the emissivity of the surface strongly affects the shape of the curve. Comparison of Figures 7 and 8 with burning rate data for 4 vol % oxygen* shows a similar dependence of

---

* See AI-AEC-12638, pg 68, Figure 7

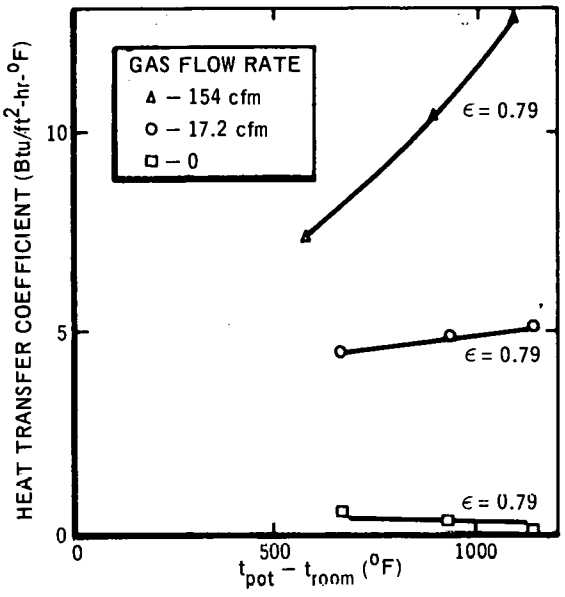

Figure 7. Heat Transfer Coefficient vs (T_{pot} - T_{room}) (Heat Balance Run)

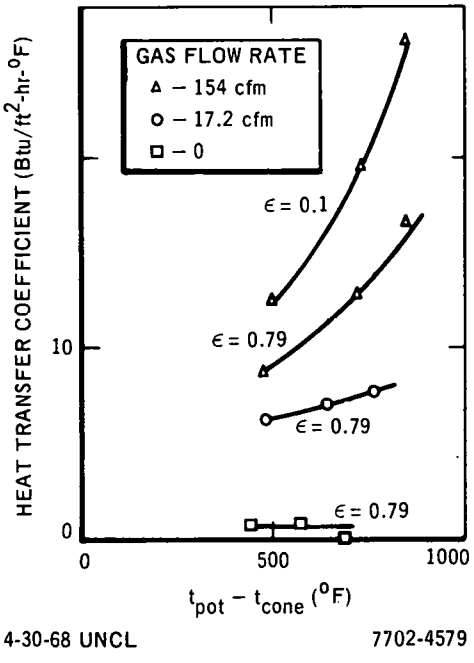

Figure 8. Heat Transfer Coefficient vs T_{pot} - T_{cone} (Heat Balance Run)

burning rate upon the flowrate, as exhibited by the heat transfer coefficient in the heat transfer coefficient increase with flowrate and pot temperature indicates that these parameters improve the accessibility of air to the heat transfer region, namely the pot surface. This is also instrumental in improving the rate of oxygen arrival to the burning region of a sodium fire.

IV. EVALUATION OF EFFORT TO DATE

A preliminary evaluation of the data from the initial experiment on sodium spray aerosol characterization indicates that the resultant aerosol behaved in a manner which was expected based on previous pool fire experience in the laboratory test chamber. However the need for improvement of the spray production technique was apparent.

The empirical models derived from the LTC experiments for evaluating fast reactor safeguards offer a simple, economical technique which is finding wide application in safeguard studies.

The results from the recent Phase I fire with a 9.5 vol % oxygen gas mixture have provided some initial information on two characteristics of a sodium fire which will eventually have to be factored into the detailed burning models. One of these characteristics is related to the observed plateau in the dependence of burning rate on sodium temperature. This effect may be due to an increased buildup of a surface layer of sodium oxides on the pool surface, resulting in an appreciable resistance to diffusion of sodium vapor to the reaction zone. If this were the case, the burning rate could be controlled by this oxide layer and not by sodium temperature, regardless of the initial mechanism involving temperature dependence. The occurrence of this effect (not apparent in the 4 vol % oxygen tests) is probably related to the increased oxidation rate with the 9.5 vol % oxygen gas mixture and a time-dependent buildup of the oxide layer, rather than being attributed to reaching any specific temperature level. This observation suggests that, for a sodium pool fire in air (21 vol % oxygen) the controlling oxide layer will develop more rapidly due to higher initial burning or oxidation rates resulting in a virtual elimination of any significant dependence of burning rate on temperature. Information on another sodium fire characteristic indicated from the recent Phase I test was that of the relative

contributions of the two sodium oxidation reactions, i.e., the formation of Na_2O vs Na_2O_2. The increased contribution from the peroxide reaction, with increasing oxygen concentration, is not unexpected and indicates that the heat of combustion (20% higher for the peroxide) specified in the burning models will have to be adjusted accordingly. Additional information in each of the above areas will be obtained in the forthcoming Phase I fire with air.

The preparations for the activation of the Phase II test system are proceeding satisfactorily.

V. NEXT REPORT PERIOD ACTIVITIES

A Phase I sodium fire test will be conducted with air.

The LTC tests on UO_2 aerosol characteristics will be resumed and the spray aerosol studies will continue.

The activation of the Phase II test system will be completed and the initial Phase II test will be conducted.

The two topical reports initiated during the previous report period will be published.

Program: Fast Reactor Development
AEC Task: 6-G — Nuclear Safety (Kinetics) Boiling Studies
Project Manager: H. A. Morewitz
Reporting Period: January-March 1968
General Order: 7702 Subaccount: 13410 AEC Category: 04-60-01-09.1

Principal Investigators: D. Logan, J. Landoni, and C. Baroczy

I. PROJECT OBJECTIVES

The general objective of this project is to develop basic information on two-phase flow and boiling required in the safety evaluation of LMFBR designs. This information is important because of the key role that sodium boiling plays in reactor dynamics, in fuel meltdown accidents, and in the ultimate shutdown mechanism of the reactor. Specific objectives of the experimental program include the development of reliable high-flux heaters as well as the measurements of: boiling heat transfer characteristics; two-phase pressure drop; void fraction; liquid superheating; transient voiding rates and pressures in single channels; and hydrodynamic instabilities. Specific objectives of the theoretical study, in addition to any analyses required to support the experimental work, are: the development of digital computer codes which will predict transient void fraction, flow rate, and heat transfer for single and multichannel sodium flow; and the incorporation of these codes into a general reactor kinetics code.

II. MAJOR ACCOMPLISHMENTS IN FISCAL YEAR 1968

Liquid superheat testing has progressed substantially. Three hundred and sixty-four sodium liquid superheat tests have been performed at pressure levels to 12 psia. In the AI two-phase sodium loop, an engineering loop with normally controlled test variables, the liquid superheat tests have demonstrated that incipient boiling occurs in a random manner with the data filling in the area under the curve of maximum superheats measured at a given pressure (Figure 1). Maximum obtainable wall superheats agree fairly well with the predictions of the pressure-temperature history theory of Holtz, provided the following conditions are met: (1) predicted wall superheat minus the convection thermal drive does not exceed the values in Figure 1, (2) heater surface has random

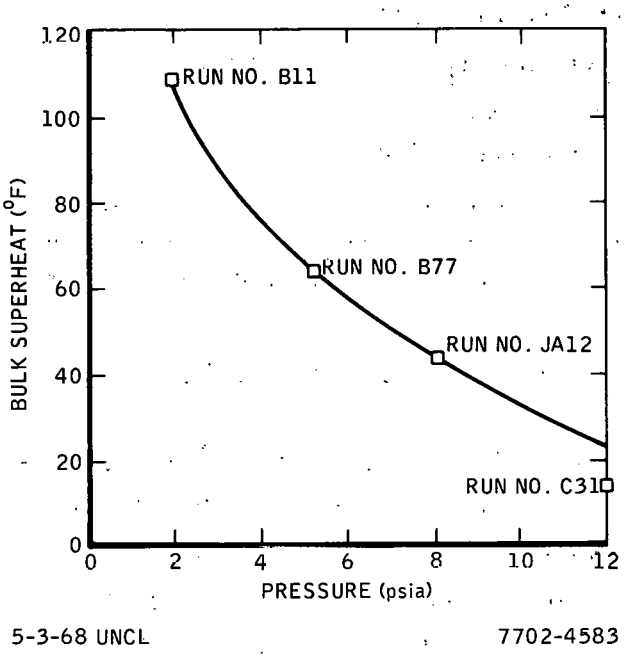

Figure 1. Maximum Measured Bulk Liquid Superheats

cavities larger than those with the minimum radius calculated for liquid sodium penetration based on Holtz's theory, and (3) attack of the heater surface has not produced well defined prominences and pits.* In Figure 1, the maximum measured bulk superheats at four pressures (2, 5, 8, and 12 psia) show a strong decreasing effect in maximum superheats as pressure is increased.

The 15-in. high-heat flux heater has been demonstrated as a useful and dependable heater for transient testing. In the development of longer heaters, premature failures have been related to the voltage across the boron nitride insulation, independent of other variables. This discovery permits a more direct attack on the development problems.

The boiling detection system has been improved allowing a more positive identification of incipient boiling. The critical instrumentation readout has been tied in to the Santa Susana data reduction center in order to obtain on-line evaluation of test data.

* "Quarterly Technical Progress Report AEC Unclassified Programs, July-September 1967," NAA-SR-12570.

A topical report, NAA-SR-12503, describing the single channel transient boiling code: TRANSFUGUE IIa, its use, and a sample problem solution was published March 15, 1968.

The SODIFAZE code (a two-phase, multichannel code which has been converted for use with sodium) is available for general usage.

The TRANSODIFAZE code (a transient, two-phase, multichannel code) converted to use with sodium is operating and preliminary comparison (at the end of a transient) with SODIFAZE shows that it is debugged.

III. PROGRESS DURING REPORT PERIOD

A. SODIUM-LIQUID SUPERHEATING

1. Experimental

Sodium-liquid superheat tests are being run to determine the extent of liquid superheating required to initiate boiling in a single LMFBR coolant channel as influenced by parameters such as velocity, heat flux, subcooling, coolant purity, pressure, heater surface finish, etc. Another 15-in. heater (Heater J) was made and used to perform 69 liquid superheat tests* during this report period. After the first 51 tests on the as-received tubing surface, Heater J was resurfaced with 600 grit abrasive and used for an additional 18 superheat tests. These data (see Table 1) are now being evaluated. Loop modifications made during this report period now permit the test section pressure to be controlled independently of the cover gas pressure, provided test section pressure is the higher pressure. During the J1 to J35 tests the cover gas pressure was maintained constant at the pressure at which the boiling test was made. Pressure changes in the test section during an experiment, such as for runs J6, J7, J8, J14, etc., were obtained by valving against the pump pressure head. This should cause a constant amount of dissolved gas and/or gas entrainment independent of pressure history, thus isolating the presure history effect. The cover gas pressure for runs J36 through J51 and JA1 through JA18 was maintained constant at 2 psia and test section pressure was obtained by valving

* Heater J is still intact and usable.

TABLE 1

SUPERHEAT TESTS USING RESURFACED HEATER J

Run	Condenser (psia)	Test Section (psia)	Maximum Test Section (psia)	Time at Maximum Pressure (min)	Inlet Temperature (°F)	Heat Flux (Btu/hr/ft^2)	Flow (ft/sec)	Bulk Superheat (°F)
J-1	5.00	5.04			1272	0.296×10^6	2.94	-4
J-2	5.00	5.00			1281	0.320×10^6	2.94	17
J-3	5.00	5.03			1277	0.342×10^6	2.94	18
J-4	5.00	5.05			1285	0.349×10^6	3.00	29
J-5	5.00	5.15			1285	0.333×10^6	2.98	20
J-6	5.00	5.13	25.5	1	1292	0.350×10^6	2.98	38
J-7	5.00	5.14	25.5	1	1286	0.329×10^6	2.88	26
J-8	5.00	5.19	26.0	5	1282	0.329×10^6	3.00	8
J-9	5.00	5.17			1279	0.329×10^6	2.94	7
J-10	5.00	5.10			1281	0.308×10^6	2.92	-3
J-11	5.00	5.02			1279	0.283×10^6	2.90	-5
J-12	5.00	5.03			1280	0.329×10^6	2.98	9
J-13	5.00	5.06			1282	0.342×10^6	2.94	2
J-14	5.00	5.01	25.5	5	1282	0.313×10^6	2.96	4
J-15	5.00	5.04	25.5	5	1278	0.325×10^6	3.00	2
J-16	5.00	5.07	25.5	10	1275	0.338×10^6	3.07	8
J-17	5.00	5.12	25.5	10	1279	0.342×10^6	3.17	5
J-18	5.00	5.03			1279	0.346×10^6	2.98	3
J-19	5.00	5.00			1281	0.325×10^6	2.96	6
J-20	5.00	5.03			1283	0.350×10^6	2.98	14
J-21	5.00	5.07			1283	0.333×10^6	3.00	10
J-22	5.00	5.10			1284	0.333×10^6	3.00	9
J-23	2.00	1.98			1133	0.358×10^6	2.98	22
J-24	2.00	1.95			1136	0.346×10^6	2.98	18
J-25	2.00	2.00			1136	0.379×10^6	2.98	28
J-26	2.00	1.99	25.5	5	1136	0.392×10^6	2.98	41
J-27	2.00	2.01	25.5	10	1133	0.479×10^6	2.96	82
J-28	2.00	1.98	25.5	10	1135	0.363×10^6	3.00	22
J-29	2.00	2.10	25.5	10	1134	0.392×10^6	3.00	14
J-30	2.00	1.99	25.5	10	1137	0.342×10^6	3.00	14
J-31	2.00	2.00			1134	0.383×10^6	3.00	33
J-32	2.00	2.04			1137	0.454×10^6	3.02	60
J-33	2.00	2.04			1131	0.433×10^6	3.22	40
J-34	2.00	2.00			1142	0.354×10^6	3.00	11
J-35	2.00	2.04			1135	0.396×10^6	2.94	36
J-36	2.00	5.54			1294	0.264×10^6	2.92	-10

TABLE 1 (Continued)

Run	Condenser (psia)	Test Section (psia)	Maximum Test Section (psia)	Time at Maximum Pressure (min)	Inlet Temperature (°F)	Heat Flux (Btu/hr/ft^2)	Flow (ft/sec)	Bulk Superheat (°F)
J-37	2.00	5.09			1290	0.274×10^6	2.94	7
J-38	2.00	4.97			1295	0.271×10^6	2.90	-2
J-39	2.00	5.00			1292	0.276×10^6	2.98	9
J-40	2.00		25.1	5	SEE SECTION III A1			
J-41	2.00		25.0	1/2	SEE SECTION III A1			
J-42	2.00	5.51	17.3	5	1292	0.229×10^6	3.02	43
J-43	2.00	5.20			1294	0.263×10^6	2.98	8
J-44	2.00				SEE SECTION III A1			
J-45	2.00	5.03	22.5	1/12	1293	0.244×10^6	2.98	-3
J-46	2.00	3.80			1290	0.191×10^6	3.00	4
J-47	2.00	4.95			1287	0.256×10^6	3.00	-3
J-48	2.00	5.09			1290	0.356×10^6	4.15	-7
J-49	2.00	5.03			1291	0.353×10^6	4.15	-6
J-50	2.00		30.0	1/12	SEE SECTION III A1			
J-51	2.00	5.03	25.5	5	1284	0.276×10^6	4.24	-22
JA-1	2.00	4.97			1287	0.321×10^6	4.15	-20
JA-2	2.00	4.93			1287	0.306×10^6	4.11	-25
JA-3	2.00	5.02			1287	0.376×10^6	4.30	-9
JA-4	2.00	4.80			1287	0.321×10^6	4.28	-21
JA-5	2.00	5.00			1289	0.338×10^6	4.37	-16
JA-6	2.00	5.08	15.0	5	1288	0.396×10^6	4.32	-3
JA-7	2.00	5.00	15.0	5	1286	0.425×10^6	4.32	7
JA-8	2.00	5.00	15.0	5	1277	0.463×10^6	4.28	9
JA-9	2.00	5.05			1282	0.440×10^6	4.30	-6
JA-10	2.00	4.97			1281	0.440×10^6	4.30	-5
JA-11	2.00	7.65			1336	0.504×10^6	4.20	35
JA-12	2.00	8.10			1329	0.558×10^6	4.24	44
JA-13	2.00	8.05			1328	0.525×10^6	4.24	28
JA-14	2.00	8.05	15.0	5	1334	0.521×10^6	4.26	36
JA-15	2.00	8.01	15.0	5	1344	0.517×10^6	4.26	37
JA-16	2.00	8.00			1341	0.423×10^6	4.28	-5
JA-17	2.00	8.10			1335	0.517×10^6	4.28	26
JA-18	2.00	8.12			1334	0.442×10^6	4.28	-7

against the pump pressure head. In runs where test section pressure is maintained by valving, as the exit temperature from the test section approaches the saturation temperature, a self-pressurizing effect occurs requiring constant valve control. In runs J40, J41, J44, and J50, self-pressurizing could not be controlled and thus prevented the occurrences of boiling and the obtaining of meaningful data.

Recent in-loop calibration of thermocouples requires corrections to the previously reported data.*

---

*Runs B22 through B100 reported in NAA-SR-12492 ("Annual Technical Progress Report AEC Unclassified Programs, 1967"), and B101 through B170 and C1 through C34 reported in NAA-SR-12570 (op. cit.) should be corrected as follows:

1) Reported superheat values should be increased by
   - 5°F for runs at 2 psia
   - 7°F for runs at 5 psia
   - 9°F for runs at 8 psia
   - 10°F for runs at 10 psia
   - 11°F for runs at 12 psia

2) Inlet subcooling values should be decreased by

2 psia subcooling of 50	5°F
2 psia subcooling of 100	5.8°F
2 psia subcooling of 150	6.5°F
5 psia subcooling of 50	4°F
5 psia subcooling of 100	4.5°F
5 psia subcooling of 150	5°F
8 to 12 psia subcooling of 50	4°F
8 to 12 psia subcooling of 100	4°F
8 to 12 psia subcooling of 150	4°F

Also, run CA13 should have a bulk superheat of -23°F instead of 74°F.

2. Data Analysis

The maximum bulk liquid superheats measured for 2, 5, 8, and 12 psia are shown in Table 2. These four points, as plotted in Figure 1, demonstrate a strong pressure effect on the maximum obtainable bulk liquid superheat. The remainder of the data completely spans the envelope below these four points and some nominal negative value. It is interesting to note the wide range of parameters (heat flux, velocity, etc.) under which these values were obtained.

All of the experimental data to date tend to fall into four categories: (1) Little or no superheating is obtained when the heater surface has been attacked by the sodium, producing well-defined surface prominences and pits.* (2) Little or no superheating is obtained when the velocity is above 4 ft/sec. There are exceptions to this cut-off velocity concept,† however; for example the

TABLE 2

Run	Condenser (psia)	Test Section (psia)	Max Test Section (psia)	Time at Max Press. (min)	Inlet Temp (°F)	Heat Flux (Btu/hr/ft^2)	Flow (ft/sec)	Bulk Super-Heat (°F)
B11	1.91	1.91	1.91	N. A.	1249	370,000	3.35	109
B77	5.23	5.23	5.23	N. A.	1280	310,000	2.17	64
JA12*	2.00	8.10	8.10	N. A.	1329	558,000	4.24	44
C31	12.00	12.00	12.00	N. A.	1483	250,000	3.39	14

*Heater resurfaced with 600 grit abrasive.

maximum bulk superheat above 4 ft/sec at 2 psia is 24°F, 5 psia is 12°F, and at 8 psia it is 44° F. (3) A wide spread in superheating is obtained with a heater surface before it reaches the condition stated in Category 1 and when the velocity is below the condition stated in Category 2. The statistical distribution of the data with common pressure temperature histories approaches a bell-shaped curve. The upper values for common pressure-temperature

* Discussed NAA-SR-12570, op. cit.
† This velocity effect is discussed in NAA-SR-12492, op. cit.

histories* are in fairly good agreement with Holtz's (ANL-7184) pressure-temperature history theory except at high-pressure histories. (4) Maximum attainable superheats appear to exist at any given operating pressure regardless of operating pressure history, with a strong decreasing effect as operating pressure is increased (Figure 1).

B. HEATER DEVELOPMENT

A method has been developed for spring-loading the boron nitride sleeves to prevent gaps from occurring at the joints between sleeves. A gap as great as 0.2-in. can be obtained in a 30-in. heater due to thermal expansion differences between the boron nitride and the stainless steel sheath. This could have contributed to the failure of the two 30-in. heaters tested last quarter as they both failed at the upper sleeve joint. This spring-loading has been used in the 15-in. Heater J, which has been used in 69 tests and is still operable. The spring-loading was also used in a 30-in. heater tested during the quarter.

The cause of failure in the 30-in. heater tested this report period cannot readily be identified because of the large amount of damage which occurred when the heater arced through the Type HP boron nitride sleeve. As a result of this failure, further use of the dc power must be postponed until a method is devised to prevent the discharge of the stored energy from the filter capacitors in the dc power unit. This stored energy resulted in considerable damage when the 30-in. heater failed. The problem is not unsolvable as the stored energy may either be diverted through a shorting bar or left stored by rapid decoupling of the capacitors from the dc power unit.

A rhenium wafer has been used at the molybdenum-graphite interface in the last few heaters in order to suppress arcing and to prevent the formation of a brittle molybdenum-carbide joint. Examination of the failed 30-in. heater showed that the rhenium was metallurgically bonded to the molybdenum and appeared to make a molded contact with the graphite. It appears that the

---

* This category of data is extensively covered in "Quarterly Technical Progress Report AEC Unclassified Programs, October-December 1967," AI-AEC-12638.

molybdenum-graphite joint is improved by the rhenium wafer; however, none of the long-life heaters have failed or been cut apart to allow evaluation of long term effects.

C. THEORY: TRANSFUGUE IIa DEVELOPMENT

The TRANSFUGUE IIa topical report NAA-SR-12503 was published March 15, 1968. The report described TRANSFUGUE IIa, its use, and application to a sample problem.

The code has been modified to incorporate variable friction factors in the all-liquid and two-phase flow region and to include the capability to analyze the case where dry (superheated) vapor occurs. The dry vapor modifications are being debugged. In addition, the existing subroutines have been broken into smaller subroutines to facilitate the debugging process for this and future modifications.

D. THEORY: CONVERSION OF TWO-PHASE STEAM CODES TO USE WITH SODIUM

The transient, multichannel boiling sodium code, TRANSODIFAZE, has operated successfully and preliminary results indicate it is debugged. For a 3-channel test case, the steady-state results from this code (flow rate, quality, void fraction) compare well with the results previously obtained from the steady-state, multi-channel boiling sodium code, SODIFAZE.

COBRA,* the steady-state, multi-channel boiling water code, which includes cross flow mixing, has been checked out and has operated successfully on the IBM System 360, Model 50. This code will be converted to use with sodium and, in this form, will be called COBRANA.

---

* D. S. Rowe, "COBRA Computer Program for Coolant Boiling in Rod Arrays," BNWL-371, Pt. 1, March 1967.

IV. EVALUATION OF EFFORT TO DATE

Progress is considered satisfactory in both the experimental and analytical phase of the project.

Liquid superheat testing has substantially progressed, with testing including pressure-temperature history and heater surface effects. TRANSFUGUE IIa has been published in NAA-SR-12503, March 15, 1968. TRANSODIFAZE is operable and appears to be debugged. The boiling water code COBRA has been checked out and is ready for conversion to (COBRANA) use with sodium. The long-length high-heat flux heater development is slower than desired. Only one 30-in. heater was tested during this report period due to the sequential development required by budgetary reasons.

V. NEXT REPORT PERIOD ACTIVITIES

Additional liquid superheat testing will be performed. Emphasis will continue on defining the effect of heater surfaces on the maximum attainable superheats, and attempts will be made to study higher pressure effects by pressurizing the test section by valving against the pump pressure head.

TRANSFUGUE IIa with the dry (superheat) vapor modifications will be debugged and checked out. Additional modifications will be started to permit the flow to converge within a boiling node and to handle the case where there is departure from thermal equilibrium (liquid superheating and supersaturation).

Check out of the TRANSODIFAZE code will be completed.

Conversion of the boiling water code COBRA for use with sodium (COBRANA) will be started.

Heater development will be continued with testing proceeding of a shaped flux heater, and of thicker boron nitride insulation of both types A and HP, and other development steps as permitted within the budget.

Program: Liquid Metal Fast Breeder Reactor Technology
AEC Task: Sodium Reactor Experiment
Project Manager: C. W. Wheelock
Reporting Period: January-March 1968
General Order: 7704 AEC Category: 04-01-61-07.3

Project Engineer: W. C. Sturtevant
Principal Investigator: R. W. Woodruff

I. PROJECT OBJECTIVES

In April 1967, a plan, TI-599-19-001, was approved for the deactivation of the SRE facility to a "stored-in-place" condition so that components would not be damaged and costs would be minimized during an undefined period of storage.

In September 1967, direction was received to prepare plans to dispose of the plant, render the site safe from hazards, protect equipment until transferred, and dispose of unsalvageable scrap. Components are to be made available to other AEC programs, with priority to LMEC, FFTF, EBR II, ZPPR, and AARR.

II. MAJOR ACCOMPLISHMENTS IN FISCAL YEAR 1968

Four alternate plans for plant disposition were prepared and submitted as Engineering Document TI-599-19-101. Later, a less extensive plan was written and submitted to AEC on November 17, 1967. This plan, described in TI-599-19-003, defines the activities and schedule for deactivating the SRE so that its final disposal can be carried out at a later date. This plan was approved and deactivation is in progress.

The sodium heat transfer systems were drained. The reactor and all sodium systems were cooled to ambient temperature, and shift operations were terminated. Deactivation of the kerosene cooling systems, inert gas systems, hot cells, component handling machines, core components, and R/A liquid waste system was completed, and responsibility for surveillance of these systems was transferred from Nuclear Operations to Facilities and Industrial Engineering (F & IE).

III. PROGRESS DURING REPORT PERIOD

The inert gas systems were prepared for plant deactivation as required in procedure PR-599-69-001. Responsibility for the systems was transferred from the Nuclear Operations Department to Facilities and Industrial Engineering by executing the transfer agreement in Specification SS599N69001.

The two SRE inert gas systems normally supply helium to the sodium systems and nitrogen to the kerosene systems and sodium vaults. Both systems will remain in service to provide cover gas for the sodium and kerosene systems. Corrosion in these systems will thus be limited. To reduce the cost of makeup gas, the helium system was converted to nitrogen. NaK bubblers were installed in series in the inert system supply line to remove trace amounts of oxygen and water from the supply gas and minimize corrosion damage to the sodium systems during an extended period of storage (under the "stored-in-place" objective). Until January, the bubblers functioned normally. Plugging then occurred intermittently in the upstream unit. This continued until the sparger holes were cleared by heating the bubbler to ~180°F and rapping it sharply with a mallet. Because plant restart capability is no longer a requirement, it has been recommended that the bubblers be removed from service in order to reduce surveillance costs.

With two exceptions, deactivation of the R/A liquid waste system was completed as required in procedure PR-599-63-001. The sanitary R/A liquid waste tank will not be deactivated until all contaminated work is completed. The excavation to the obsolete R/A liquid waste tanks will not be filled until it is determined if additional work is required on the buried R/A piping. A summary of the status was submitted by letter to the AEC. Responsibility for the R/A liquid waste system was transferred to F&IE by executing the transfer agreement in specification SS599N63001.

In deactivating the R/A liquid waste system, the fuel wash cells were flushed with a solution of sodium dichromate. This was done to inhibit corrosion in the black iron portions of the system. The R/A sump tanks were then drained and the liquid was shipped for disposal.

The system for treating the wash cell effluent contained fission and activated corrosion products, resulting in radiation levels ranging from 40 to 100 mr/hr at the exterior of the piping and components. This source of contamination was easily removed because the system was constructed as a package on a steel pallet. Unions connecting the system to the R/A liquid and gaseous waste system, kerosene system, and the water and steam supplies were disconnected. The pallet was lifted from the trench. After capping all lines, the system was boxed and shipped for disposal.

Most of the work required to deactivate the hot cell, component handling machines, and core components was completed last quarter. Transfer of responsibility to F&IE was formalized by signature of the transfer agreements in the appropriate specifications.

Deactivation of the R/A gaseous waste system, sodium systems, and contaminated support facilities is essentially complete.

Procedure PR-599-28-001 was revised to require storage of unirradiated SRE fuel in the new fuel storage building. Since all irradiated fuel has been removed from SRE, the radiation alarm system and the emergency diesel generator can be deactivated after unirradiated fuel is transferred. Specification SS599N70001 for the electrical system was revised to reflect this change and to reduce surveillance costs. The electrical procedure requirement now can be deleted because no active systems will remain in service.

Southern California Edison Company (SCE) provided the principal heat sink for SRE in the form of a 6 Mwe steam-electric plant. The AEC-owned portion of the main secondary sodium system was decoupled. SCE can now remove their equipment at their convenience. At SCE's request information on sodium handling and site renovation was provided for use in preparing specifications for this effort. The possibility of including the AEC-owned SIR steam generator in this package is being considered. Scrapping of the steam generator at least cost to the government may be accomplished in this way.

Equipment requested by AEC-RDT designated priority groups was deleted from the SRE inventory. It was then submitted by CPAO to other RDT contractors. Seventy-nine instruments requested by priority groups have been removed from control panels. Most of these instruments are recorders and temperature controllers.

A representative from FFTF, which is one of the priority groups, reviewed the secondary sodium pumps, auxiliary airblast heat exchanger, secondary fill and transfer tanks, and dehumidification (DH) systems. Their need for the pumps, airblast, and DH system freon units was verified. Plans were initiated for removal of the pumps and freon units.

A draft of NAA-SR-12572, "Retirement of SRE," was prepared. It includes the following summaries: (1) SRE description, (2) operating history, (3) deactivation and retirement plans, (4) pre-retirement action, (5) radiation and contamination survey, and (6) plant surveillance.

IV. EVALUATION OF EFFORT TO DATE

The work is essentially on schedule as required by the network for the retirement effort shown on page 8.0 of TI-599-19-003. Fuel storage is behind schedule because of problems in determining where and how it would be stored. Deactivation of R/A gaseous waste is ahead of schedule. As work has been completed, the number of people assigned to SRE has been reduced.

Instruments required for draining sodium from the primary fill tank have not been removed although they have been requested for use elsewhere. The radiation level at the surface of the tank insulation is 0.3 r/hr. Until the possibility of draining the 1000 ft^3 of sodium from the tank is eliminated from ultimate SRE retirement, this instrumentation and one of the two drain pumps should remain in place.

Removal of SCE equipment will not commence before June and may not be completed until the first quarter of calendar year 1969. Sodium handling assistance from AI will be needed by SCE during part of that period.

V. NEXT REPORT PERIOD ACTIVITIES

The approved retirement activities will be completed. However, removal of portions of the equipment and removal of the SCE equipment will not be completed until GFY 1969.

Program:	FBR Fuel Cladding and Structural Materials
AEC Task:	10A – Coolant Chemistry
Project Manager:	J. L. Ballif/J. J. Gill
Reporting Period:	January-March 1968
General Order: 7706	Subaccount: 29510 AEC Category: 04-01-61-01.1

Principal Investigator: E. W. Murbach

I. TASK OBJECTIVES

The task objectives are to,

1) Define, prepare, and manage a source of stock "systems quality" sodium for the program.

2) Develop sampling and transfer procedures for handling sodium without contamination.

3) Monitor the compositions of sodium and of gas atmospheres in use on all the tasks in this program. Provide a management system for insuring the use of proper procedures in sampling, transferring, and analyzing of sodium.

II. MAJOR ACCOMPLISHMENTS IN FISCAL YEAR 1968

Sodium meeting the specification requirements for impurity levels has continued to be dispensed for use on the program. A calibrated electrode for the oxygen meter was installed in the sodium supply loop. This electrode is quite stable and responds rapidly to changes in oxygen level. The temperature coefficient of the electrode was determined to be 0.5 mv/°F.

III. PROGRESS DURING REPORT PERIOD

Dispensing of sodium was continued on an as-needed basis. Six retorts were loaded for biaxial testing and three were loaded for uniaxial testing during the report period. Sodium was also dispensed to the Sodium Chemistry Project for use in preparing samples for the spark source mass spectrometer.

Routine sampling of the retorts and loops was continued. Nine retort samples were taken this quarter. The oxygen analyses were mostly between 10 to 20 ppm, which is higher than obtained earlier. It is believed that a problem has developed in the oxygen technique. The purification train for the dry box was regenerated, which should have eliminated one problem.

Analysis of the sample of sodium taken from the supply loop during the oxygen addition experiment (reported in the previous quarterly) gave 5 ppm oxygen, which represents no increase. The oxygen meter reading decreased 40 mv and the plugging temperature increased to 325°F, so there was a marked change in oxygen content of the sodium. Therefore, the chemical analysis must have been in error.

To further evaluate the electrode, the loop was operated at different temperatures to determine the temperature coefficient of the electrode. The results are given in Table 1. The first and last rows show normal operating conditions with the electrode temperature, "T", running a little higher than the nominal loop temperature. The other data are arranged in chronological order.

TABLE 1

OXYGEN METER READING VERSUS VARIOUS TEMPERATURES AROUND SUPPLY LOOP

Temperature (°F)				emf
"T"	Fins	Pump	Tank	Volts
520	169	490	497	1.117
571	169	524	530	1.134
551	169	520	522	1.132
575	169	521	530	1.135
575	169	568	569	1.155
552	169	547	550	1.146
527	170	520	521	1.131
514	170	498	505	1.119

The location for the thermocoupler for the other temperature in the table are: Fins are on the meter housing, Pump is about 5 feet upstream, and Tank about 5 feet downstream from the electrode. As can be observed, the meter readings are more responsive to the loop temperature than to the temperature at the electrode. No immediate explanation for this behavior is available; however, the equilibrium in the oxygen-sodium stainless steel system must be involved. Under the conditions of this experiment, the temperature coefficient of the electrode is 0.5 mv/°F, when compared to loop temperatures.

The gas chromatograph to monitor helium purity for Sub-task C has been set up. A tank of high purity helium has been ordered to be used as the carrier gas.

The topical report, "Sampling Blanks for the LMFBR Cladding Program," NAA-SR-12616, was issued.

The draft of a topical report on evaluation of the electrochemical oxygen meter was written and is currently undergoing revision.

IV. EVALUATION OF EFFORT TO DATE

Dispensing and sampling of sodium proceed as before on a routine basis. The mercury amalgamation procedure for the determination of oxygen continues to present minor problems. In particular, the method does not appear adequate for the less than 5 ppm oxygen level. The supply loop probably operates with 1 to 2 ppm oxygen in the sodium.

The latest experiment with the oxygen meter provided puzzling results. Besides the apparent anomaly in the dependence of the temperature coefficient on loop temperature, the temperature coefficient under saturated conditions (unit activity of sodium oxide, or oxygen) should be negative.

V. NEXT REPORT PERIOD ACTIVITIES

Routine activities of dispensing and sampling sodium will continue. The topical report on the oxygen meter will be completed.

THIS PAGE

WAS INTENTIONALLY

LEFT BLANK

Program:	FBR Fuel Cladding & Structural Materials
AEC Task:	10B — Materials Management
Project Manager:	J. L. Ballif/J. J. Gill
Reporting Period:	January-March 1968
General Order: 7706	Subaccount: 29520 AEC Category: 04-01-61-01.1

Principal Investigator: D. F. Atkins

I. PROJECT OBJECTIVES

The objectives of this task are:

1) To procure and characterize a supply of the selected material required by the program (304 SS, 316 SS, Incoloy-800, and Inconel-625).

2) To manage, store and issue to authorized persons, the supply of selected material.

II. MAJOR ACCOMPLISHMENTS IN FISCAL YEAR 1968

Annealed 304 SS tubing and annealed 316 SS tubing have been added to the supply of characterized, as-received tubing of reference heats of 304 SS and 316 SS. This annealed material will be used for comparison with the as-received material containing 10 to 15% cold work.

The reference heat of Incoloy-800 was fabricated into six sizes of thin-walled seamless tubing to meet requirements of the Program. This heat has a lower-than-nominal aluminum and titanium content. A quantity of tubing from another heat of nominal commercial composition was purchased so that the low Ti + Al content can be evaluated.

III. PROGRESS DURING REPORT PERIOD

The reference heat of Incoloy-800 (0.01% Al and 0.20% Ti) has been fabricated into thin-walled tubing to meet the requirements of the Program. The size and quantity of this tubing is tabulated below.

Item	Size (in.)	Amount Ordered (ft)	Amount Received (ft)
1	0.275 ID x 0.010 wall	500	474
2	0.275 ID x 0.020 wall	200	149
3	0.315 ID x 0.020 wall	100	101
4	0.210 OD x 0.008 wall	400	213
5	0.145 ID x 0.035 wall	50	57
6	0.230 ID x 0.010 wall	50	56

This tubing has been received and has undergone inspection and acceptance tests. The fine grain structure on the surfaces of Items 2 and 4 was successfully removed by chemical milling, and these items now meet specification.

The purchase of 460-ft of Incoloy-800 pressure tubing (0.126-in od x 0.063-in. id) has been received for stress rupture retort fabrication. This tubing was made from a heat which was representative of a nominal Incoloy-800 composition (0.40 Ti and 0.36 Al). From this heat, about 70-ft of tubing, 0.275 in. ID x 0.010 in. wall, from the original order of 200-ft, was received for stress rupture test specimens. A reorder for the balance of this tubing will have to be from another heat.

Characterized tubing (190-ft, 0.210-in. OD x 0.008 in. wall) of reference heat 316 SS was issued to Battelle Northwest Laboratories for development studies. A short length of tubing from both the 304 SS and 316 SS reference heats was supplied to Brookhaven National Laboratory for heat transfer studies in sodium.

IV. EVALUATION OF EFFORT TO DATE

The low titanium and aluminum content (0.10% Al and 0.20% Ti) of the reference heat of Incoloy-800 must be studied to determine the importance of these elements on mechanical behavior and fabrication processes. This feature must be resolved before an extensive mechanical testing program can be started on the tubing of this heat.

V. NEXT REPORT PERIOD ACTIVITIES

All activities, except routine release of 304 SS and 316 SS tubing from controlled storage for use on other subtasks, have been completed for the present time. Characterization of the Incoloy-800 tubing will not be carried out since this material has been deleted from the GFY 1968 test program.

Program: FBR Fuel Cladding and Structural Materials
AEC Task: 10-C – Mechanical Properties
Project Manager: J. L. Ballif/J. J. Gill
Reporting Period: January-March 1968
General Order: 7706 Subaccount: 29530 AEC Category: 04-01-61-01.1

Principal Investigator: D. F. Atkins

I. PROJECT OBJECTIVES

The objectives are to determine the individual and combined effects of environment (sodium and helium), strain rate (10^{-7} to 10^{-3}/hr) and stress condition (uniaxial and biaxial) on the creep, stress rupture, and fatigue characteristics of selected cladding alloys. The alloys selected for study will be those which have greatest potential for fast reactor applications.

II. MAJOR ACCOMPLISHMENTS IN FISCAL YEAR 1968

Scoping tests to provide early biaxial stress rupture information on the behavior of 304 SS and 316 SS in system quality sodium have been completed. These tests define the 100 to 1000-hr stress rupture properties at temperatures of 1000 to 1400°F and provide data to select appropriate stress levels for long-term tests. These tests also served to study the influence of cold work and decarburization (by the action of a zirconium getter in the sodium) on the stress-rupture properties of the alloys.

Studies have been completed on the effect of copper-contaminated sodium on the biaxial stress-rupture behavior of 304 SS at 950 and 1100°F. No detrimental effect of Cu in sodium was observed under exposures up to 1000 hours at 1100°F.

Creep/stress rupture studies on sheet stock of the reference 304 SS heat have been completed. Specimens in the annealed condition, and with two levels of cold work, were tested in the uniaxial tensile mode in high purity static sodium. This work provided information on the effects of state-of-stress and cold work to complement the biaxial testing program.

TABLE 1

STATUS OF BIAXIAL STRESS-RUPTURE TESTS

Retort No.	Test Temperature (°F)	Alloy	Clad Condition*	Environment	Life Span Hrs	Status		Remarks	Date Start/Completed
						Test	Examination		
1	1300	304SS	AR	Na + Zr	100-700	Comp.	Comp.	Scoping Test	2-11-67/3-13
2	1400	304SS	AR	Na + Zr	100-400	Comp.	Comp.	Scoping Test	2-6-67/2-22
3	1400	304SS	AR	He	100-800	Comp.	Comp.	Effect of Sodium	3-18-67/4-21
4	1200	304SS	AR	Na + Zr	100-2600	Comp.	Comp.	Scoping Test	3-27-67/7-14
5	950	304SS	AR	Na + Cu	100-3000	Comp.	Comp.	Effect of Copper	4-21-67/9-18
6	1400	304SS	AR	Na	100-900	Comp.	Comp.	Scoping Test	6-2-67/7-7
7	1100	304SS	AR	Na	100-3000	Comp.	Comp.	Scoping Test	6-9-67/10-30
8	1400	304SS	Ann	Na	100-2000	Comp.	Comp.	Effect of Cold Work	6-15-67/9-12
9	1000	304SS	AR	Na	100-700	Comp.	Comp.	Scoping Test	8-12-67/9-11
10	1400	304SS	AR	Na	1000-3000	Comp.	Comp.	Extension of Data	8-10-67/12-18
11	1200	304SS	AR	Na	100-4000	Comp.	Comp.	Extension of Data	8-12-67/1-10-68
12	1100	304SS	AR	Na + Cu	100-700	Comp.	Comp.	Effect of Copper	8-18-67/9-18
13	1200	304SS	AR	He	100-5000	3/4 Comp.	-	Effect of Sodium	10-20-67
14	1200	304SS	AR + Aged	Na	100-1000	Comp.	-	Effect of Thermal Aging	11-2-67/3-6-68
15	1200	304SS	AR	Na	5000-10,000	In prog.	-	Extension of Data	11-9-67
16	1000	304SS	AR	Na	100-5000	3/4 Comp.	-	Extension of Data	11-22-67
17	1200	304SS	Ann	Na	5000-10,000	In prog.	-	Extension of Data	2-22-68
18	1200	304SS	Ann	Na	100-5000	3/4 Comp.	-	Effect of Cold Work	1-25-68
20	900	304SS	AR	Na	100-1000	1/2 Comp.	-	Scoping Test	12-1-67
21	1000	304SS	Ann	Na	100-5000	1/2 Comp.	-	Effect of Cold Work	2-15-68
22	1000	304SS	Ann	Na	5000-10,000	In prog.	-	Extension of Data	2-29-68
101	1400	316SS	AR	Na	100-1000	Comp.	Comp.	Scoping Test	8-10-67/9-21
102	1200	316SS	AR	Na	100-10,000	3/4 Comp.	-	Extension of Data	8-12-67
103	1000	316SS	AR	Na	100-1000	3/4 Comp.	-	ScopingTest	9-14-67
104	1400	316SS	AR	He	100-1600	Comp.	Comp.	Effect of Sodium	8-31-67/11-15
105	1400	316SS	Ann	Na	100-800	Comp.	Comp.	Effect of Cold Work	10-19-67/11-27
106	1200	316SS	Ann	Na	100-1000	Comp.	-	Effect of Cold Work	10-24-67/1-18-68
107	1000	316SS	Ann	Na	100-1000	Comp.	Comp.	Effect of Cold Work	12-6-67/1-8-68
108	1000	316SS	AR	He	100-1000	3/4 Comp.	-	Effect of Sodium	1-12-68
109	1200	316SS	AR	Na	100-1000	3/4 Comp.	-	Scoping Test	2-9-68

*AR = As-received tubing containing 10-15% cold work
Ann = Annealed tubing

III. PROGRESS DURING REPORT PERIOD

Biaxial stress rupture tests on tubing from the reference heats of 304 SS and 316 SS have continued in system-quality sodium. Four 12-specimen retorts of 304 SS and two 12-specimen retorts of 316 SS were placed on test under a biaxial (1/2:1) stress mode. This extends to 22 the total number of biaxial 12-specimen retorts placed on test during GFY 68 (264 specimens, 0.275-in. ID x 0.010-in. wall). Uniaxial stress rupture tests on 20 sheet specimens (0.062 in.) of 304 SS in sodium were completed. These specimens, representing annealed, 11% cold work and 38% cold work, were tested to provide further insight into cold work and state-of-stress effects. A summary and status of all the biaxial retorts assembled on this program is given in Table 1. Table 2 lists the uniaxial tests and the creep of stress-rupture results.

A. TYPE 304 SS

Diametral strain measurements taken on 24 specimens of 304 SS tubing, biaxially stress-rupture tested in 1400°F high purity sodium, are shown in Figure 1. This tubing contained 10 to 15% cold work, introduced during the final drawing operation in tubing manufacture. The strain data, although somewhat scattered, exhibit a definite trend to increase with increasing rupture time (lower stress). This behavior is attributed to recovery effects of the cold-worked specimens as the test time at 1400°F increased. Annealed specimens of the same alloy heat are plotted for comparison. Since the annealed and cold-worked specimens approach a common value, it would seem that the cold-work effects disappear in about 2500 hours at 1400°F. A similar convergent behavior of strain to a common value for annealed and cold-worked M-316 SS has also been reported.*

Metallographic examination of the cold-worked 304 SS specimens tested in 1400°F sodium for 3000 hours revealed the normal intergranular fracture with

---

* H. K. Richardson and R. McDowell, "Elevated Temperature Stress Rupture Properties of M316, FV548, and Nimonic PE16 P. F. R. -Type Tube," TRG Report 1482(c), 1967.

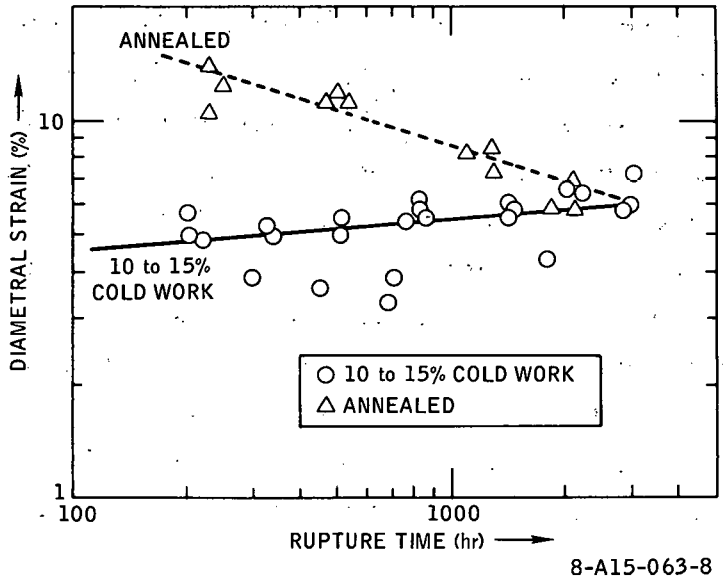

Figure 1. Strain Variation with Rupture Time for 304 SS in 1400°F Na

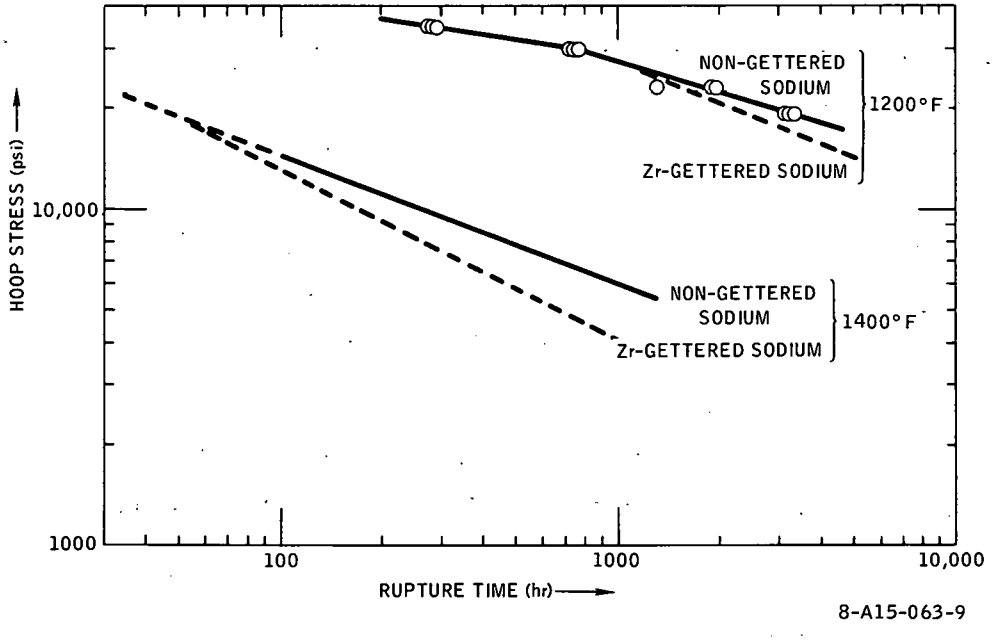

Figure 2. Reduction of Stress Rupture Properties of 304 SS Tubing (10-15% cold-worked) due to Zr in the Na

TABLE 2

STATUS OF UNIAXIAL STRESS-RUPTURE TEST OF 304SS SHEET IN 1200° F SODIUM

Sample No.	Sample Condition	Stress, psi	Rupture Time, hrs	Elongation, %	Steady-State Creep Rate in/in/hr
8A	Anneal	30,000	143*	44	1.15×10^{-3}
9A	Anneal	30,000	55	17	1.27×10^{-3}
12A	Anneal	30,000	69	-	-
4A	Anneal	25,000	421	40	2.4×10^{-4}
5A	Anneal	25,000	388†	33	3.4×10^{-4}
11A	Anneal	25,000	383	41.5	2.76×10^{-4}
6A	Anneal	21,000	1233	29	8.0×10^{-5}
7A	Anneal	21,000	1253	29	6.3×10^{-5}
1C3	38% Cold Work	35,000	46	3	2.9×10^{-4}
2C3	38% Cold Work	35,000	47	3	1.9×10^{-4}
3C3	38% Cold Work	30,000	66	3.5	1.9×10^{-4}
4C3	38% Cold Work	30,000	72	3	2.3×10^{-4}
5C3	38% Cold Work	20,000	187	6.5	1.2×10^{-4}
6C3	38% Cold Work	20,000	147	6	1.64×10^{-4}
2C1	11% Cold Work	39,000	Discontinued§	-	-
1C1	11% Cold Work	39,000	47	15	8.6×10^{-4}
4C1	11% Cold Work	35,000	105.6	10	2.0×10^{-4}
5C1	11% Cold Work	35,000	93	13	3.8×10^{-4}
3C1	11% Cold Work	27,000	1290	7	2.0×10^{-5}
7C1	11% Cold Work	27,000	897	11.5	-

NOTES: *Specimen aged in 1200° F Na without load for 120 hrs due to furnace controller problem
†Specimen failed at gage mark
§Test discontinued due to furnace controller problem

a large amount of r-type grain boundary voids. Normal carbide precipitation and morphology were observed on slip bands and grain and twin boundaries. Large amounts of sigma particles (~5%) of relatively large size, when compared to the short-term (1000-hr) stress-rupture specimens tested at the same temperature, were found randomly across the tubing wall. This increase in sigma particle density and size due to the increase in test time is in accord with the particle nucleation and growth processes as controlled by diffusion.

A biaxial stress-rupture scoping test on the reference heat 304 SS (as-received condition with 10 to 15% cold-work) in 1200°F system quality sodium has been completed. The results are plotted in Figure 2 and are compared with some early test results where zirconium foil was used in the sodium for oxygen-gettering purposes. The reduction in stress-rupture strength due to the presence of zirconium in 1400°F sodium was also observed at 1200°F. Decarburization of the stainless steel tubing by the zirconium foil in sodium was the cause of this weakening effect.

Visual examination of the tubing stress-rupture tested in the zirconium-free 1200°F sodium revealed the normal clean and metallic bright tubing. Three of the tubular specimens exhibited explosive type ruptures. One of the specimens had collapsed after rupture — most probably due to the shock-wave generated by subsequent specimen fractures. This rupture behavior has been observed on previous tests at 950, 1000, and 1100°F in sodium. This type of damage to ruptured tubing has been minimized by use of solid inserts, decreasing the volume of pressurizing gas inside the specimens.

The total exposure time for these specimens in 1200°F sodium was about 3500 hours. The microstructure exhibited large amounts of carbides on slip bands within the grains and in grain boundaries. A slight amount of sigma phase (~1%) was also found randomly scattered in grain boundaries. All ruptured specimens exhibited intergranular fracture with some internal fissures.

To determine the effect of thermal aging on the stress rupture behavior of 10 to 15% cold-worked 304 SS tubing, twelve specimens were soaked in 1200°F sodium for 2000 hours without stress. The specimens were then biaxially stressed to provide rupture over 100 to 1000 hours. The results, plotted in Figure 3, indicate that there is little change in stress rupture strength as a

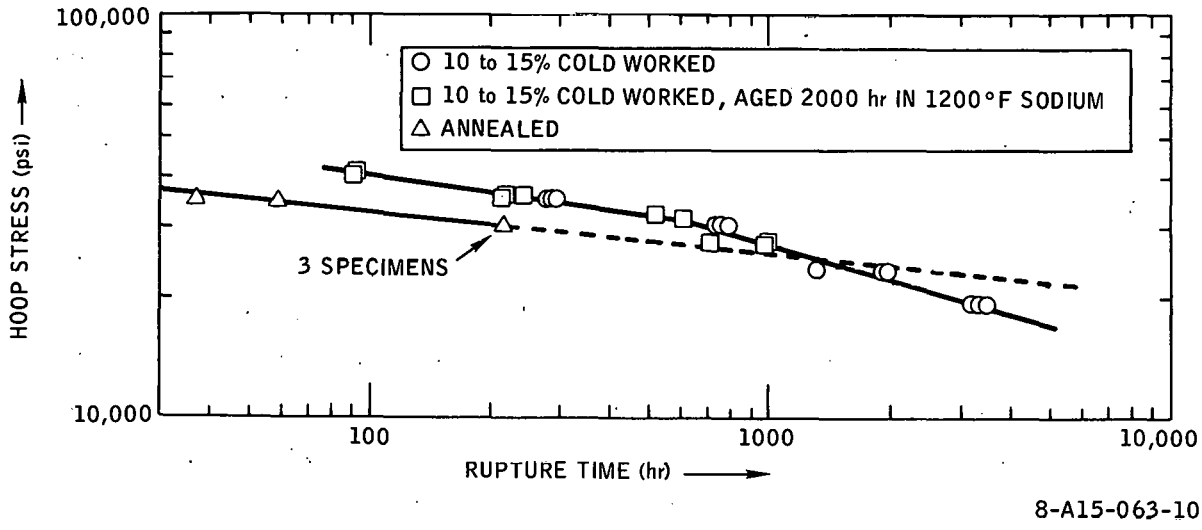

Figure 3. Biaxial Stress Rupture Properties of 304 SS in 1200°F Na

consequence of the thermal aging step. Apparently the temperature-time combination was not sufficient to effect any significant recovery processes in the cold-worked tubing. On disassembly of the test retort, it was found that all but three specimens had ruptured in an explosive manner. Compared with other tests at 1200°F, it appears that the aging treatment enhanced the mechanism which causes the explosive type ruptures.

Specimens of as-received 304 SS (10 to 15% cold-work) tested in 1100°F sodium were examined metallographically. Fractures were intergranular, with fissuring along grain boundaries in areas away from the fracture. Carbide precipitation along grain boundaries, along twin boundaries, and on slip bands within grains was observed. A very thin and continuous second-phase layer (~0.1 mil) was also detected on the surfaces of tubing exposed to sodium. Metallographic techniques identified the layer as ferrite, and subsequent x-ray diffraction confirmed the presence of ferrite on the OD surfaces of the tubing. A weak indication of ferrite on the ID of the tubing (exposed to helium gas) was also found by x-ray. Since this ferrite layer developed in static sodium, its origin is rather uncertain at this time. Due to the thinness of the layer, it is possible that the layer might be due to a leaching effect by the sodium at 1100°F. Another strong possibility is that the layer is a direct consequence of inhomogeneous cold-working of the tubing during fabrication, since the ID and, particularly the OD of tubing could conceivably have received higher deformation. Microstructural studies employing selective etching techniques failed to detect any sigma phase in the tubing.

Four biaxial 12-specimen retorts of annealed 304 SS tubing were placed on test during this period. These 48 specimens, all in high purity sodium at 1200 and 1000°F, possess stress levels which will give ruptures over the range of 100 to 10,000 hours.

To further study the effect of copper-contaminated sodium on the stress rupture behavior of 304 SS, a biaxial test retort has been assembled which contains four copper-plated stress rupture specimens, eight non-plated stress rupture specimens, four Charpy impact samples and two pure copper corrosion tabs. The retort has been loaded with high-purity sodium and is ready to be placed on test at 1300°F. This work will complement the previous tests at 950 and 1100°F.

Uniaxial creep rupture tests on 304 SS sheet stock (0.062-in., reference heat) have been completed. The specimens in the O (annealed), 11% and 38% cold worked condition were tested to provide further information on cold-work effects. As with the biaxial tests, the cold-worked specimens exhibited a steeper stress-rupture slope. All tests were conducted in 1200°F sodium. The results are summarized in Table 2.

In actual fuel element performance, the cladding may be subjected to simultaneous hoop and axial stresses in the latter stages of life. To simulate this condition, a test was devised using a tubular specimen internally pressurized with gas while under axial tension. Conditions were chosen such that the tension and hoop stresses were equal (1:1 biaxiality). Figure 4 shows a photograph of the test assembly. In the initial checkout test of this assembly, a 304 SS specimen was subjected to 30,000 psi stress in both the tensile and hoop directions. Although the test retort was designed for testing in sodium, helium was used in this initial test. After 165 hours under test, a failure was detected by loss of internal gas pressure. This rupture life was considerably shorter than predicted from individual stresses due to either applied gas pressure or axial load. On disassembly, the fracture was found in the heat-affected zone of one of the end-plug welds. The use of a longer specimen is now being considered to extend the end plugs into cooler regions of the retort.

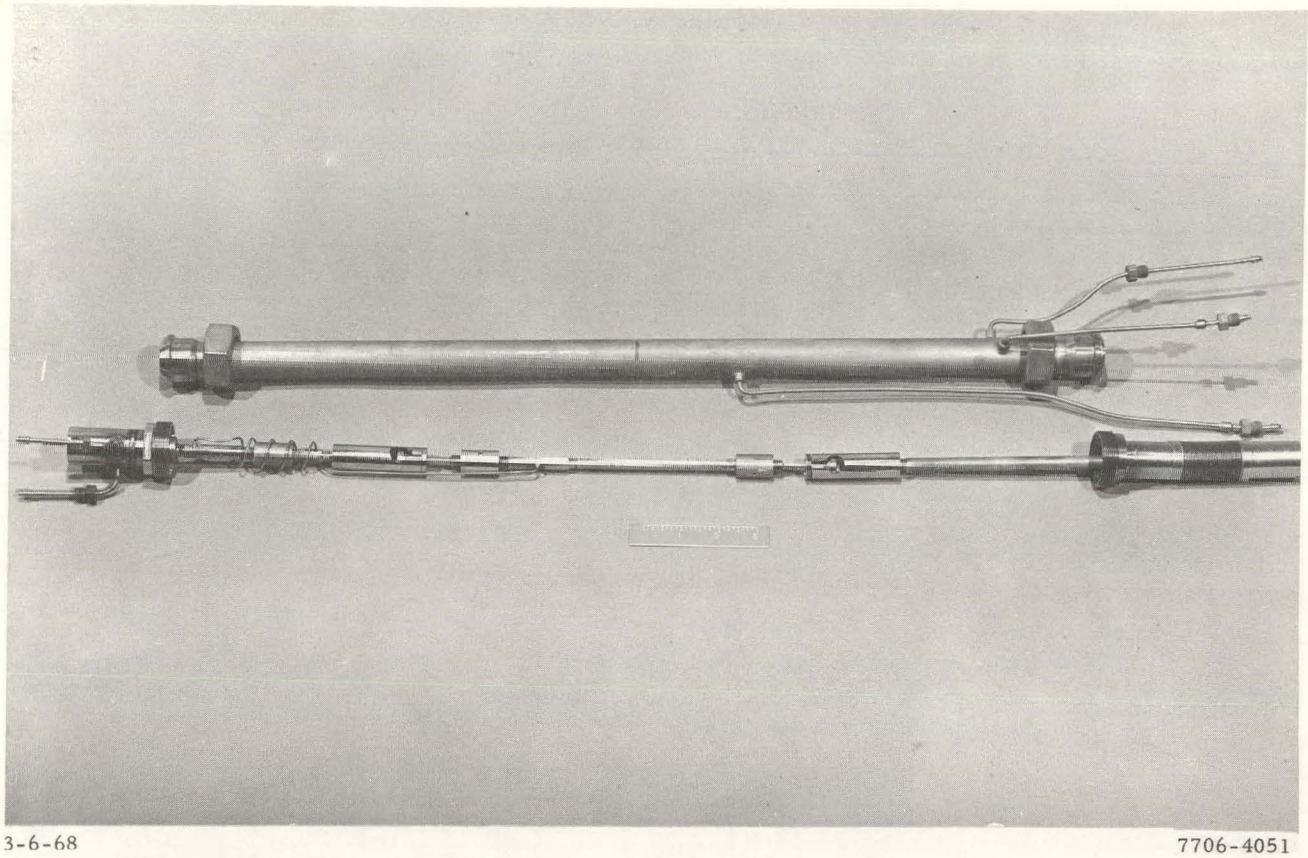

3-6-68 7706-4051

Figure 4. Test Assembly for 1:1 Biaxial Stress-Rupture Testing

B. TYPE 316 SS

The effect of annealing on the creep behavior of reference heat Type 316 SS tubing in 1400°F sodium is shown in Figure 5. Annealed 316 SS tubing has a higher strain rate at a given stress than the cold-worked (10 to 15%) 316 SS tubing. It is interesting to note that annealed 316 SS has a comparable strain rate to annealed 304 SS tubing. However, the rupture strain of the annealed 316 SS tubing was found to be almost double that of annealed 304 SS in 1400°F sodium. Metallographic examination of the annealed 316 SS tubing tested in 1400°F sodium revealed very little intergranular voids or cracks. Grain deformation was observed, particularly at the rupture area. The specimens exhibited carbide precipitation within the grains and along grain boundaries; little or no sigma precipitation was observed in the specimens tested in 1400°F sodium for 740 hours.

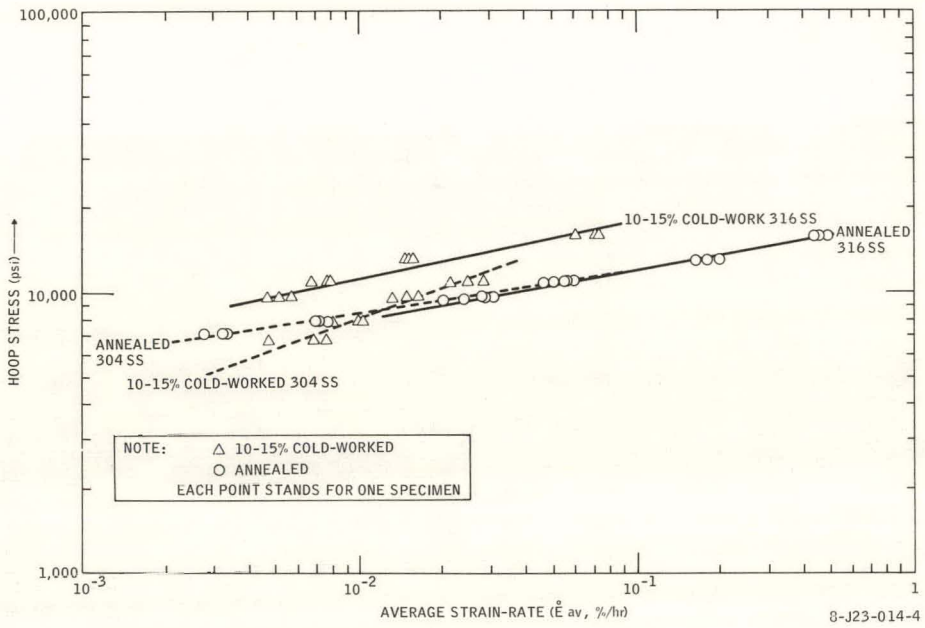

Figure 5. Strain Rate Behavior of 304 SS and 316 SS in 1400°F Sodium

Microstructural comparison of the annealed and cold-worked specimens of 316 SS is shown in Figure 6. The large quantities of intergranular voids or cracks in the cold-worked samples are evident. The voids are attributed to the fact that cold-work enhances precipitation in the grain-matrix and possibly on grain boundaries. Grain matrix precipitation on slip lines and twin boundaries strengthens the grain, thus reducing the deformability of the grain. Furthermore, precipitation on grain boundaries tends to limit grain boundary migration. Both processes, coupled with strain-hardening due to dislocation tangle within the grains, reduce the ability of the material to relax stress concentrations. This is particularly important along grain boundaries because grain boundary sliding is a dominant deformation process at high temperatures and low strain-rate.

As-received 316 SS (10 to 15% cold-work) specimens stress-rupture-tested in 1400°F helium exhibited a similar microstructure to that of cold-worked 316 SS specimens tested in 1400°F sodium. This observation supports the previously-reported observation on 304 SS that the sodium environment has no effect on 1000-hr creep or rupture strength at 1400°F.

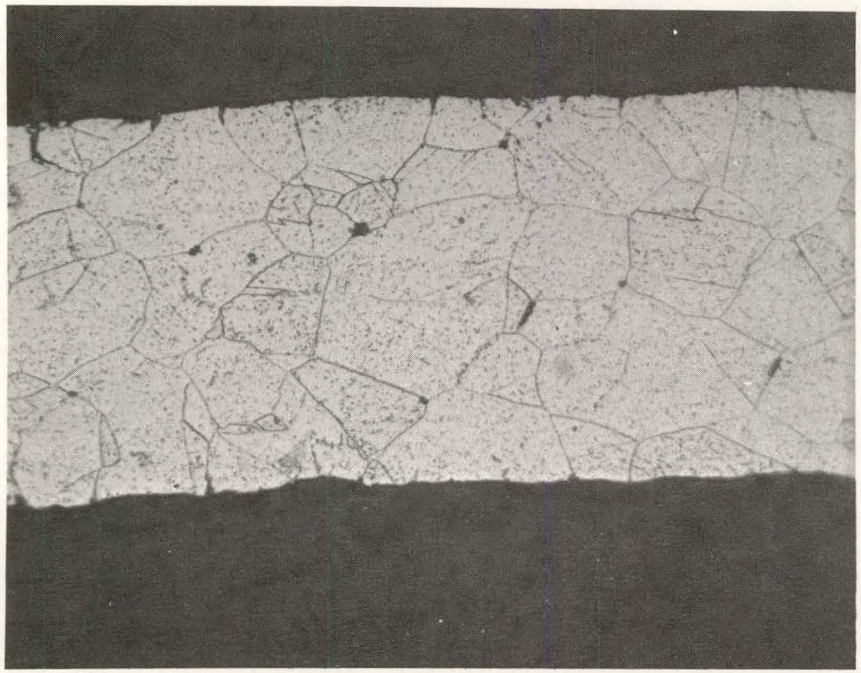

MARBLE ETCH 250X

ANNEALED

σ = 9600 psi, RUPTURE TIME = 731 hr ϵ = 19.5%

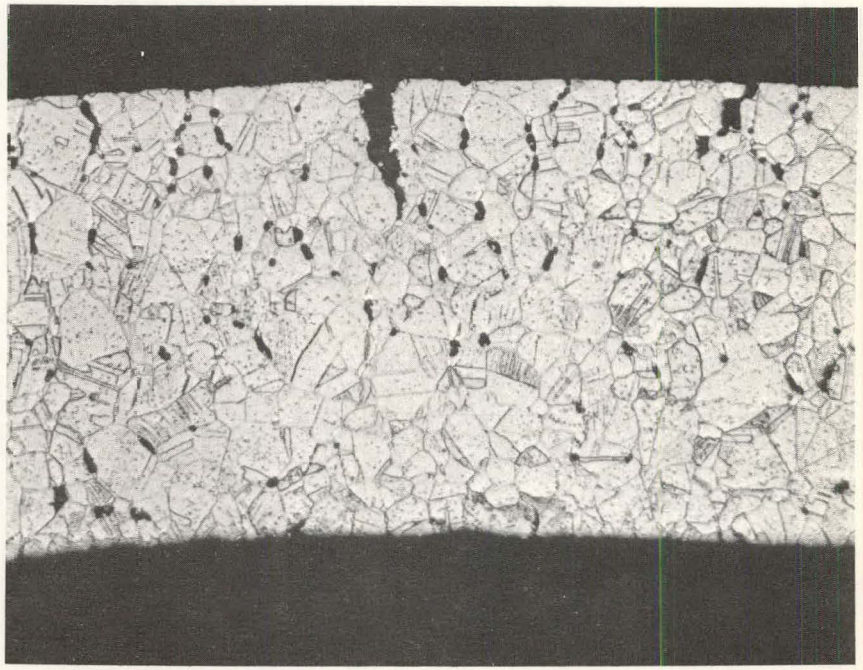

MARBLE ETCH 250X

10-15% COLD-WORK

σ = 13,000 psi, RUPTURE TIME = 405 hr ϵ = 6%

8-J23-014-10

Figure 6. Microstructure Comparison Between Cold Work and Annealed 316 SS Tested in 1400°F Sodium

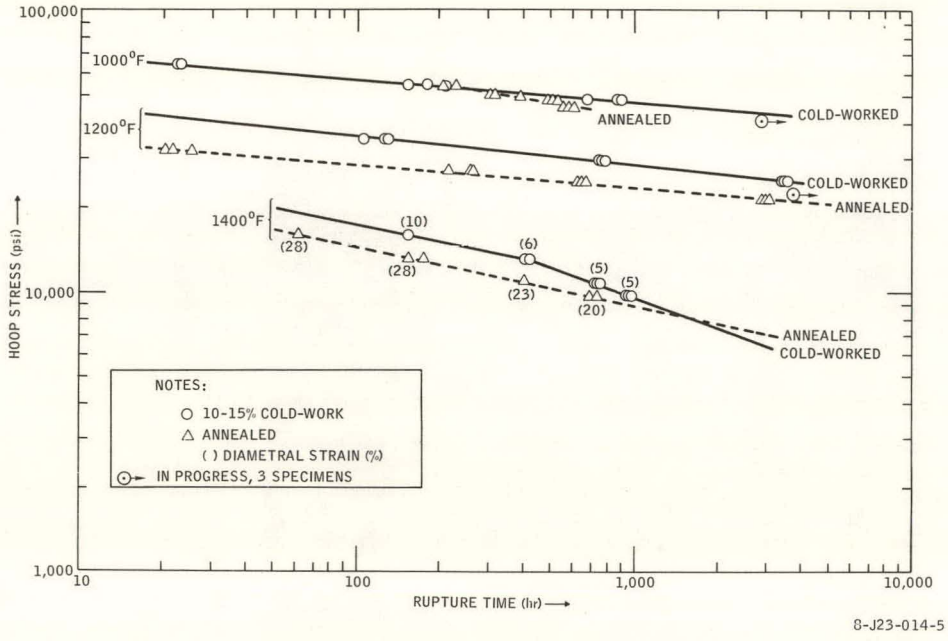

Figure 7. Effect of Annealing on the Stress-Rupture Properties of 316 SS

A biaxial stress-rupture test on annealed 316 SS tubing in 1200°F sodium has been completed. The results, shown in Figure 7 with other pertinent data for comparison, show that annealed tubing has lower stress-rupture strength than the cold-worked tubing when tested at 1200°F for up to 3100 hours. However, the slope of the curve for annealed material is less steep that that of the curve for 10 to 15% cold-worked material. This behavior is in accord with the previously reported data at 1400°F.

The biaxial stress rupture properties of annealed 316 SS in 1000°F sodium are also plotted in Figure 7. The annealed specimens have comparable stress-rupture strength to that of the 10 to 15% cold-worked 316 SS material. This behavior differs from the results obtained at 1200 and 1400°F. The cause for the deviation is uncertain at this time. Further tests of the annealed 316 SS tubing for a longer time (1000-10,000 hours) is expected to clarify the reasons for this behavior.

Before the start of the biaxial test at 1000°F, the annealed 316 SS specimens were loaded with solid 316 SS plugs to reduce gas volume, with intent of limiting specimen damage by the explosive type ruptures. When the retort was

opened after testing, visual examination revealed that the specimens were not damaged as badly as previously found. No collapsed tubing was found, although some large rupture openings due to sudden yielding of the material still occurred. It is clear therefore, that the insertion of solid rods was effective in reducing the damage to the tubing from explosive force accompanying specimen rupture.

Two additional biaxial retorts have been placed on test. Specifically, a retort containing 12 as-received (10 to 15% cold-work) 316 SS tubing specimens in 1000°F high-purity helium is on test to obtain rupture lives within 1000 hours. This is to study the effect of sodium environment at 1000°F. Another retort with 12 annealed 304 SS specimen has been filled with sodium. Four stress levels will be applied to produce ruptures within 5000 hours in 1200°F sodium.

IV. EVALUATION OF EFFORT TO DATE

The multiple specimen biaxial stress-rupture testing concept continues to produce accurate, consistent data with a high statistical confidence. The static sodium is sampled several times during each test and the ability to maintain a high-purity sodium environment for the test specimens has been demonstrated.

The presence of a thin ferritic layer on the surface of cold-worked 304 SS tubing which was tested in 1100 and 1000°F sodium was unexpected. On similar tests at 1200 and 1400°F, such a layer was not found. However, sigma-phase was found at 1200 and 1400°F, whereas, at lower temperatures, this phase was absent. The evidence suggests that ferrite, formed by transformation of austenite due to cold-work, is stable at 1100°F and below. At higher temperatures, the ferrite in the alloy promotes sigma formation. In annealed tubing, sigma-phase was not found in 1200 and 1400°F stress rupture specimens.

V. NEXT REPORT PERIOD ACTIVITIES

Biaxial stress rupture testing (1/2:1) will be continued on the long-term (to 10,000 hr) tests on both 304 SS and 316 SS. Five new 12-specimen retorts will be assembled and placed on test. This will complete the test matrix which was specified for this fiscal year. These final retorts will include one 304 SS test and four 316 SS tests. Scoping tests on Incoloy 800 were originally scheduled, but these retorts have been diverted to 316 SS tests to provide additional

low temperature data (900°F) in the range of the FFTF Program interest. These retorts are included in the four 316 SS retorts mentioned above.

The biaxial retort containing copper-contaminated sodium will be tested at 1300°F and the stress rupture results evaluated. Charpy impact specimens, which are also included in the retort, will be tested.

Microstructural studies on specimens will be conducted as tests are completed. These studies will reveal further information on cold-work effects, stress-induced reactions and fracture modes.

Modification to the 1:1 biaxial test assembly will be made to lower the temperature in the region of the specimen end plugs. The use of a longer specimen will be the initial approach.

Program: FBR Fuel Cladding and Structural Materials
AEC Task: 10D-1 – Dynamic Loop Operation
Project Manager: J. L. Ballif/J. J. Gill
Reporting Period: January-March 1968
General Order: 7706 Subaccount: 29541 AEC Category: 04-01-61-01.1

Principal Investigator: D. K. Darley

I. PROJECT OBJECTIVES

The objective of this project is to operate and maintain the 2-in. sodium loop facility in support of activities under S/A 29542 and 29543.

II. MAJOR ACCOMPLISHMENTS IN FISCAL YEAR 1968

The 2-in. dynamic loop has operated satisfactorily at 1200°F for testing of clad specimens and high-flux heater development. Four series of tests have been completed. High-flux heater life in excess of 1,000 hours has been demonstrated.

III. PROGRESS DURING REPORT PERIOD

The stress-rupture test series of five clad heaters, initiated during the last quarter, was terminated when the last cladding ruptured. The test status at the time of completion is tabulated below:

Heater No.	Time at Test (hr)	Cladding Pressurized (Time-hr)	Hr at Temperature >1000°F	Heater Hr	Operation Cycles	Cladding Remarks
40	172.4	172.6	193.8	86.3	865	Ruptured
42	134.0	134.0	163.5	67.0	4026	Ruptured
44	163.2	163.2	187.5	81.6	4902	Ruptured
46	384.6	398.5	499.5	192.3	1925	Ruptured
48	392.8	418.8	499.5	196.5	1961	Ruptured

NOTE: Heaters #42 and 44 were programmed for 2-minute cycles and Heaters #40, 46 and 48 were on 12-minute cycles.

All five high-flux heaters were in operating condition at the time cladding failures occurred. The five test assemblies were removed from the 2-in. test loop for examination. The cladding was removed from Heaters 40, 42, 44, and 48, and the bare high flux heaters were reinstalled in the 2-in. test loop for additional heater life testing. The cladding was removed from heater No. 46 and the high flux heater was disassembled for examination and analysis.

Another clad heater (Heater 50) was installed in the loop with the four bare heaters to measure mass transfer rates under conditions simulating those of the fuel cladding in a fast reactor. Prior to being assembled on the heater the cladding was irradiated in a reactor to allow use of an activation analysis technique to determine the amount of metal removal. This test was terminated after 182 hours because of a heater failure. Two of the bare heaters also failed due to shorts during this run. The test status at the end of this run is shown in the following table.

Heater No.	Time at Test Cond. (hr)	Cladding Pressurized (Time-hr)	Hr at Temperature >1000°F	Heater Operation		Heater Remarks
				Hr	Cycles	
40	238.0	0	240.7	238.0	0	Shut-down
42	109.4	0	112.1	54.7	3282	Failed - Short
44	148.7	0	151.4	148.7	0	Failed - Short
48	237.7	0	240.4	118.8	1195	Shut down
50	181.5	181.5	184.2	181.5	0	Failed - Short

NOTE: Heater 42 was programmed for a 2-min cycle, Heater 48 a 12-min cycle, and Heaters 44 and 40 were operated at steady-state conditions; heaters were not covered with cladding.

The last test run in the loop prior to shutdown was made with a second irradiated clad heater (Heater 52). The two bare heaters that were operating satisfactorily at the termination of the previous run, Heaters 40 and 48, were also placed on test. The mass transfer test was terminated after 12 hours because of the heater failure. The bare heaters were operating satisfactorily when the loop was shut down after accumulating an additional 260 hours of testing. The following table summarizes the total operating history of the heaters that were operated during the last three test runs.

Heater No.	Hours at Test Cond. Cyclic	Steady State	Total	Hours Run with Cladding	Hours in >1000°F Na	Heater Operation Hours	Cycles	Shut-Down Condition
40	172.6**	497.6	670.2	172.6	697.6	583.9	865	Operating
42	243.4*	-	243.4	134.0	275.6	121.7	7308	Failed-Short
44	163.2*	148.7	311.9	163.2	338.9	230.3	4902	Failed-Short
46	384.6**	-	384.6	384.6	499.5	192.3	1925	Operating
48	890.1**	-	890.1	392.8	1003.0	445.0	4457	Operating

* 2 min. cycle: 1-min. power on, 1-min. power off
** 12 min. cycle: 6-min. power on, 6-min. power off

All heaters were removed from the loop and the loop was placed in a low temperature stand-by condition. The plugging temperature at the time of shut-down from 1200°F was <235°F.

IV. EVALUATION OF EFFORT TO DATE

The integrity, reliability and operation of the 2-in. dynamic loop for the purpose of testing fuel cladding material under simulated reactor operating conditions has met or exceeded project objectives as to schedule, availability and operating costs. The purity of the sodium in the loop has been verified by sodium sampling during periods of loop operation. The plugging temperature of the sodium has been maintained between 250 and 300°F by operation of the cold trap.

V. NEXT REPORT PERIOD ACTIVITIES

Since all planned tests have been completed, the test loop will remain in a stand-by condition until the end of the fiscal year.

THIS PAGE

WAS INTENTIONALLY

LEFT BLANK

Program: Fuel Cladding and Structural Materials		
AEC Task: 10-D-2 – Dynamic Loop Testing (Mechanical Properties)		
Project Manager: J. L. Ballif/J. J. Gill		
Reporting Period: January-March 1968		
General Order: 7706	Subaccount: 29542	AEC Category: 04-01-61-01.1

Principal Investigator: J. H. Shively

I. Project Objectives

The objectives of this program are listed below.

1) Test, evaluate, and demonstrate the performance capability of candidate fast reactor clad and structural materials in a dynamic sodium environment.

2) Determine the nature of combined effects of mass transfer, temperature, low-cycle thermal fatigue, and biaxial stresses on the stress-rupture and creep behavior of these alloys.

II. MAJOR ACCOMPLISHMENTS IN FISCAL YEAR 1968

Ten internally heated and pressurized clad assemblies, and four internally pressurized clad control assemblies, all immersed in dynamic sodium, were tested this year. On the basis of these tests, it was learned that thermal cycling reduced the life under stress but enhanced the creep rate. Steady heat flux, NaK and ferrite layer formation did not influence the life of these specimens. The stress-rupture behavior for a steady heat flux, or without internal heating, can be rationalized from the temperature-stress sensitivity of creep. On the other hand, cyclic operation of the heat flux cannot be explained using equations describing secondary creep.

III. PROGRESS DURING REPORT PERIOD

A. BACKGROUND

The combined effects of static biaxial stresses due to fuel swelling and fission gases and of steep thermal gradient due to internal heating on the

TABLE 1

STRESS-RUPTURE IN DYNAMIC SODIUM WITH INTERNAL HEATING

Specimen No.	Heat Flux (Btu/ft^2-hr)	Heat Flux Condition	Rupture Time (hr)	Mechanical Hoop Stress (psi)	Calculated Thermal Stress (psi)	Peak Strain (%)	Peak Strain Rate* (in/in/hr)	$\frac{\text{Actual Life}}{\text{Predicted Life}}$†
30	1×10^6	Steady	177	21,000	8,300	2.2	1.2×10^{-4}	.9
36	1×10^6	Steady	558	16,000	8,300	2.8	4.5×10^{-5}	1.1
34	1.5×10^6	12 min cycle	5§	21,000	12,400	3.6	-	-
38	1×10^6	12 min cycle	198§	16,000	8,300	1.0	1.1×10^{-4}	-
32	1×10^6	12 min cycle	227	21,000	8,300	3.6	3.2×10^{-4}	.57
40	1×10^6	12 min cycle	173	21,000	8,300	3.6	4.2×10^{-4}	.43
42	1×10^6	2 min cycle	134	21,000	8,300	3.6	5.4×10^{-4}	.33
44	1×10^6	2 min cycle	163	21,000	8,300	3.6	4.4×10^{-4}	.41
46	1×10^6	2 min cycle	398	17,700	8,300	3.6	1.8×10^{-4}	.55
48	1×10^6	2 min cycle	419	17,700	8,300	3.6	1.8×10^{-4}	.56

*Based on the time the heat flux is on
†Prediction is based on isothermal data obtained in static sodium
§Heater failed prior to cladding

stress-rupture life of fuel cladding comprise an important design consideration. In addition, thermal cycling as a result of daily reactor load variations may bring into play deformation mechanisms which enhance the creep rate and reduce the life of the cladding more than anticipated from conventional creep equations. While the idea has been the subject of considerable theoretical speculation, it has not been confirmed experimentally for conditions approaching those anticipated in fast reactors. The purpose of the work described below is to assess the influence of thermal cycling on the life of cladding without the complicating effects of radiation.

To accomplish the objectives of this program, it was necessary to design and build a high flux heater to internally heat cladding while it is subjected to an internal pressure. So that this dual purpose can be met, it is necessary to use NaK as a pressurization and heat transfer media.

Control tests, without the presence of a heat flux, are employed to determine the effects, if any, of NaK pressurization on the stress rupture behavior. This need arises because NaK may reduce the life of cladding by action at the inside surface of the cladding. For example, removal of oxide surface layers may reduce the surface barrier to dislocation movement, or grain boundary penetration of NaK would help to promote intergranular corrosion. In any case, these control specimens serve to determine the NaK pressurization effect by comparison with suitable stress rupture data obtained in static sodium.

B. SUMMARY OF TEST RESULTS

Five cladded heater assemblies (Nos. 40, 42, 44, 46, and 48) were tested in the 1200°F flowing sodium loop. The conditions related to these and other tests are outlined in Table 1. The primary objectives of this latest series of tests were: (1) to determine the effect of frequency on the thermal fatigue life of cladding, and (2) to determine the effect of mechanical stress on the thermal fatigue life of cladding. Both aspects are important to the design of fuel assemblies.

The strain profiles of the cycled tubes were measured and found to be more localized for thermal cycling than with steady-static heating. In addition, examination of metallographic specimens revealed that less grain boundary

void formation takes place. This points to a different mode of deformation for cycled tubes than for the steady-state tubes. The results of the analysis based on tests in static sodium project the life of the thermally cycled specimens to be approximately twice that actual observed (see Figure 1). Thus it appears that, when thermal cycling effects are superimposed on an internal pressure effects, the stress-rupture life of unirradiated cladding is substantially reduced.

In addition to the thermal cycling effects, mass transfer effects were manifested on all specimens tested in flowing sodium. Both polished regions, less than 0.05-mils-thick corrosion, and ferrite layers up to 0.43-mils-thick selective leaching were found on the specimens. This layer growth was determined to be diffusion-controlled with an activation energy of 64,000 cal mole °K. While the time of these tests was too short to observe any detectable influence of mass transfer on the stress-rupture behavior, the life will, in the actual reactor application, be reduced by depletion of alloying constituents and surface layer recession.

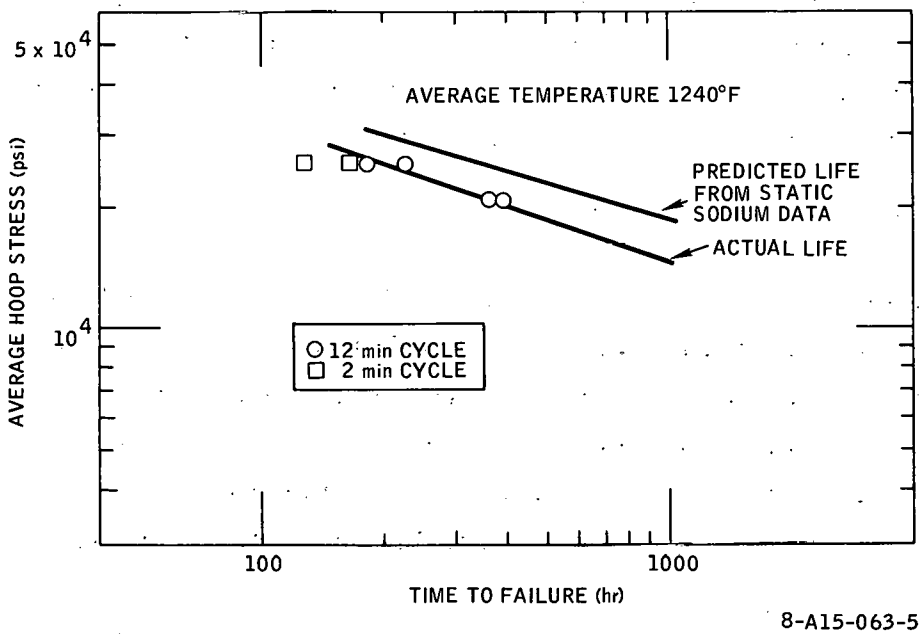

Figure 1. A Comparison of the Expected Life Based on Creep Parameters from Static Sodium Tests and the Actual Life of Thermally Cycled Cladding

C. STRESS-RUPTURE WITH NO INTERNAL HEATING

Stress-rupture results of NaK pressurized Type 304 stainless steel tubes without internal heating and in flowing sodium were evaluated. Stress-rupture data were compared to the stress-rupture data obtained in static sodium. The static sodium specimens were pressurized with high purity helium. The comparison is a natural consequence of the fact that static sodium testing supplies the backbone of the LMFBR test program under Subtask C. Therefore, using the interpolation routine discussed in the last quarterly, it appears that NaK pressurization does not substantially alter the life of cladding, at least within the first 1000 hours.

The absence of a NaK effect is not unexpected when consideration is given to recent tests in static sodium. Stress-rupture tests with types 304 and 316 stainless steels demonstrated that the stress-rupture behavior in static sodium is essentially identical to that in helium. In addition, the stress-rupture behavior of internally heated cladding in a steady-state heat flux were in accord with tests in static sodium. Thus, the results in static sodium, helium, and dynamic sodium, taken together, support the idea that the pressurization with NaK did not affect the life of cladding. This idea confirms the validity of the results of stress-rupture tests with internal heating.

Considerable evidence was found for mass transfer effects on the control specimens. A polished zone associated with the wire helix for centering the cladding in the sodium stream was observed on one specimen (Figure 2). In addition, evidence of ferrite layers uniformly distributed along the outside surface was also detected in the cross-sections. This layer is understandable when cognizance of the condition necessary for attack are considered. The presence of a temperature gradient due to local heating of the sodium from a high flux heater upstream raises the solubility and renders the sodium unsaturated. As a result of the increased flow rate associated with the control specimens, the surface of the cladding is selectively attacked with regard to nickel and chromium. Depletion in the concentration of these alloying elements at the surface establishes a concentration gradient in the cladding resulting in selective leaching of these alloying elements. A loss of nickel then permits the metastable austenite to transform to the stable ferrite. The table below

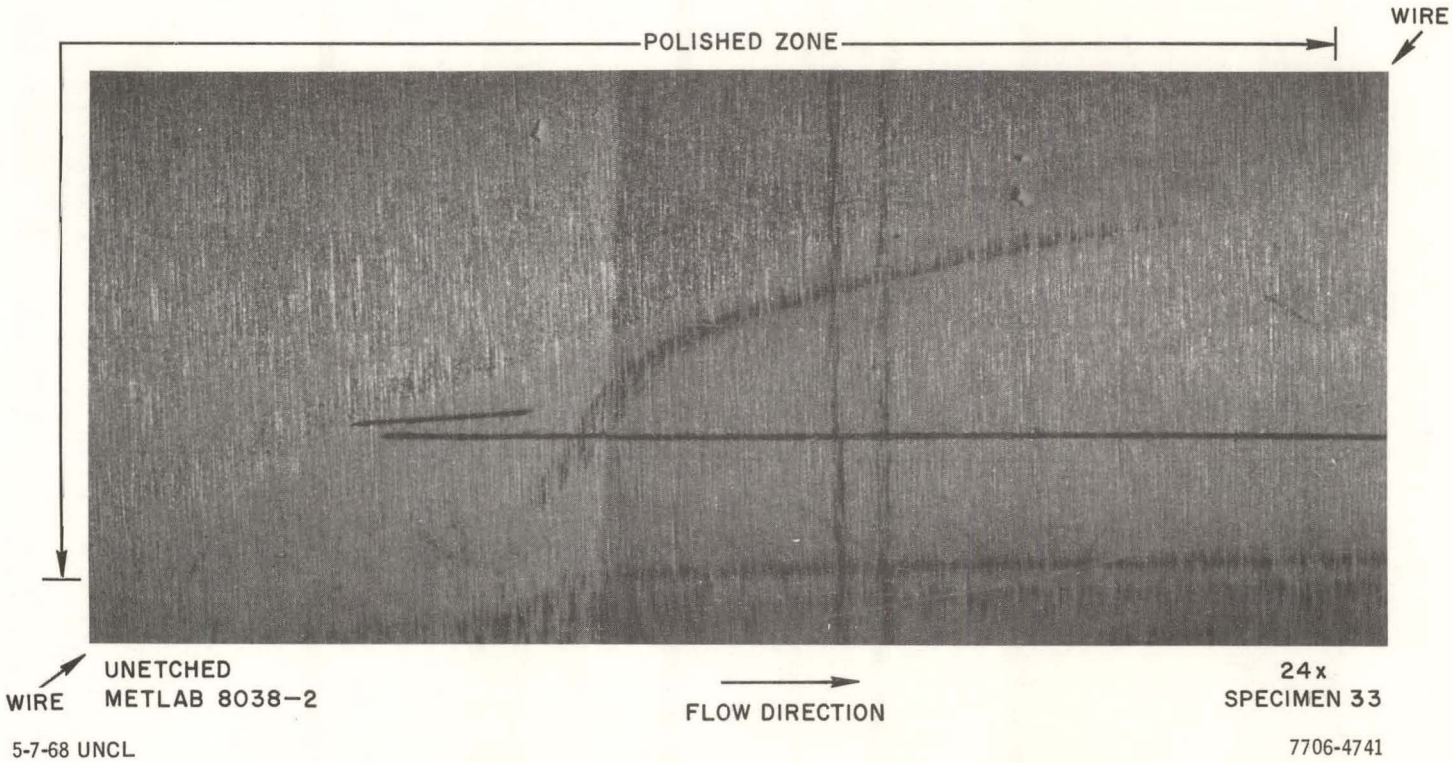

Figure 2. Polished Zone Associated With the Wire Helix for Centering the Cladding

gives the ferrite layer thickness and the time the sodium was heated by an upstream heater. These values represent more accurate measurements of the thickness of the ferrite layer than previously reported.

Specimen No.	Layer Thickness x 10^3 in.	Time at 1240°F
31	0.125	78
33	0.350	823
35	0.175	300
37	0.200	400

The limit of resolution is about 0.1 x 10^{-3} in., so that values close to this are less accurately measured than those which are much larger.

D. INTERNALLY HEATED AND PRESSURIZED CLADDING TESTS

The results of the stress-rupture test of thermally cycled cladding have been compared with results of stress-rupture of the same material under isothermal (steady state) conditions. This comparison is relevant because design analysis of fuel cladding employs equations describing creep behavior as a function of stress and temperature. Whether or not the equations are valid for thermal cycling, or if low cycle thermal fatigue conditions must be considered, is crucial to design of LMFBR fuel pins.

The expected life of a cyclic thermally stressed specimen, as compared to a static stressed specimen, is under question. In these tests the heat is turned on and off for equal times. Thus, during a "heat-on" half cycle, the cladding outer fibers experience static biaxial mechanical stresses and static biaxial thermal stresses. For the "heat-off" cycle, only a mechanical stress is applied.

One point of view that can be adopted in evaluation of test results is that the life is determined by competition between creep processes; i.e., thermal recovery and work hardening. If the only effect of cyclic heating is to alter the creep rate through the changes in stress and temperature, it should be possible to estimate the life by comparing creep rates with and without a heat flux applied. The following creep rates were estimated by use of data obtained from tests conducted in static sodium.

Heat Status	Static Stress (psi)	Thermal Stress (psi)	Wall Temperature (°F)	Avg. Creep Rate (in./in.-hr)
On 1/2 cycle	21,000	8,300	1260°F	1.3×10^{-4}
Off 1/2 cycle	21,000	0	1220°F	1.2×10^{-5}

Analysis of the cyclic creep from this table reveals a very interesting point. On the average, the specimen creep rate is 10 times faster during the heat-on portion of the cycle than during the heat-off portion. If creep processes where the stress and temperature are greater determine the life of the specimen, the difference in creep rates strongly suggests that rupture life is essentially determined by the time the heat flux is passing through the wall. Consequently, an internally heated specimen operated cyclically should last twice as long as a specimen operated under steady heating at the same maximum stress and temperature.

In terms of this analysis, the predicted life of a cycled specimen is 400 hours if a steady heated specimen will rupture after 200 hours. This was not the case, however, rather, the thermally cycled cladding ruptured prematurely in every case, as is illustrated in the table below.

Specimen No.	Hoop Stress		Actual Life / Predicted Life*
	Mechanical (psi)	Thermal (psi)	
32	21,000	8,300	0.57
40	21,000	8,300	0.43
42	21,000	8,300	0.33
44	21,000	8,300	0.41
46	17,700	8,300	0.55
48	17,700	8,300	0.56

* Prediction is based on isothermal data obtained in static sodium.

Another approach to the analysis of cyclic thermally stressed tubes under biaxial tension is that creep rate is a known junction of stress and temperature. While the approach is not fundamentally different from the previous method, it is analytical rather than graphical. We may assume the average creep rate obeys a law of the form:

$$\dot{\epsilon} = A\sigma^n \exp\left[kn\, T/100\right] \qquad \ldots(3)$$

where

$\dot{\epsilon}$ = average creep rate

σ = hoop stress

A = material constant

n = stress parameter = 3*

kn = temperature parameter = 0.9*

T = average temperature in °F

The outer surface of the specimen spends half its life at $+\Delta T$ and $+\Delta\sigma$ above the average condition and half at $-\Delta T$ and $-\Delta\sigma$ below the average condition. Therefore, the net creep rate is given by

$$\dot{\epsilon} = \dot{\epsilon}_o \left\{\left[1 + \frac{n(n+1)}{2}\left(\frac{\Delta\sigma}{\sigma}\right)^2\right] \cosh \frac{kn\Delta t}{100} + \left(\frac{n\Delta\sigma}{\sigma}\right) \sinh \frac{kn\Delta T}{100}\right\} \qquad \ldots(5)$$

where

$\dot{\epsilon}_o$ = creep rate at the average temperature and stress.

On the basis of the calculated temperature change ($\Delta T = 25°F$), the calculated thermal stress change ($\Delta\sigma$ = 4,200 psi) and the creep parameters (k,n), the net creep rate should increase by 34% over that at the average condition.

---

* Values derived from static sodium tests.

Therefore, from Figure 1 at the average temperature (1240°F), the specimen life should be 370 hours at an average stress of 25,000 psi. In contrast, the tubes ruptured at 200 hours. This may mean that thermal cycling brings into play mechanisms which accelerate creep beyond that anticipated from stress and temperature cycling alone and that this reduces the life.

There is some evidence from the literature[1-6] supporting the view that cyclic stresses superimposed on a static stresses enhance the creep rate, produce localized damage, and alter the creep mechanisms. Photomicrographs of thermally cycled specimens from these tests give added support to the literature evidence.

The strain profile for cycled specimens is sharper, and displays more peak strain, than for steady-heated specimens. This behavior has also been seen by other observers as a result of mechanical fatigue and creep.[3] In general, the superposition of cyclic and static stresses tends to localize the strain and leads to synergistic effects on the rate of deformation. If this action by thermal cycling is correctly interpreted, low cycle thermal stresses present a serious limitation on the life of cladding.

The frequency of the internal heating cycle apparently plays a role in the life of cladding under a static stress. In this work, the frequency was increased by a factor of 6, while all other parameters were held constant. The average life at the peak stress and temperature was reduced from 200 to 150 hours as a consequence of the frequency change. This effect is illustrated in Figure 3 for the 2- and 12-min periods. Also presented is a band which represents the predicted life based on creep at the maximum temperature of the outside wall and under the total hoop stress. Clearly, the life is adversely affected by cycling on the basis that creep alone determines the life.

Another interesting result, while preliminary, is that the ratio of the mechanical stress to combined thermal and mechanical stress does not change the extent of the life reduction at the same cycling frequency. The stress ratio, when varied from 0.4 to 0.5, resulted in the same fractional loss of life in comparison to the base line for each stress level. This is evident in Figure 1 by the parallel slope of the predicted and actual stress curves of the thermally cycled tests. Similar behavior was found from the peak stress-temperature

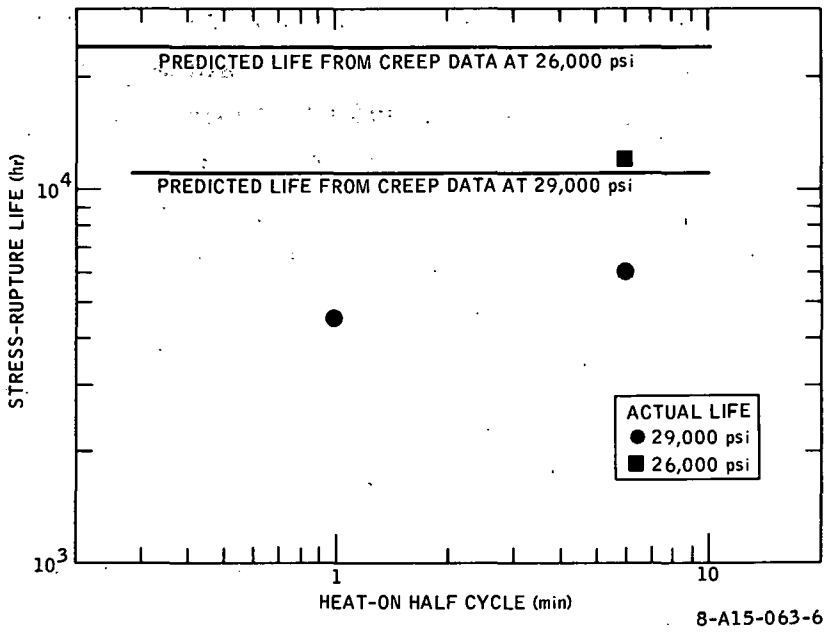

Figure 3. Influence of Cycle Rate on the Life of Cladding in Relationship to the Anticipated Life

analysis. It should be noted that the combined effects may require a greater change in the ratio of the thermal stress to the mechanical stress, or longer times, due to a dependence on relative proportions of loading mode. Intuitively, a very small ratio should result in no cycling effect, while ratios greater than one should eventually lead to thermal fatigue. Steady creep and thermal fatigue would then establish the limits on the thermal cycling effect.

E. MICROSTRUCTURES OF INTERNALLY HEATED AND CONTROL SPECIMENS

The microstructures of the thermally cycled specimens are essentially identical. It is not possible to discern any differences in the microstructure due to either a higher cycle rate or a lower internal pressure. This leads to the conclusion that changing the cycle rate or decreasing the mechanical hoop stress does not alter the mode of deformation and failure when the heat flux is cycled.

The microstructures of the cycled specimens were definitely different from those in specimens exposed to a steady heat flux or tested under isothermal conditions. In all cases, the thermally cycled specimens showed considerably

less void formation at grain boundaries than the steady-heated specimens. This clearly means that deformation involves less grain boundary sliding and is more localized when the heat flux is turned off and on. The importance of these observations to the analysis of the thermally cycled specimens becomes evident. Secondary creep, which is related to the amount of grain boundary sliding, cannot completely explain the amount and the type of deformation observed under the cyclic conditions used for these tests. Rather, it appears that considerably more primary creep occurs during the life of a cycled specimen.

Each specimen tested in flowing sodium, whether internally heated or not, exhibited a ferrite layer at the surface. The presence of a ferrite layer on the surface of the control specimens has been rationalized. In the case of the internally heated specimens, it is easy to explain why a ferrite layer is observed. As a result of the heat flux through the wall of the tubes, during the heat-on portion of the cycle, the bulk sodium temperature is sufficiently increased to raise the local solubility of the sodium for chromium and nickel. These elements are selectively removed from the cladding surface by a corrosion mechanism. When the alloy composition is sufficiently depleted in nickel, the metastable face-centered-cubic structure (austenite) transforms to the stable body-centered-cubic structure (ferrite). This new phase boundary moves away from the surface as more and more nickel is removed from the surface. The movement of the interface should therefore be under diffusion control and propagate as the square root of the time of heating; this is what is observed, as shown by Figure 4. The slope of the line gives an indication of the diffusivity which was calculated to be $D = 5.35 \times 10^{-13}$ cm^2/sec at 1265°F. For the control specimens, the time that the bulk sodium temperature was raised can be used to obtain a similar plot for 1240°F. This is also shown in the figure. As a result, the change in the diffusion rate with temperature was used to calculate the activation energy for the growth of the ferrite layer. This value was estimated to be $\Delta H = 64{,}000$ cal/mole °K, and it agrees favorably with the activation energy for self-diffusion of iron in iron.[7, 8]

If the diffusion of nickel in iron is comparable to self-diffusion, the rate of growth of the ferrite layer is controlled by diffusion in the ferrite.[9, 10, 11] This result is somewhat surprising because the diffusion rate of nickel in

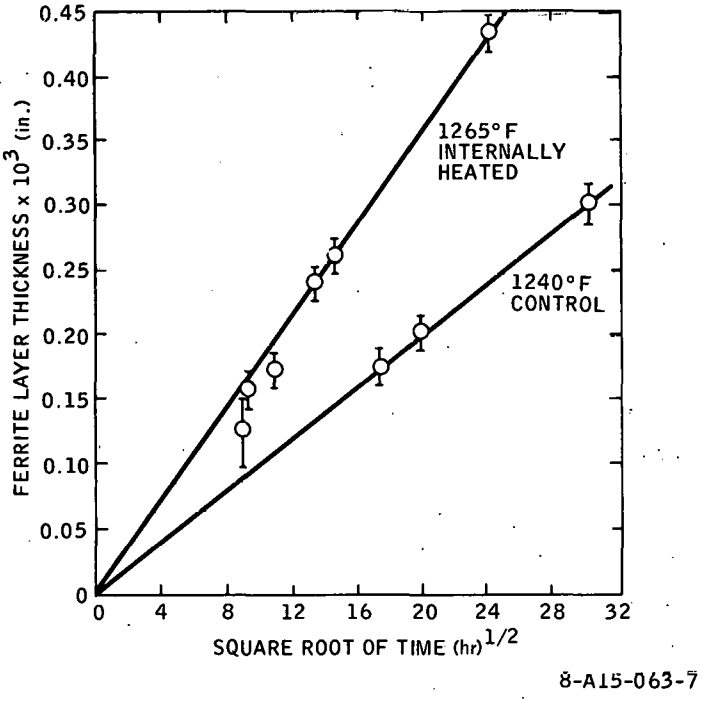

Figure 4. Growth of Ferrite on the Surface of Type 304 Stainless Steel in Sodium Flowing at 20 Ft/Sec

austenite is two orders of magnitude less than in the body-centered-cubic phase. Thus, the diffusion rate in the phase should limit the rate of ferrite layer. However, this assumes that the concentration at the exit surface is constant. In any case, these results will require additional analysis before the paradox can be removed.

IV. EVALUATION OF THE EFFORT TO DATE

The activities of this subaccount during the current budget fiscal year have met the desired project goals for determining the combined effects of internal pressure, a high heat flux, high temperature, and flowing sodium on the creep-rupture behavior of Type 304 stainless steel. While much of the phenomena remains to be studied, the impact of a preliminary evaluation of these results for reactor technology has prompted a growing interest in the high flux heater assembly as a device for simulating reactor conditions. Several important milestones were achieved which bear a direct relation to the fast reactor field:

1) NaK pressurization and thermal bonding do not influence the life of cladding when compared to isothermal tests in static sodium or helium.

2) The effects of a static heat flux superimposed on an internal pressure on the stress-rupture life can be rationalized by the temperature-stress sensitivity of secondary creep.

3) The effects of a cyclic heat flux, added to the internal pressure, increases the creep rate and decreases the life of cladding more than expected on the basis of secondary creep deformation.

The significance of these results, coupled with increasing interest in the prlblem of thermal ratcheting, have warranted additional consideration by the reactor technology field; therefore, a topical will be issued on the results and analysis of thermal gradients on the biaxial stress-rupture behavior of cladding. Hopefully, these preliminary results, when added to future studies, will constructively lead to an improved basis of alloy selection and design criteria for fuel cladding in liquid-metal-cooled fast reactors.

V. NEXT REPORT PERIOD ACTIVITIES

1) Develop analysis of thermal cycling effect.

2) Release topical report on mechanical property testing in flowing sodium.

REFERENCES

1. A. H. Meleka, "Combined Fatigue and Creep," Met. Rev. 7 43 (1962).
2. J. Bree, "Ratchet and Fatigue Mechanism in Sealed Fuel Pins for Nuclear Reactors," TRG Rep 1214(D) March 1966.

   J. Bree, "Ratchet and Enhanced Creep Strains in Sealed Fuel Pins for Nuclear Reactors," TRG Rep 1311(D) August 1966.
3. G. J. Moyar and G. M. Sinclair, "Cyclic Strain Accumulation under Complex Multiaxial Loading," Paper 35, International Conference on Creep (1963), Inst. Mech. Eng. London, p a (47).
4. A. J. Kennedy, "Interactions Between Creep and Fatigue in Aluminum and in Certain of its Alloys," Paper 13, International Conference on Creep (1963), Inst. Mech. Eng., London, p3 (17).
5. I. Finnie and W. R. Heller, "Creep of Engineering Materials," McGraw-Hill New York (1959) Chapter 10.

6. S. Tarra and M. Ohnami, "Fracture and Deformation of Metals Subjected to Thermal Cycling Combined with Mechanical Stress," Paper 25, International Conference on Creep (1963) Inst. Mech. Eng., London, p 3-57.

7. D. Y. F. Fai and R. J. Borg, Trans. AIME 233, (1965).

8. C. E. Birchenall and R. F. Mehl, Trans AIME 188 (1950).

9. F. S. Buffington, K. Hirano, and M. Cohen, Arta Met 9 434 (1961).

10. R. J. Borg and C. E. Birchenall, Trans AIME 218 980 (1960).

11. J. E. Dorn, Creep and Recovery, ASM, Cleveland 1956 p 255.

THIS PAGE

WAS INTENTIONALLY

LEFT BLANK

Program: FBR Fuel Cladding and Structural Materials
AEC Task: 10 D-3 — Dynamic Loop Testing (Mass Transfer)
Project Manager: J. L. Ballif/J. J. Gill
Reporting Period: January-March 1968
General Order: 7706 Subaccount: 29543 AEC Category: 04-01-61-01.1

Principal Investigators: R. L. McKisson, J. Hopenfeld

I. PROJECT OBJECTIVES

The objectives of the project are listed below.

1) Develop a model to describe the mass transfer process in cladding materials in a sodium environment and with a temperature gradient

2) Develop a high heat flux heater capable of operating for a minimum of 1000 hours at a minimum heat flux of 1×10^6 Btu/hr/ft^2.

II. MAJOR ACCOMPLISHMENTS IN FISCAL YEAR 1968

A tracer technique method for directly measuring the corrosion of stainless steel components in flowing sodium has been devised and its feasibility has been demonstrated.

A modification to the high heat flux heater design, involving the use of an impermeable metal bellows to prevent the inward diffusion of air into the upper electrode chamber, has been tested and has proven to be effective.

Two heaters have achieved the desired 1000-hr minimum service lives at 1.3×10^6 Btu/hr/ft^2 heat flux levels.

III. PROGRESS DURING REPORT PERIOD

A. MASS TRANSFER

Two mass transfer tests (Nos. 50 and 52) were run during the quarter. The test durations were shorter than were desired in both cases. Test 50 was terminated by a heater failure after 182 hours, and Test 52 operated only 12 hours before the heater failed. Summaries of the test conditions are shown in

TABLE 1

HEATER TEST SUMMARY*

Heater	Service Time (hr)†	Mode	Time Above 1000°F (hr)§	Construction Features	Remarks
40	173	Cyclic (6 min. "on", 6 min. "off")	194	Bellows; Mo Electrode; Clad Heater	This clad heater has been operating normally since the beginning of the test period. The total "on" time in this test sequence is 86.5 hours. The test was continued as No. 40A.
40A	238	Steady	238	Clad of No. 40 Removed	This heater was still operating when the loop was shut down to remove No. 50, and was left in place for re-use as No. 40B.
40B	260	Steady	262	Unclad, No. 40A Continuing	This heater was still operating when the loop was shut down. An x-ray of its upper electrical contact showed it to be in very good condition. The total "on" time for heater No. 40-40A-40B is: 86 + 238 + 260 = 584 hours of which the first 86 were on 12 minute, 50% duty cycle service. A total of 870 cycles were experienced.
42	134	Cyclic (1 min. "on", 1 min. "off")	134	Bellows; Mo Electrode; Clad Heater	Cladding failed after 3966 cycles. The heater was still operable. The total "on" time was 67 hours. The test was continued as No. 42A.
42A	109	Cyclic (1 min. "on", 1 min. "off")	112	Clad of No. 42 Removed	Heater failed by short circuit. Total "on" time to failure, 67 + 55 or 122 hours, all on 2 minute, 50% duty cycle service. 7308 cycles were experienced.
44	163	Cyclic (1 min. "on", 1 min. "off")	163	Bellows; Mo Electrode; Clad Heater	Cladding failed after 4842 cycles. Heater was still operable. The total "on" time was 82 hours. The test was continued as No. 44A.
44A	149	Steady	151	Clad of No. 44 Removed	Heater failed by short circuit. Total "on" time to failure, 82 + 149 = 231 hours, of which 82 were on 2 minute, 50% duty cycle service. 4902 cycles were experienced.
46	385	Cyclic (6 min. "on", 6 min. "off")	500	Bellows; Mo Electrode; Clad Heater	This clad heater operated normally during the test period. Upon removal, a 4-mils diametral swelling was noted at the position of the W wafer. The heater was dismantled and examined. The upper electrical contact had obviously run very hot. See Figure 2. The total "on" time was 193 hours. 1925 cycles were experienced.

(continued)

TABLE 1. (Continued)

Heater	Service Time (hr) †	Mode	Time Above 1000°F (hr)§	Construction Features	Remarks
48	393	Cyclic (6 min. "on", 6 min. "off")	500	Bellows; Mo Electrode Clad Heater	Cladding failed after 1961 cycles. Heater was still operable. The electrical safety gear of this clad heater was too sensitively set during the first few days of the test, and it was switched "off" probably because of electrical disturbances on the line caused by the switching of other heater units. The total "on" time to date is 197 hours. The test was continued as No. 48A.
48A	238	Cyclic (6 min. "on", 6 min. "off")	240	Clad of No. 48 Removed	This heater was still operating when the loop was shut down to remove No. 50, and was left in place for re-use as No. 48B.
48B	260	Cyclic (6 min. "on", 6 min. "off")	262	Unclad, No. 48A Continuing	This heater was still operating when the loop was shut down. An x-ray of its upper Mo electrical contact showed it was beginning to expand and to put lateral pressure on the BN insulator. The total "on" time for the heater No. 48-48A-48B is: 197 + 119 + 130 = 446 hours, all on 12 minute, 50% duty cycle service. 1870 cycles were experienced.
50	182	Steady	184	Bellows; Mo Electrode; Clad Heater	Heater failed by short circuit. Total "on" time to failure, 182 hours. 3 cycles were experienced.
52	12	Steady	12	Double Boot; Mo Electrode; Clad Heater	Heater failed by short circuit after several momentary low-power cycles were experienced. Total "on" time to failure, 12 hours.

* All heaters were operated at 1.3×10^6 Btu/hr/ft^2 at the heater sheath and at 1.0×10^6 Btu/hr/ft^2 at the clad sample surface. The loop sodium temperature was nominally 1225°F.
† Service time is the total operating time experienced by the heater in 1225°F sodium.
§ Time above 1000°F is the time during which the heater was in contact with sodium above 1000°F.

TABLE 3

HEATER PERFORMANCE ANALYSIS

No.	Total Service Life (hr)	Unclad Steady (hr)	Clad Steady (hr)	Unclad Cyclic (hr)	Clad Cyclic (hr)	Heater Heat Flux ($\times 10^{-6}$)	Failure Mode				
							Open	Short	MoO_3	Other	Still Operable
12	1117	1117	0	0	0	1.3					Yes
32, A	1044	898	0	0	146	1.3			X		Barely
11	763	763	0	0	0	1.3				Stiff Bellows	Yes
6	657	0	657	0	0	1.0	X				No
36	589	0	589	0	0	1.3	X		X	W-C Reaction	No
10	463	0	463	0	0	1.3	X		X	Re-Disc	No
7	462	0	0	0	462	1.3		X			No
40, A, B	584	498	0	0	86	1.3					Yes
8	433	0	433	0	0	1.3					Yes
9	410	0	410	0	0	2.0		X			No
48, A, B	446	0	0	249	197	1.3					Yes
30, A	330	107	0	0	223	1.3	X		X		No
44, A	231	149	0	0	82*	1.3		X			No
46	192	0	0	0	192	1.3				W-C Reaction	Yes
50	182	0	0	182	0	1.3		X			No

* 2-min cycle, all others are on a 12-min cycle.

Table 1. Both tests involved the use of an irradiated cladding, whose radioactivity was determined before it was assembled onto the heater. In addition, a number of DPH hardness indentations were made on the clad surface. Measurements of the change in the radioactivity due to material loss, and of the change in surface size of the DPH hardness indents due to surface recession, are the raw data from which the mass transfer rates can be deduced. The advantage of the activation technique is that specific elemental loss rates for Fe-59 and Cr-51 can be determined by an analysis of the gamma ray energy spectrum. (Incidentally, Co-60 and Mn-56 can be detected and their losses evaluated by proper analysis.)

The indent technique has an inherent uncertainty in that the formation of an indent cavity forces some metal to move toward the sample surface to form a ridge around the opening. This raised material is more heavily cold-worked than the surrounding surface and may tend to corrode more rapidly. The ridges also slightly protrude into the sodium stream. There is a question, therefore, about the effects of these factors on the local corrosion rate. For this reason, the present tests should be considered to be exploratory.

When Test 50 was removed from the test loop for examination, it was found that the heater failure involved the melting of about 1/4-in. of the end of the molybdenum electrode and a portion of the heater sheath wall. During the heater wall failure, the molten metal became very firmly attached to the inner wall of the cladding and also distorted the wall. Because of this, it was necessary to cut the clad sample off the heater and to perform the counting on the recovered piece. The accuracy of the indent size measurements was also affected because of the handling and bending of the sample during the removal operation. The results of both the activation-method and the indent-method analyses are shown in Table 2. The positions of the indents along the length of the tube specimen are shown in Figure 1.

The material losses indicated by the indentation method represent average values obtained from one to three indents located 90° apart at each position. The range in the reported corrosion rate represents the uncertainty in the measurements of the size of the indent. The uncertainty in the activation method result represents an estimate of the effects of the loss of material from

the cut and the change in the counting geometry from the initial pre-test configuration to the post-test configuration of the slit tube.

It is of interest to note that both techniques yield data which are in agreement with the results of other researchers, 1-2 mil/year. Further, there is an unmistakable difference in the upstream rate and the rate in the heated zone, as measured by the activation technique. This is in general agreement with the theory of operation of the 2-in. loop because the sodium which approaches the heated section, and has been circulating in the loop at 1225°F, should be saturated with metallic corrosion products at 1225°F. Therefore, the corrosion rate of the sample should be nominally zero, as found by the activation method. The observance of a small corrosion rate by the indent method may be illustrating, at least in part, the effect of the indent ridge on the corrosion rate. However, based upon these first results, it is concluded that both methods of measurement warrant further study.

An investigation of the feasibility of using "Kryponates" for corrosion and temperature measurements has begun. This is a technique developed by Panametrics, Inc., and is reported to permit the accurate measurement of corrosion rates in very short times. According to the developers, corrosion rates are measurable in exposure times of less than 200 hours. If the technique is usable in the sodium systems of interest, it may be preferable to either the activation or indent methods. Basically, the technique involves the use of Kr-85 as a tracer

TABLE 2

SUMMARY OF MASS TRANSFER RESULTS

Test 50

Heat Flux = 10^6 BTU/ft^2-hr Loop Temperature = 1225°F
Sodium Velocity = 20 ft/sec Time of Exposure = 182 hours

Position	Metal Losses (mils/year)		
	Indentation Method	Number of Indents Averaged	Activation Method
3	0.817-0.860	1	
4	1.07-1.15	2	1.4 ± 1.2
5	1.47-1.56	3	
10	0.206-0.500	2	0

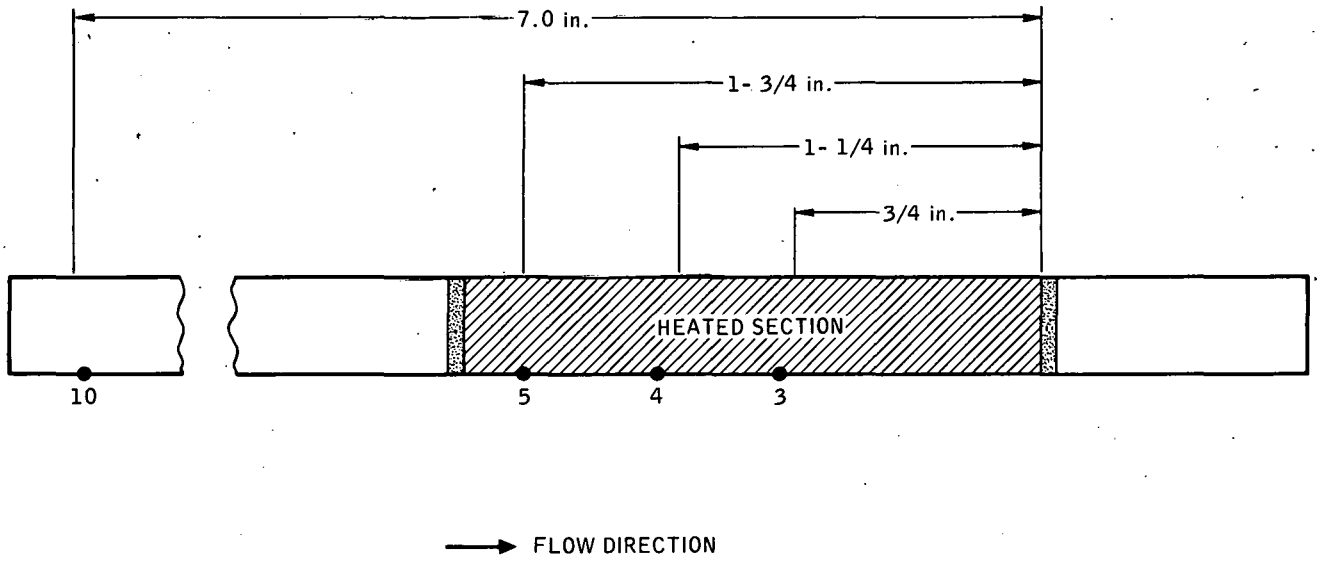

Figure 1. Positions of Indents Along the Length of a Tube Specimen

material which is diffused into the test samples, and whose loss can presumably be related to the corrosion rate, or, in other circumstances, to the service temperature of the specimen.

An abstract entitled "A Method for Studying Corrosion Mechanisms in High Temperature Flowing Sodium" has been submitted for presentation at the AEC Corrosion Symposium to be held at BMI in May.

2. High Heat Flux Heaters

Tests of seven clad heaters were performed during the quarter. In each, the primary purpose of the test was to obtain stress-rupture or corrosion data on the cladding rather than to test the heater performance per se. Therefore, the heater test sequences show a mixed history with various combinations of 2-min and 6-min cycles and steady-state heating modes. Table 1 summarizes the tests performed. The original series of the five cladding stress-rupture tests was begun in December, 1967. The cladding had failed on all of these by January 5, 1968. All the heaters were operable, but the sheath of Heater 46 showed evidence of degradation. There was a diametral swelling of about 4 mils at the level of the upper contact. Heater 42 also showed a swelling (~2-3 mils), but it was returned to service as Test 42A.

The examination of Heater 46 showed that the lower diffusion barrier (platinum) had operated very well. It showed some evidence of having extruded laterally, but it was not a marked effect, and the wafer, though distorted, was still in good condition. However, there was unmistakable evidence of malfunction at the upper contact. It had obviously run very hot, so much so that the tungsten diffusion barrier wafer reacted with the graphite electrode to form a button, presumably of tungsten carbide, in the contact. At the center-line, nearly all of the tungsten had reacted, but there was less reaction at the periphery. The end of the molybdenum electrode had expanded against the BN insulator, and had partly cut through the insulator in one spot. The swelling observed in the heater sheath was probably due to the radial forces generated by the molybdenum's distortion. These effects can be seen in the photograph shown in Figure 2.

After the cladding was removed from Heaters 40, 42, 44, and 48, they were reinserted into the loop as "A" samples, and were tested as indicated in Table 1 during the test period of clad heater 50, the first activated cladding mass transfer test. Heaters 40A and 48A were then re-used as 40B and 48B during the test period of clad Heater 52, the second activated cladding mass transfer test. After the failure of the heater in Test 52, Heaters 40B and 48B were continued on test for several days until the 2-in. loop was shut down on March 11, 1968.

A review of the performance of the several heaters tested over the last two years was made in an effort to establish the probable cause of the premature heater failures. The heaters can be grouped as shown in Table 3 to show a correlation of heater life versus construction features and the type of service. The best combination for long life is the "unclad, steady"; "clad, steady" shows next-longest lives. The cyclic mode is clearly more severe than the steady mode, as one would expect.

A review of the behavior of the most recently fabricated heaters, in which the bellows or the double boots were used, shows that the problem of MoO_3 buildup (which caused several early failures in heaters not shown in Table 3) is under control. The bellows are the best seals, but they must be soft to avoid the need for heavy weight loadings to provide the needed contact pressure. The

major disadvantage of the bellows is that the electrode cannot be rotated with the bellows as it can with the boots. In some tests, the ability to rotate the electrode enabled the operator to re-start an otherwise open-circuited heater.

At the present time therefore the upper electrical contact appears to be the most serious problem in heater life, and future heater development efforts must be concentrated on improving this joint. It would seem that it is very desirable that the number of non-bonded interfaces be reduced because each of them is almost certainly a point of high resistance. Further, in the case of clad heater service, the incremental temperature rise caused by the presence of the added NaK and cladding heat flow resistance causes an imperfect joint to run hot enough that the tungsten and the carbon begin to interact. When tungsten carbide is formed, the failure of the joint is imminent because of its higher electrical resistance.

IV. EVALUATION OF EFFORT TO DATE

A heater design, capable of attaining 1000 hours of service life at 1.3×10^6 Btu/hr/ft^2 under limited circumstances, has been developed. However, in order that it fully meet the requirements of providing a heat flux of 1.0×10^6 Btu/hr/ft^2 in a cladding specimen, an improvement in the hot-end electrical contact is needed.

A radioactive tracer technique for measuring mass transfer of stainless steel components in flowing sodium has been devised. The first tests of the technique indicate the technique to be quite useful, and to merit further study.

An indent method for measuring mass transfer of a metal surface has been devised. A first test of the method indicates the method has merit. Further study is indicated.

V. NEXT REPORT PERIOD ACTIVITIES

A status report of the high heat flux heater development will be prepared.

THIS PAGE

WAS INTENTIONALLY

LEFT BLANK

Program: FBR Fuel Development, Fuel Cladding, and Structural Materials
AEC Task: 10E — Modes of Failure and Helium Degradation Studies
Project Manager: S. C. Carniglia
Reporting Period: January-March 1968
General Order: 7706 Subaccount: 29550 AEC Category: 04-01-61-01.1

Principal Investigator: D. Kramer

I. TASK OBJECTIVES

The objectives of this task are to, (1) obtain a detailed understanding of the motion, agglomeration, and trapping of helium atoms and bubbles in fast reactor cladding and structural materials, including the effects of initial distribution of helium atoms and the ultimate distribution of these trapped product atoms, (2) investigate the basic nature and form of the mechanical property changes induced by fast reactor transmutation damage, (3) assist in the translation of these into interpretation of environmental behavior of cladding alloys and the selection, heat treatment, and design of fast reactor materials.

II. MAJOR ACCOMPLISHMENTS IN FISCAL YEAR 1968

The third and fourth cyclotron injections of helium were performed on samples of 304L, 316, and 405 stainless steels; Incoloy 800; 19-9DL; Inconel 625; IN 102; and Inconel X-750. Helium concentrations ranged from 1×10^{-6} to 4×10^{-5} atom fraction.

Tensile testing and metallography were completed for 316 stainless steel. The mechanism of helium embrittlement was determined to be similar to that previously reported for 304 stainless steel, but the extent of ductility loss is sensitive to the presence of dispersed sigma precipitates.

Helium was determined to embrittle Incoloy 800 to approximately the same degree as it does 304 stainless steel.

The energies of formation, and the binding energies of a number of (001) and (111) vacancy clusters, have been determined. The stability of a 13-vacancy clusters, have been determined. The stability of a 13-vacancy sphere, with respect to planar 13-vacancy clusters in either the (001) or (111) plane, and the

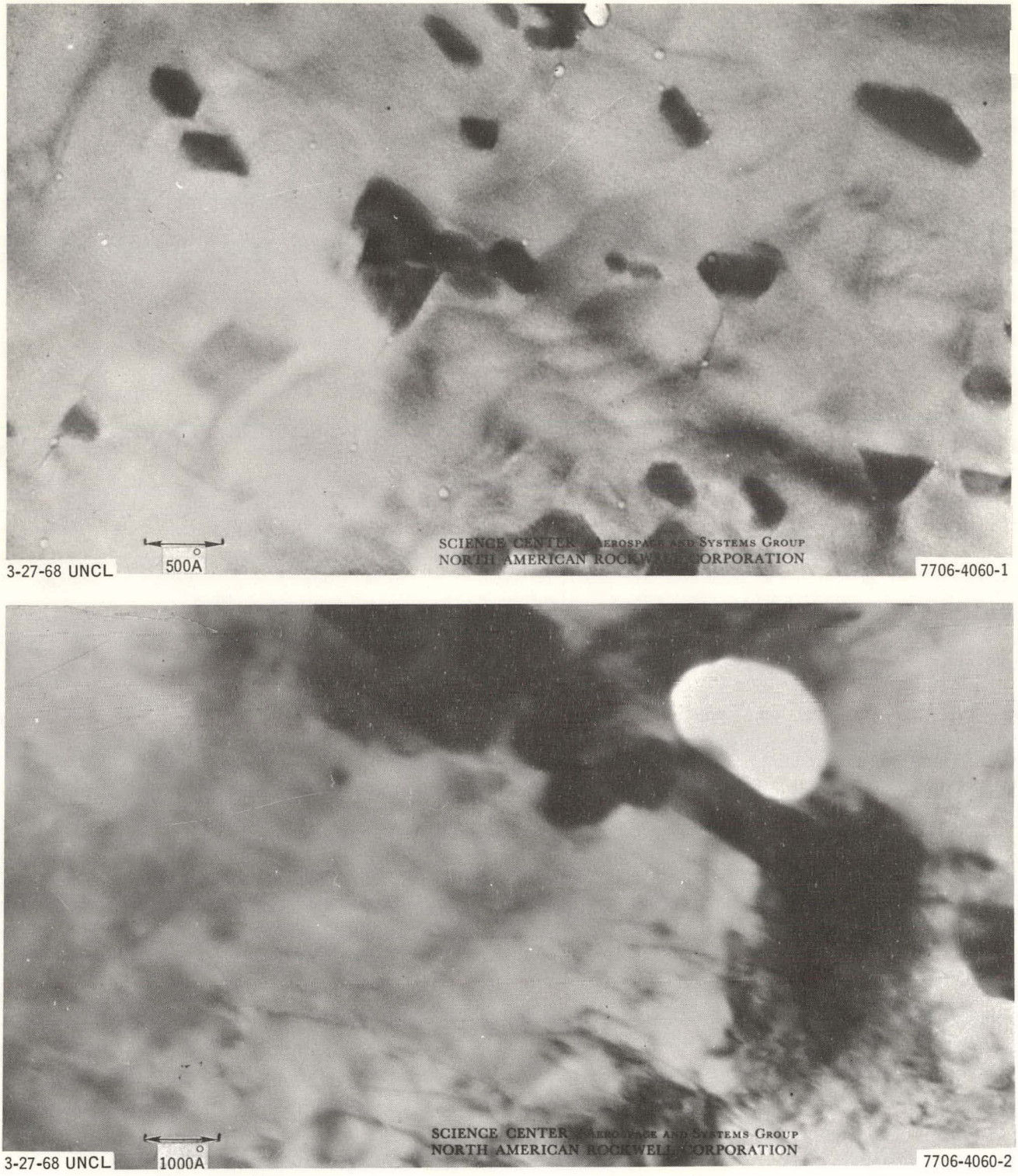

Figure 1. Replica Electron Micrograph 316 SS With 4×10^{-5} At. Fraction Helium Tested at 760°C (Showing Voids Adjacent to Grain-Boundary Carbides)
(a) Treatment 6, (b) Treatment 13

non-collapse of the planar clusters, indicates that gas atoms may not be necessary for the nucleation of voids recently detected in highly irradiated metals. The positive binding energy of all the vacancy clusters studied shows that there is no minimum-size cluster that must be reached before stability is achieved. This absence of a nucleation barrier means that the mechanism of void formation is diffusion-controlled. The key driving force for the formation of voids is the reduction in the internal energy that results when vacancies condense.

The high sensitivity gas mass spectrometer has been put into operation. Analyses of helium at the 10^{-6} atom fraction level in milligram pieces of stainless steel have an absolute uncertainty of less than 5%.

III. PROGRESS DURING REPORT PERIOD

A. 316 STAINLESS STEEL

The matrix precipitates produced by treatment 13 (25% CR → 24h 480°C → 144h 705°C) and assumed in the previous quarterly progress report,* to be carbides, were ascertained, by electron diffraction, to be sigma-phase. Those precipitates located on grain boundaries are $M_{23}C_6$ carbides. The helium concentration was analyzed on the new gas mass spectrometer and found to be $4 \pm 0.3 \times 10^{-5}$ atom fraction. The calculated value used heretofore should be disregarded.

Further electron microscopy has allowed us to propose the mechanism of helium embrittlement. Loss of ductility was always accompanied by a failure that was partially or completely intergranular and by the presence of intergranular cracks along the gage length. In their incipient state, these cracks are located adjacent to grain-boundary carbide particles, as seen in Figure 1. Grain boundary sliding, which probably occurred during testing, was obstructed by these carbides, leading to the nucleation of voids at the carbide-matrix interface.

---

* "Quarterly Technical Progress Report AEC Unclassified Programs October-December 1967," AI-AEC-12638.

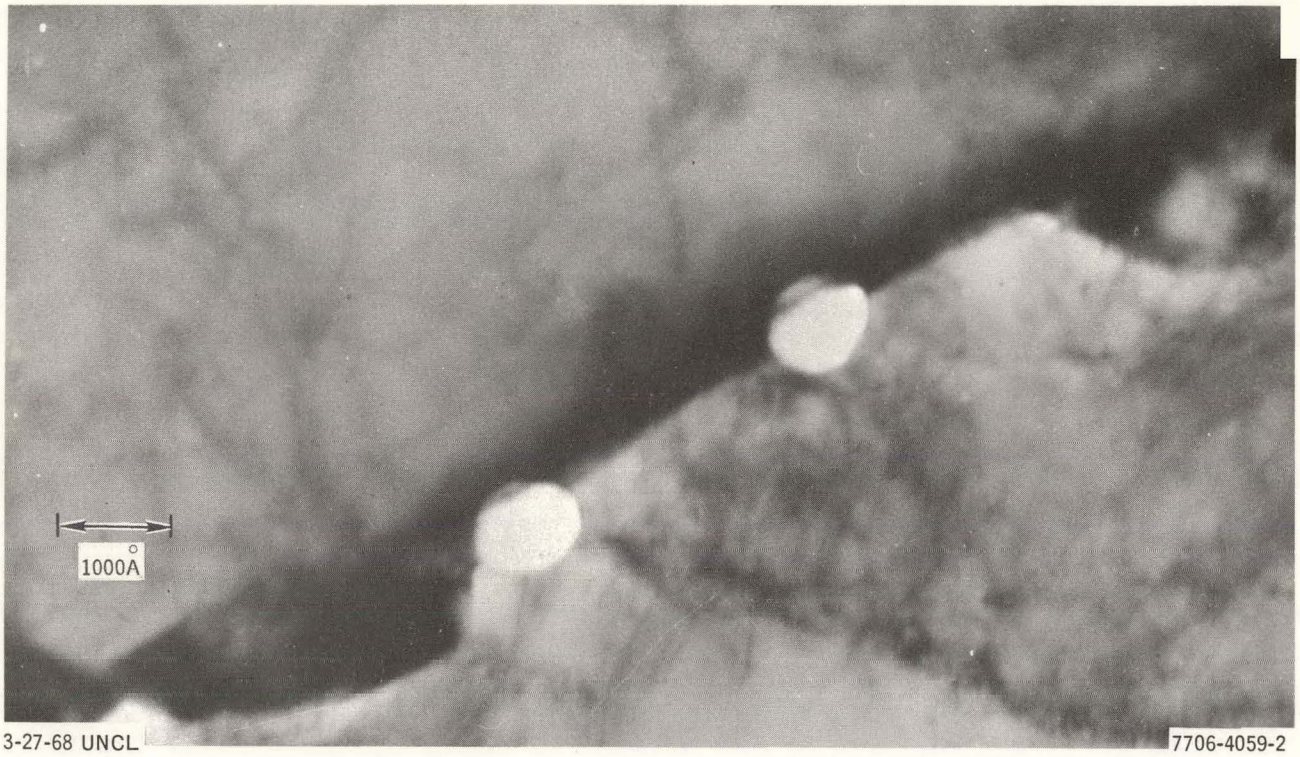

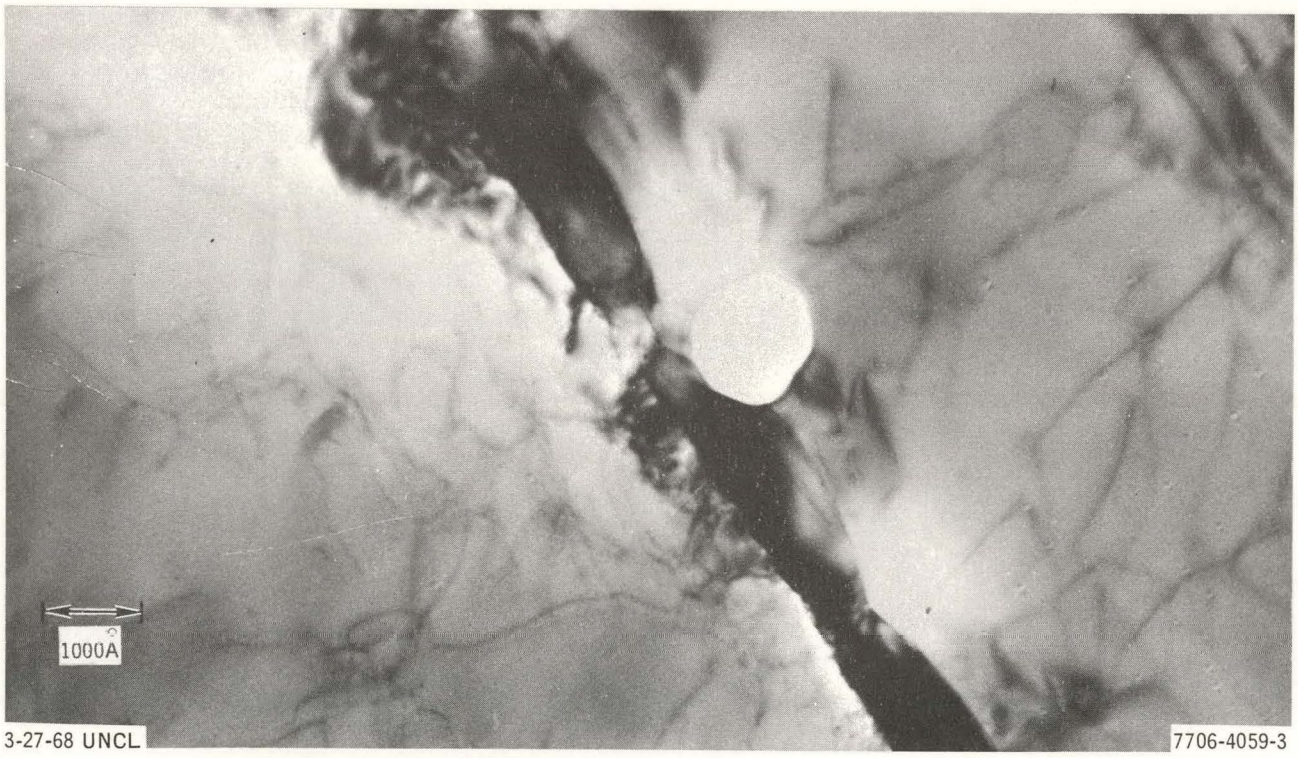

Figure 2. Transmission Electron Micrographs Showing Helium Bubbles in 316 SS Given Treatment 6 with 4×10^{-5} at. Fraction Helium, Tested at 760°C

This mechanism is valid whether or not helium is present and, when it is, grain-boundary voids and cracks are present to a much greater extent for equivalent amounts of strain. A large helium bubble (> 500 Å) attached to a grain-boundary carbide is already a void. Under the action of grain-boundary sliding, such large bubbles will grow as voids and cracks. Figures 2 and 3 are examples of bubbles on grain-boundary carbides which had the potential of growing as cracks. Helium embrittles 304 stainless steel in the same way.

The fine dispersion of sigma particles produced by Treatment 13 was effective in trapping helium bubbles in the matrix, as seen in Figure 4. This delayed the accumulation of helium at grain boundaries and explains why ductility loss is not manifest at 650°C or below.

B. INCOLOY 800

Tensile tests of samples containing $4 \pm 0.3 \times 10^{-5}$ atom fraction helium were completed. As in the case of 316 stainless steel, the calculated value of the helium concentration has been replaced by the measured value. The tensile samples were treated to produce two different microstructures prior to helium injection. These were:

Treatment 4: 50% CR → 1h 1010°C → 100h 760°C

Treatment 11: 50% CR → 100h 760°C

The tensile data appear in Tables 1 and 2, and the total elongation as a function of temperature appears in Figure 5.

Helium causes a loss in ductility above 500°C regardless of the treatment received prior to injection. However, the amount of ductility loss is greater in samples given Treatment 11. Helium bubbles were detected in samples tested throughout the temperature range 500 to 800°C. Previously, the lowest test temperature that resulted in helium bubbles was 650°C for 304 stainless steel.

Treatment 11 resulted in matrix precipitation (10^{12} particles/cm^{-3}) but not in as fine a dispersion as was obtained in 316 stainless steel. The particular heat used in this study (HH7531A) is low in Al, Ti and Cu; other heats may behave in a different manner. The mechanism of helium embrittlement appears to be the same as for 304 and 316 stainless steels.

Figure 3. Transmission Electron Micrograph Showing Helium Bubbles in 316 SS Given Treatment 13 with 4×10^{-5} at. Fraction Helium, Tested at 760°C

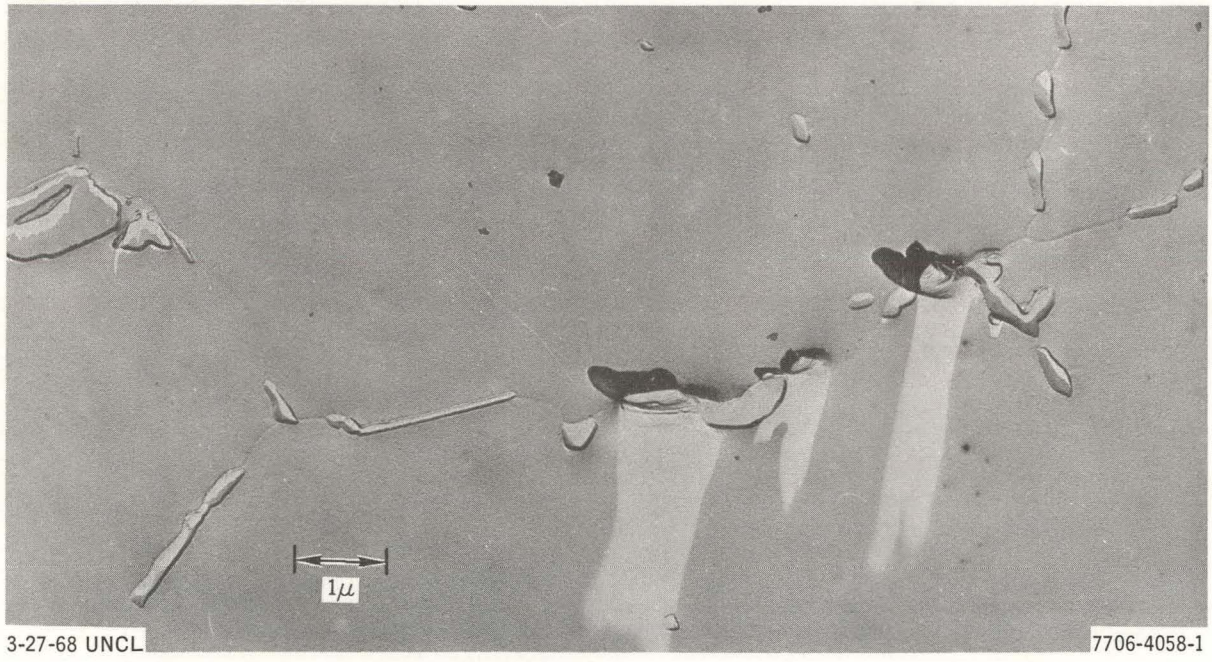

Figure 4. Transmission Electron Micrograph Showing Helium Bubbles in 316 Stainless Steel Given Treatment 13 with 4×10^{-5} at. Fraction Helium, Tested at 760°C

TABLE 1

TENSILE DATA OF INCOLOY 800 WITH TREATMENT 4

σ_Y = yield strength σ_T = tensile strength

ϵ_U and ϵ_T = uniform and total elongation

Atom Fraction Helium	Test Temperature (°C)	σ_Y (kpsi)	σ_T (kpsi)	ϵ_U (%)	ϵ_T (%)
0	500	15.4	53.1	28.4	30.3
4×10^{-5}	500	15.3	52.9	29.2	30.3
0	600	16.6	47.5	25.7	28.0
4×10^{-5}	600	15.5	47.3	25.6	39.2
0	700	14.2	30.6	13.0	39.2
4×10^{-5}	700	15.8	30.3	10.6	13.9
0	800	12.7	17.7	6.9	38.4
4×10^{-5}	800	12.0	17.1	4.6	10.1

TABLE 2

TENSILE DATA OF INCOLOY 800 WITH TREATMENT 11

Atom Fraction Helium	Test Temperature (°C)	σ_Y (kpsi)	σ_T (kpsi)	ϵ_U (%)	ϵ_T (%)
0	500	17.9	52.9	24.8	25.9
4×10^{-5}	500	16.0	52.4	25.2	26.1
0	600	18.3	43.1	22.6	34.3
4×10^{-5}	600	17.0	42.0	15.7	16.4
0	700	14.2	27.0	12.0	45.5
4×10^{-5}	700	14.8	26.0	6.1	7.1
0	800	10.6	14.4	6.5	45.7
4×10^{-5}	800	12.1	14.2	3.0	5.8

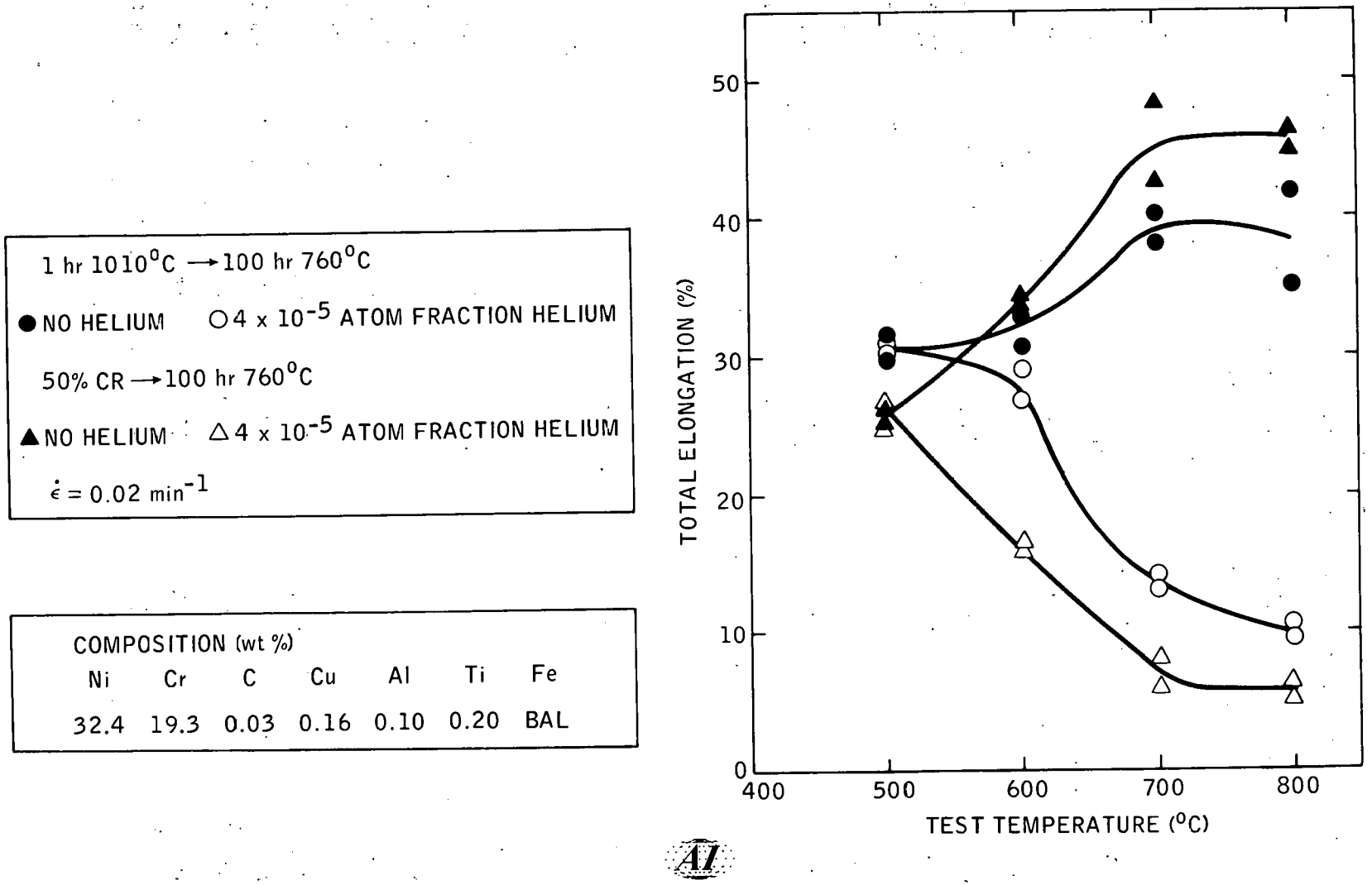

JANUARY 1968

8-J23-003-13

Figure 5. Total Elongation as a Function of Test Temperature for Incoloy 800

C. 405 STAINLESS STEEL

Tensile tests on 405 stainless steel have begun. This alloy is ferritic at temperatures of interest and, its composition is given below in wt %. The tensile data appear in Table 3.

C	Cr	Al	Ni	Fe
0.56	15.4	0.15	0.27	bal.

Prior to helium injection the samples were given either one of the following treatments:

Treatment 5: 40% CR → 1h 980°C

Treatment 10: 1/2h 715°C → 40% CR → 24h 760°C

TABLE 3

TENSILE DATA OF 405 STAINLESS STEEL TESTED AT 750°C

Treatment	Atom Fraction Helium	σ_Y (kpsi)	σ_T (kpsi)	ϵ_U (%)	ϵ_T (%)
5	0	5.6	6.6	2.3	44.0
5	4×10^{-5}	6.8	7.5	1.7	28.2
10	0	4.5	4.7	1.7	48.5
10	4×10^{-5}	5.8	6.3	3.5	22.4

The ductility loss experienced by the austenitic alloys at 750°C with about the same helium concentration ranges from 65 to 88%. However, the ductility loss for 405 stainless steel is 36 and 54% for samples with Treatments 5 and 10.

D. STRESS-RUPTURE TESTS OF 304 STAINLESS STEEL

Four samples, without helium, were tested in vacuum; the results are shown in Table 4. The next tests will be done on samples with 3×10^{-5} atom fraction helium.

TABLE 4

STRESS-RUPTURE DATA OF 304 STAINLESS STEEL, WITHOUT HELIUM, AT 760°C

Stress (kpsi)	Rupture Time (hours)
7.7	507
7.7	516
8.5	324
11.1	82

E. FOURTH HELIUM INJECTION

The fourth helium injection was accomplished; details are given in Table 5. The Incoloy 800 used was from another heat with higher Al, Ti and Cu concentrations.

TABLE 5

THE FOURTH HELIUM INJECTION

Alloy	Estimated Atom Fraction Helium	Number of Samples
304L	3×10^{-5}	30
19-9DL	3×10^{-5}	30
316	3×10^{-5}	20
Incoloy 800	3×10^{-5}	20
Inconel 625	3×10^{-5}	13
IN 102	3×10^{-5}	13
Inconel X-750	3×10^{-5}	12
304L	1×10^{-6}	23
316	1×10^{-6}	45

F. COMPUTER CALCULATIONS OF HELIUM AND VACANCIES IN GAMMA-IRON

Earlier in this study, an approximate rule was reported: $E_B \sim 0.25\ (ev) N_B$, which related the binding energy, E_B, of a vacancy cluster to the number N_B of nearest neighbor Fe-Fe bonds that are broken when the originally isolated vacancies are coalesced into a cluster. The application of this rule to a 43-vacancy cluster led to $E_B \sim 39$ ev, which agreed within 1% of the computer value of 38.68 ev.

One important aspect of the approximate rule lies in the possibility of making hand calculations of the binding energy of other clusters. Two such calculations have been carried out during this report period, one for a 55-vacancy cluster, $E_B \sim 51$ ev, and the other for a 79-vacancy cluster, $E_B \sim 75$ ev. The 55-vacancy cluster consists of a central vacancy plus vacancies at the lattice sites of the 12 first, 6 second, 24 third, and 12 fourth neighbors of the central vacancy. The 79-vacancy cluster adds on one shell of vacancies, i.e., the 24 fifth neighbor sites.

The most important aspect of the approximate rule lies in the insight the above type of application gives into the energetics of formation of large voids, e.g., a million vacancies clustered together. The originally isolated vacancies which coalesce to form a cluster fall into two classes: (1) interior vacancies, which are surrounded by 12 other vacancies, and (2) surface vacancies, which have less than 12 vacancies around them with the deficit being made up by metal atoms at the surface of the void. The calculations show that the energy of formation of the originally isolated vacancies, E_V, is completely returned if a given vacancy ends up as an interior vacancy of the void. A lesser energy, on the average $0.5\ E_V$, is returned if a given vacancy becomes a surface vacancy. Thus, for large voids with a small surface-to-volume ratio, all but a few percent of the total formation energy of the originally isolated vacancies is recovered by the formation of the void. Therefore, if the reference point is the high steady-state supersaturation of vacancies which are generated by a high steady neutron flux, the internal energy of the system can be drastically reduced by the formation of large voids. This reduction in internal energy is the principal driving force for the formation of large voids.

Two defects lying in a (111) plane have been studied in addition to the eight (001)-plane defects studied earlier. Defect 9 is an equilateral triangle trivacancy, and defect 10 is a 13-vacancy planar cluster (Figure 6). The most significant result is that neither defect exhibited large relaxation effects. For example, the atom above the center of the equilateral triangle (indicated by the cross in defect 9 in Figure 6) moved downward toward the plane of the triangle by only 0.07 A, or 3.3% of the interplanar spacing. This result is directly contradictory to that of Damask, Dienes, and Weiser (Phys. Rev. 113, 781 [1959]) who reported this atom to move 75% of the interplanar spacing to form a tetrahedron of four vacancies with an atom in the center. The difference in the two results arises from the difference in the interatomic potentials used in the two studies. The Johnson potential used in the present study only extends to first nearest neighbors whereas the Morse potential used by Damask et al. interacts out as far as the fourth neighbors. Analysis of a crystal model of the tetrahedral configuration shows clearly that the difference in the results is due directly to the difference in the number of neighbors with which the central atoms interact. The Johnson potential leads to much better agreement with experimental energies of formation of defect configurations than the earlier

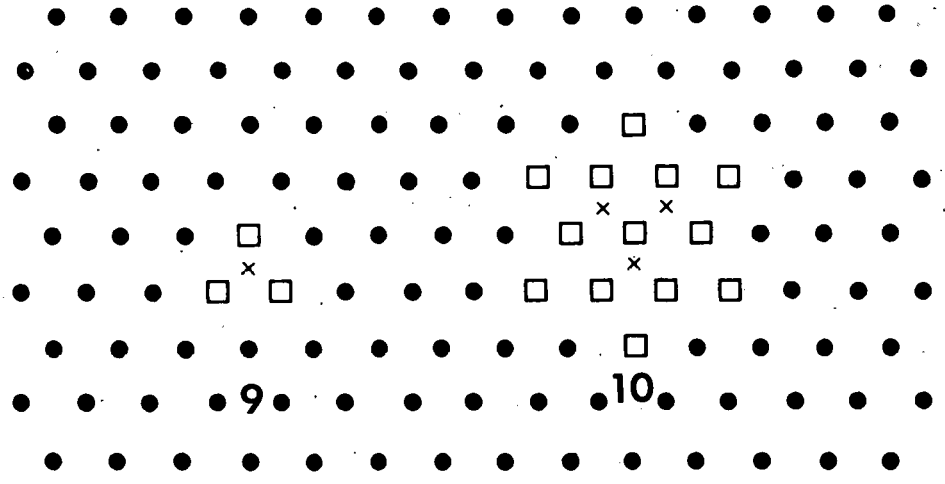

3-22-68 UNCL 7706-1006

Figure 6. Vacancy Clusters in a (111) Plane of FCC γ-Fe

developed Morse potential; thus, the present result of a stable triangular configuration for the (111) trivacancy can be accepted with confidence.

The validity of the present result with the trivacancy is confirmed by the non-collapse of the 13-vacancy star (Defect 10). However, it is known that large enough (111) clusters will collapse to form a stacking fault surrounded by a dislocation loop. The present result is not in contradiction with this experimental fact; it means only that there is a minimum size cluster that must be attained before the energy increase due to the formation of the dislocation loop is offset by the energy decrease due to the formation of the stacking fault in the center of the loop. A very crude model suggests that this minimum size would be a 91-vacancy planar (111) hexagon, but this is an extreme lower limit since such a cluster is only 25 Å in diameter whereas the sizes of observed loops are at least 100 Å in diameter.

The interaction of helium atoms with γ-Fe has been initiated this report period. The placement energy, E_p, of a substitutional helium atom in an otherwise perfect γ-Fe lattice has been found to have the very low value of 0.01 ev. For a substitutional He atom adjacent to a vacancy, E_p = 1.38 ev, the He atom will move 0.033 Å toward the vacancy which is 1.3% of the first nearest neighbor separation distance in γ-Fe (2.5767 Å). Finally, the diffusional activation energy of a helium atom jumping from a substitutional site to the saddle point between the original site and an adjacent vacancy is 1.96 ev. This value should be compared to the following values: (1) 2.80 ev for the self-diffusion of Fe in γ-Fe, (2) 0.43 ev for the jump of H in γ-Fe, (3) 1.75 ev for the jump of N in γ-Fe, and (4) 0.69 ev for the jump of He in germanium.

G. MASS SPECTROMETER ANALYSIS OF HELIUM IN METALS

The high sensitivity gas mass spectrometer for the analysis of low levels of helium and other noble gases has been completely assembled and put into operation. During this quarter, the vacuum system was assembled from stainless steel and aluminosilicate glass sections. All the volumes necessary for the isotope dilutions with ^{3}He were calibrated. A bakeout oven was made to surround the entire high-vacuum part of the system and zirconium-titanium alloy getters were made and placed into individual furnaces.

Determination of the helium content is made by cutting a suitable size sample (1 mg), weighing it, and melting it in a tungsten helix furnace in vacuum. Immediately after the material is melted and the ^{4}He is released, a precisely known volume of ^{3}He ($\sim 10^{-5}$ cc STP) is added. Mixing of ^{3}He and ^{4}He is very rapid. Other gases released by the sample are gettered and a part of the ^{3}He and ^{4}He mixture is allowed to go quickly and directly into the mass spectrometer volume, after the vacuum pumps are sealed off. A measurement of the ^{3}He/^{4}He ratio, and a knowledge of the weight of the material, gives the helium concentration. Two independent checks have been built into the mass spectrometer system for calibrating and measuring isotope discrimination. Results of the first 11 samples are shown in Table 6.

TABLE 6

HELIUM MEASUREMENTS FROM THE GAS-SOURCE MASS SPECTROMETER

Sample	Material	Nuclear Reaction	Helium Conc. (atom fraction x 10^6)		
			Atomics International	McMaster U	Estimated
1s	stainless steel and boron	(n, α)	12.7	12.5	12.9
1s	stainless steel and boron	(n, α)	11.9	13.4	12.9
2s	stainless steel and boron	(n, α)	1.0	1.4	1.44
2s	stainless steel and boron	(n, α)	1.5	1.4	39
9-7	stainless steel	α bombard.	43	-	39
9-30	stainless steel	α bombard.	41	-	39
9-54	stainless steel	α bombard.	38	-	39
10-3	stainless steel	α bombard.	12.5	-	18
10-19	stainless steel	α bombard.	24.3	-	18
10-19	stainless steel	α bombard.	24.4	-	18
10-33	stainless steel	α bombard.	19.2	-	18

Samples 1s and 2s are two helium "standards" which were prepared at AI in 1967 by irradiating a known mixture of stainless steel and boron in the reactor STIR. Careful measurements of the flux, self-shielding, boron concentration, etc., resulted in estimated helium concentrations of 12.9 and 1.44×10^{-6} atom fraction, respectively. These values were confirmed by measurements made at McMaster University, Hamilton, Canada, in June 1967. Recent values obtained at AI are in close agreement with the above values. The slight differences seen are probably due to sample variation because repeat measurements on the more homogeneous tensile specimens gave results reproducible to within 1%. Measurements on the tensile specimens from the 9th and 10th sample plates of α-irradiations at the University of Washington, Seattle, show that the doses are close to those estimated. However, a drop in dose by a factor of 2 can be seen for a sample at the edge of the sample plate (10-3) when compared to the center (10-19). The absolute uncertainty of the concentrations is estimated to be less than 5%.

Work has commenced to determine the detection limit of the mass spectrometer. Aluminosilicate glass was used wherever possible to reduce the leak-rate of helium into the system. Preliminary observations indicate that a helium background "memory" from sample to sample may be the limiting factor. This memory is less than 1% of the samples so far analyzed, and efforts will be made to considerably reduce this. The sensitivity of the mass spectrometer is such that future samples will be made smaller so that the "between-sample memory" will drop accordingly. At present, samples whose helium concentration is greater than 10^{-8} atom fraction can be measured without difficulty.

H. EBR-II IRRADIATION EXPERIMENT

The AI samples were inserted in the reactor during February 1968. These samples are part of ORNL-Exp. 3 and ORNL-Exp. 4 which were placed in Rows 2 and 7 respectively.

I. PUBLICATIONS AND TALKS

1) W.G. Gehman, "Vacancy Clusters and Voids in FCC γ-Iron," Oral presentation at the American Physical Society meeting, Berkeley, March 1968.

2) D. Kramer, K. R. Garr, C. G. Rhodes and A. G. Pard, "Helium Embrittlement of Type 316 Stainless Steel," oral presentation at the AIME meeting, New York, February 1968.

IV. EVALUATION OF EFFORT TO DATE

The third and fourth helium injections scheduled for this fiscal year were successfully completed. Results on 316 stainless steel and on Incoloy 800, taken with the results on 304 stainless during FY 67, indicate that all simple austenitic alloys suffer helium embrittlement to about the same degree by the same mechanism. The ability of only a moderately fine dispersion of precipitates (in 316 stainless steel) to mitigate ductility loss is significant.

The influence of carbides on the mechanisms of failure in 304 and 316 stainless steels warrant a further effort on the effect of carbon content on mechanical properties both in the presence and absence of helium. Low and high carbon varieties of 304 and 316 stainless steels will therefore be studied.

We have built two stress-rupture machines that operate in vacuum and have tested four samples of 304 stainless steel without helium. These machines will allow us to measure the extent and mechanism of ductility loss, due to helium, at low strain rates which are closer to actual reactor conditions.

Computer calculations have shown that small (<25 Å) clusters of vacancies are stable without the presence of gas. This is an important step toward understanding the nature of void formation in metals exposed to high fluxes and fluences. The initiation of the helium work will evaluate the importance, if any, of helium in the formation of large voids (>100 Å).

Fast and accurate measurement of the helium content of the small tensile samples is now routinely available. This will allow check of helium distribution in samples along the plate length and along the sample itself. The high sensitivity of the gas mass spectrometer will be applied in the future to the elemental EBR-II samples yielding (n, α) cross-sections.

V. NEXT REPORT PERIOD ACTIVITIES

Electron microscopy will be completed on Incoloy 800. Tensile testing and metallography will be completed on 405 stainless steel. Stress-rupture tests on 304 stainless steel with helium will begin. Tensile testing of alloys of the fourth injection will begin.

Vacancy clusters containing helium atoms will be studied to determine if gas atoms can stabilize some clusters and thus lead to an alternate kinetics route for void formation in addition to the diffusion of vacancies alone.

Routine measurements of helium concentration in various metals will be made with the gas mass spectrometer. An effort will be made to reduce memory effects and determine the effective limit of detection.

THIS PAGE

WAS INTENTIONALLY

LEFT BLANK

Program: FBR Fuels and Cladding
AEC Task: 11-A – Mixed Carbide Fuels (Basic Properties)
Project Manager: J. L. Ballif
Reporting Period: January-March 1968
General Order: 7707 Subaccount: 28210 AEC Category: 04-40-02-01

Principal Investigator: G. Ervin, Jr.

I. TASK OBJECTIVES

The task objectives are to:

1) Determine selected microstructural attributes and mechanical and physical properties of mixed carbide fuels both to establish the potential for these materials as nuclear fuels and to provide a basis for interpreting and understanding irradiation behavior in terms of atomistic transport phenomena.

2) Develop, where necessary, preparative techniques for polycrystalline mixed carbide materials of controlled structure and stoichiometry.

II. MAJOR ACCOMPLISHMENTS IN FISCAL YEAR 1968

Some basic studies on UC were brought to completion and are now in the process of publication. These studies include high-temperature oxidation, mechanical properties, and self diffusion of uranium and carbon in UC. With the objective of starting experimental work on mixed carbides at the beginning of next fiscal year, a portion of the AI plutonium-handling facility has been allocated to this project, glove boxes for the work are in place, and equipment and material procurement has been started.

III. PROGRESS DURING THE REPORT PERIOD

Mixed carbide materials procurement was begun early in the quarter with projected delivery of portions of the order scheduled for July 1, 1968.

The conversion of the existing plutonium metal facility to handle mixed carbides and oxides is proceeding well. The glove boxes for this work are in place, and equipment procurement is underway. In the area set aside for

mixed carbides, two types of operation are planned: preparation of samples of mixed carbide, and performance of basic property studies. For the sample preparation portion, seven process flow diagrams were prepared:

1) Synthesis of (U, Pu) C from UO_2 and PuO_2.
2) Preparation of U-Pu Alloy.
3) Synthesis of (U, Pu) C from U-Pu Alloy.
4) Preparation of (U, Pu) C Slugs from Synthesized (U, Pu) C.
5) (U, Pu) C Powder Preparation, Sintered Pellet Fabrication and Vibratory Compaction.
6) Helium Bonded Fuel Encapsulation.
7) Sodium Bonded Fuel Encapsulation.

The equipment list for the operations in these flow diagrams was prepared. These plans are designed to provide a versatile facility, but not all will be operational in the early stages.

A manuscript covering the work on self-diffusion of uranium and carbon in uranium monocarbide has been reviewed and revised. The paper reviews other studies on this topic which have appeared recently in the literature, and it is shown that important areas of disagreement and incompleteness still exist both as to the experimental results and their interpretation. Hence, it is not yet very fruitful to make use of self-diffusion results in basic treatments of swelling and mechanical behavior of carbide fuels.

A paper entitled "Preparation of Fine Refractory Dispersions in UC," by B. D. Pollock and A. C. Hott, has recently been accepted for publication by the Journal of Nuclear Materials. A revised copy meeting the reviewers comments has now been returned to the Journal for publication.

IV. EVALUATION OF EFFORT TO DATE

Definite steps have been taken to convert an existing company plutonium laboratory for working with mixed carbide, and it is believed that experimental work in this facility will begin early in fiscal year 1969. Completion of previous basic studies on UC has proceeded approximately on schedule.

V. NEXT REPORT PERIOD ACTIVITIES

Company equipment for pressing and sintering modified (U, Pu) C will be ordered and at least a part of it is expected to be delivered and set up. Specific plans will be formulated for samples to be prepared and for carbon activity measurements and other basic property studies.

Program: FBR Fuels and Cladding
AEC Task: Task 11-B — Mixed Carbide Fuels (Irradiation Studies)
Project Manager: J. L. Ballif
Reporting Period: January-March 1968
General Order: 7707 Subaccount: 28220 AEC Category: 04-40-02-01

Principal Investigator: G. Ervin, Jr.

I. TASK OBJECTIVES

The objective of this task is to apply fundamental technology toward the reduction and control of swelling in mixed carbide fuels and to demonstrate the effectiveness of fine dispersion tungsten doping in improving the high-temperature irradiation stability of UC.

II. MAJOR ACCOMPLISHMENTS IN FISCAL YEAR 1968

Irradiation of the fuel swelling test of dispersed-phase UC-W alloys (the 101 experiment) is in progress at the NRX reactor at Chalk River and, as of the end of March, approximately 50% of the target burnup has been achieved. The temperature profile and other parameters have followed design predictions very closely, and we have now reached an advanced stage of what appears to be a successful experiment.

All engineering documentation of the experiment is complete, and a technical report on the preparation and properties of the fuel samples is now ready for printing.

III. PROGRESS DURING THE REPORT PERIOD

A repair on the 101 capsule was completed at AI headquarters and the capsule was shipped back to the NRX reactor. It was inserted in the reactor during the normal cycle shutdown that began January 22 and was first brought up to power on January 27. The startup produced excellent results, confirming all the major design features of the capsule.

The instrumentation of the capsule permits three independent indications of the power produced by the fuel string. The first is the set of in-capsule

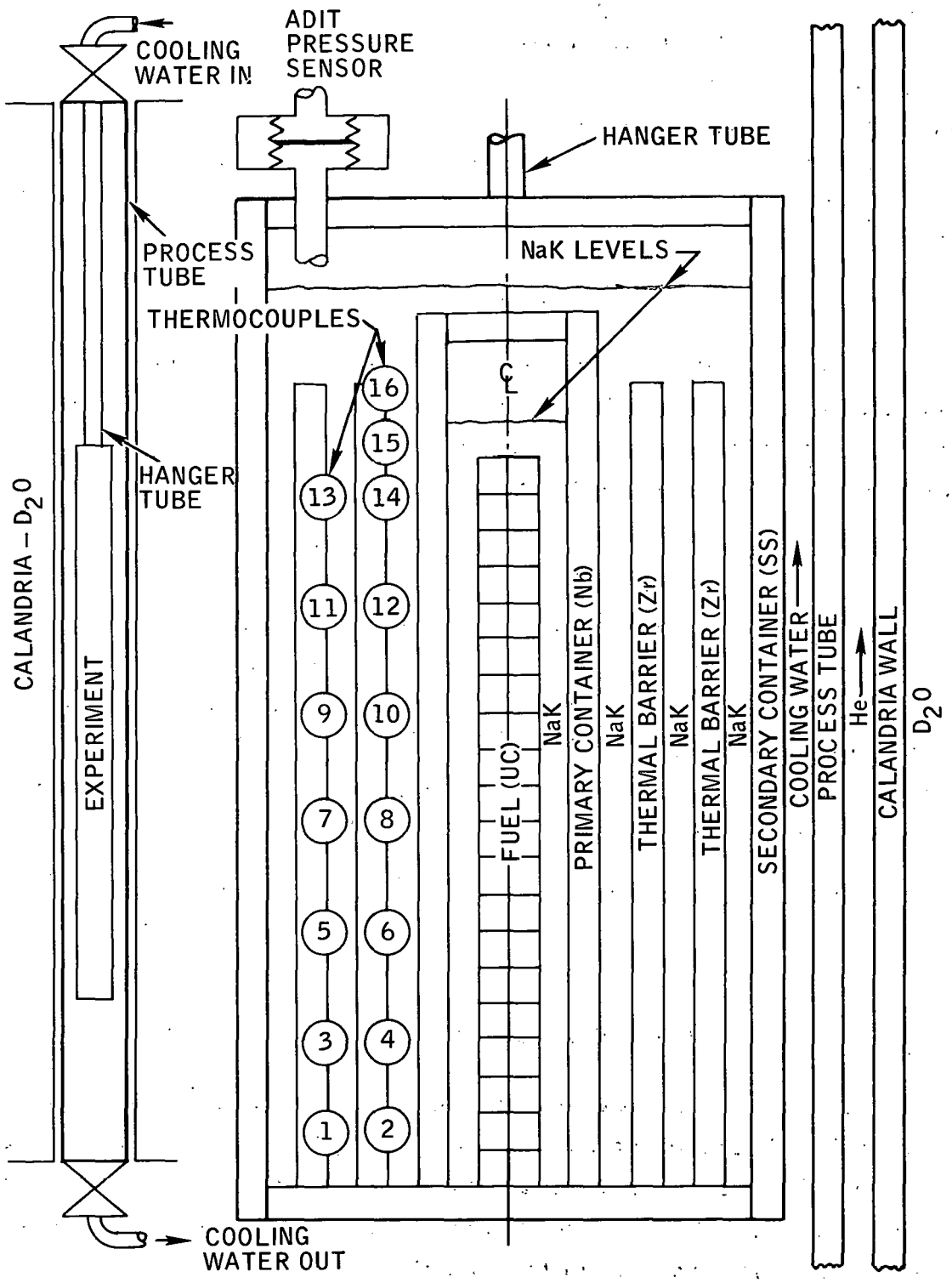

Figure 1. Schematic Drawings Indicating the Locations of the Thermocouples and the Pressure Sensor and the Positioning of the Experiment in the Reactor

temperature measurements. These are the most important because they are used to extrapolate to the fuel centerline temperatures. The arrangement of these thermocouples is indicated in Figure 1, and the readings obtained during the first operation at power in the reactor are indicated in Figure 2. It may be seen from Figure 2 that the actual temperatures are close to design but with a slight dip near the center which is so far unexplained. These temperatures will vary somewhat during a reactor cycle and from cycle to cycle, and the power to the experiment will be controlled to some extent by adjustment of neighboring fuel rods in an effort to maintain the desired temperatures.

The second indication of power to the experiment is the pressure read on the adit pressure sensor or transducer which measures the pressure in the gas space above the NaK in the secondary containment vessel. The position of this sensor is indicated in Figure 1 and readings taken while coming up to power are shown in Figure 3. The agreement here is an indication that the average temperature and power level are as calculated. The real purpose of the pressure sensor is to serve as an indication of a leak or failure of the primary container which is at a higher pressure and a failure would cause an increase in reading. This purpose has been somewhat compromised by the performance of the transducer subsequent to the startup in that it has functioned properly only intermittently.

Still a third indication of average power output of the 101 fuel string is the rise in water temperature in the channel, shown in Figure 4 as a function of reactor power. Again there was excellent agreement with design.

Performance of the capsule subsequent to startup has continued to be good, except for two over-temperature incidents. A maximum temperature has been set to avoid the danger of NaK boiling with loss of thermal bond and extreme over-heating of the fuel. The first such occurrence was during startup and was due to the failure of an alarm on the hottest thermocouple. The second occurrence was also during startup and, although the alarm functioned, the temperature was already past the danger point by the time the operator read it and lowered power. Temporary over-heating is now expected during startups due to low moderator level and skewed power distribution, and special precautions will be taken during future startups. Because temperature distribution as a

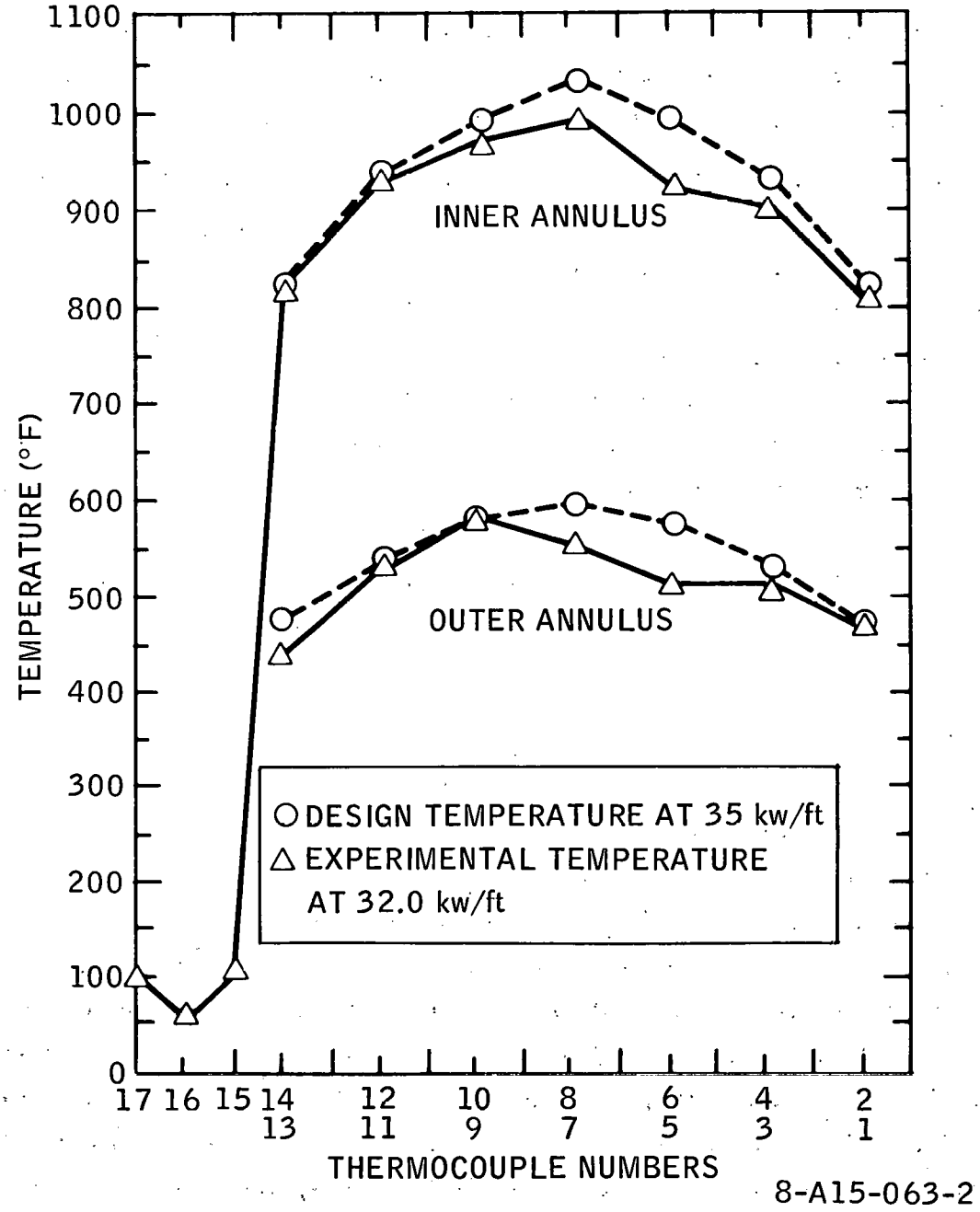

Figure 2. Thermocouple Readings After Full Power Was Reached

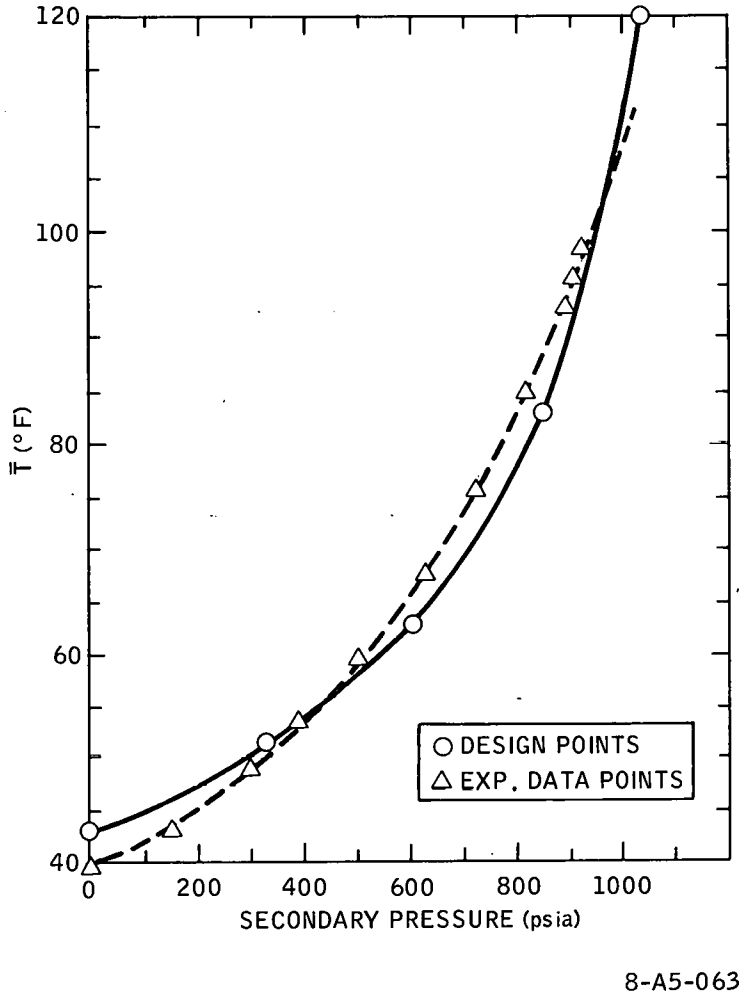

Figure 3. Pressure in Secondary Containment Vessel Versus Average Temperature During Initial Rise to Full Power

function of reactor power is still normal, indications are that no damage occurred during the two excursions.

The target burnup is 15,000 Mwd/MTU. When operating at design power of 35 kw/ft the burnup accumulates at a rate of 165 Mwd per day, but of course there are shutdowns of varying duration and frequency and the power is usually somewhat less than design. As of the end of March, burnup is approximately 50% complete, and target burnup can be expected sometime during June.

The principal measure of swelling to be used in post-irradiation examination of the fuel samples will be change in density. The changes in density of the tungsten-containing samples will be compared with the changes of the

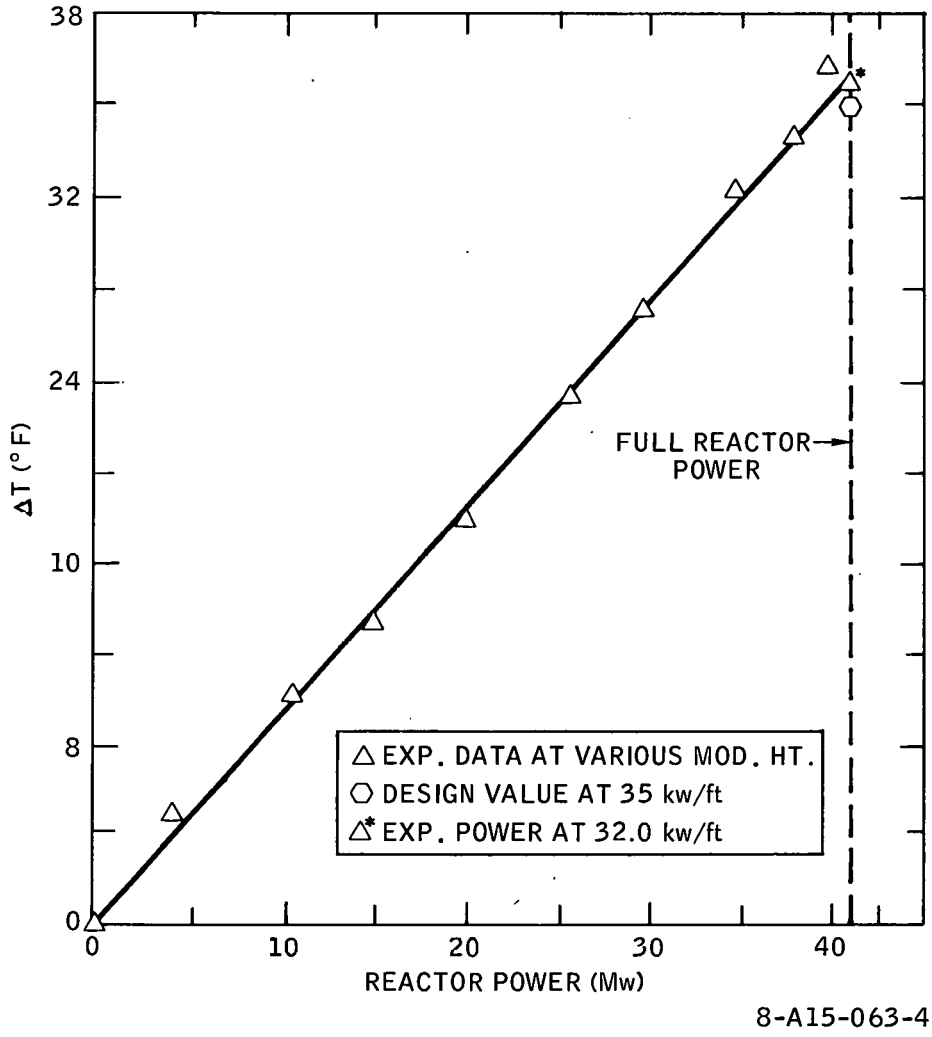

Figure 4. Temperature Difference in Water Flow Channel During Rise to Power

controls which contain no tungsten. Some of the data on pre-irradiation densities are summarized in Table 1. Values for all 120 samples are given in the report on fuel preparation and properties, which has been completed and is about to be published.

IV. EVALUATION OF EFFORT TO DATE

The successful startup of the 101 experiment, with verification of the design parameters, makes it very probable that the experiment will be completed as planned and that it will be a valid comparison experiment to show the effect of small particles in controlling fission gas swelling in ceramic fuels.

TABLE 1

DENSITY RANGES OF FUEL SAMPLES IN THE 101 EXPERIMENT

Carbon Stoichiometry	Tungsten Content, (wt % W)	Alloy Structure	Density Range (gm/cc)
$MC_{0.97}$	1.6	particle dispersion	13.62-13.71
$MC_{0.97}$	1.6	solution	13.64-13.72
$MC_{0.97}$	3.0	particle dispersion	13.69-13.76
$MC_{0.97}$	3.0	solution	13.71-13.77
$MC_{0.99}$	none	-	13.40-13.59
$MC_{0.99}$	1.6	particle dispersion	13.61-13.69
$MC_{0.99}$	1.6	solution	13.57-13.65
$MC_{0.99}$	3.0	particle dispersion	13.60-13.72
$MC_{0.99}$	3.0	solution	13.68-13.74

V. NEXT REPORT PERIOD ACTIVITIES

It is expected that the 101 experiment will achieve target burnup by June – probably about the middle of the month – and that it will be removed from the reactor and held in water storage until cool enough for shipment, at least a month. Detailed plans for hot cell examination will be formulated. The technical report on the preparation and properties of the fuel samples will be issued.

THIS PAGE

WAS INTENTIONALLY

LEFT BLANK

Program: FBR Fuels and Cladding
AEC Task: 11-C – Mixed Carbide Fuels (Casting Studies)
Project Manager: J. L. Ballif
Reporting Period: January-March 1968
General Order: 7707 Subaccount: 28230 AEC Category: 04-40-02-01

Principal Investigator: J. W. Carroll

I. TASK OBJECTIVES

The objectives of this task are to:

1) Establish optimum fabrication parameters, by calculation, for the melting and casting of mixed carbides.

2) Utilize the calculated parameters in practice by producing laboratory quantities of mixed carbide.

3) Design, procure and pilot-run a furnace for the production of melted and cast mixed carbide fuel.

II. MAJOR ACCOMPLISHMENTS IN FISCAL YEAR 1968

Two studies have been initiated, and one has been completed, on the effect of arc melting and casting in an inert atmosphere. The study has shown that the plutonium loss rates during melting can be appreciably reduced by the use of an inert gas pressure within the furnace. A study to optimize crucible configuration has been completed and shows that maximum volume to crucible cooling wall area is obtained with a hemisphere. It is closely followed by a right circular cylinder with a diameter-to-height ratio of two.

Process flow sheets, process descriptions, and equipment lists have been prepared and the equipment has been requested for installation in the NMDF.

III. PROGRESS DURING THE REPORT PERIOD

A theoretical study was completed on the vapor pressures and loss rates of Pu from UC-20 wt% PuC fuel during melting and casting. The following assumptions were used for the calculation: (1) ideal behavior of all species in the condensed and gaseous phases; (2) a rigid sphere model for the derivation

of the expression for diffusion coefficients; (3) zero concentration of plutonium vapor at 1-cm from the surface of the melt; (4) the collision diameter of gaseous plutonium atoms is equal to the molar volume of the solid divided by Avogadro's number; and (5) the vapor pressure of plutonium over the melt can be obtained by extrapolation, from 1900 to 3000°K, of the expression obtained from observed pressures over the solid.

Table 1 shows the calculated evaporation rates vs temperature for a vacuum furnace atmosphere, one atmosphere of argon, one atmosphere of krypton and one atmosphere of xenon.

TABLE 1

MAXIMUM RATE OF EVAPORATION OF Pu

Temperature (°K)	Evaporation Rate ($\mu g/cm^2/sec$)			
	Vacuum	Argon	Krypton	Xenon
2000	46.1	0.011	0.008	0.006
2250	509.	0.132	0.094	0.071
2500	3452.	0.996	0.712	0.537
2750	16420.	5.23	3.74	2.82
3000	60260.	20.9	14.9	11.3

The results given should be considered as upper limits since each of the assumptions involved in the calculations leads to high values for the vapor pressure and diffusion coefficients.

A geometric analysis was performed to optimize the size of the molten pool within a skull melting crucible. The results of the analysis are shown in Table 2.

Process descriptions and process flow diagrams were prepared for: (1) (U-Pu)C feed stock synthesis, (2) U-Pu master alloy preparation and (3) (U-Pu)C arc melting and casting.

TABLE 2

CRUCIBLE GEOMETRIC FACTOR CONSIDERATIONS

Shape	Open Top Area/Volume	Volume/Cooling Wall Area
Sphere	---	0.29
Hemisphere	1.91	0.26
Cylinder, D = 2H	1.45	0.23
Cylinder, D = H	0.92	0.22
Cylinder, D = 1/2H	0.58	0.19

IV. EVALUATION OF EFFORT TO DATE

Data are being obtained concerning the arc melting and casting process for mixed carbide so that the volume of material poured from the crucible may be increased and the volatilization loss of plutonium during melting may be decreased.

Experimental equipment requirements have been defined and the equipment is being assembled for installation in the NMDF.

V. NEXT REPORT PERIOD ACTIVITIES

The crucible geometry study will be continued by performing a three-dimensional heat transfer analysis to more clearly define the effect of the volume/cooling wall area on the volume of molten material available for casting into slugs for various crucible configurations.

A criticality analysis will be performed to determine a curve for crucible geometry vs allowable plutonium content.

A summary report will be prepared analyzing the three theoretical studies, and optimum crucible configurations and furnace atmospheres will be recommended for experimental study.

THIS PAGE

WAS INTENTIONALLY

LEFT BLANK

Program: General Chemistry and Chemical Engineering
AEC Task: 12 — Sodium Chemistry
Project Manager: S. C. Carniglia
Reporting Period: January-March 1968
General Order: 7708 Subaccount: 36110 AEC Category: 04-40-04-03.1

Principal Scientists: R. L. McKisson
R. L. Eichelberger
D. C. Gehri
J. Guon

I. PROJECT OBJECTIVES

The objective of this project is to advance the understanding of the chemistry of liquid sodium as a solvent for metals and non-metals through study of the following:

1) The equilibrium solubility and the rate of solution of selected metals and non-metals in liquid sodium, as a function of temperature, using materials of the highest purity available to minimize the perturbations caused by unwanted side reactions.

2) The nature of solute entities and their interactions in liquid sodium, from which thermodynamic properties of the solutions may be deduced.

3) The analytical chemistry of solutes in liquid sodium at very low concentrations, in order that the data developed under 1) and 2) above may have the greatest possible reliability.

II. MAJOR ACCOMPLISHMENTS IN FISCAL YEAR 1968

1) A topical report entitled "The Construction and Operation of a Sodium Purification Apparatus," NAA-SR-12444, was published and released.

2) Consistent data on the solubility of carbon in sodium, using diamond and single crystal solute materials, have been obtained.

3) The solubility of copper in liquid sodium has been determined over the temperature range 350 to 725°C, and the results compared with those from other laboratories.*

4) The solubility of molybdenum in liquid sodium has been determined to be less than 2 ppm at temperatures below 1000°C. No definable temperature dependence was found in the temperature interval 700 to 1000°C.

III. PROGRESS DURING REPORT PERIOD

A. HIGH PURITY SODIUM

The extruder which was filled with purified sodium in November, the fifth distillation product from the sodium purification system, was installed on the ion-pumped vacuum system used for capsule loading. After discarding the first six inches of extruded sodium, samples were taken to be analyzed for carbon and oxygen. The carbon level reported was 6 ppm, the average of duplicates of 5 and 7 ppm. Carbon content and analytical procedures are discussed in detail later in this report. To date, a total of 12 samples have been analyzed for oxygen, with a spread from 4.8 to 18.4 ppm, and a higher analytical blank than was formerly used. Refinements in sampling are planned to attempt to lower the spread in analyses, since it is felt that the numbers reported are not representative of the oxygen level of the sodium extruded and loaded into solubility experiments.

B. EXPERIMENTAL SYSTEM

Repeated trouble with the clutch and belt drive which couple the turbomolecular vacuum pump with its drive motor culminated in complete breakdown of the clutch. A replacement unit of a new design, which provides a direct belt drive without the need for a clutch, has been ordered. It is obvious from our experience why the manufacturer has changed the pump-motor coupling in newer models of the equipment.

A sodium extruder which failed during use, by fracture of the ram extension, was disassembled. The probable cause of the failure was faulty operation

* These results have been reported in a topical report, "The Solubility of Copper in Liquid Sodium," AI-AEC-12671.

of the quick-to-slow drive mechanism in the unit. The extruder has been repaired and the design modified so that a similar failure cannot occur in this unit. Other units will be modified as time permits.

Design and detailing continues for a small sodium chemistry loop (SCL) to be used in solute interaction studies. In at least the initial phases of the SCL experimental program, oxygen-metal-sodium interactions will be studied utilizing a United Nuclear Corporation oxygen meter to follow changes of oxygen activity in sodium. The program as presently envisioned will be divided into the following phases:

Phase 1	Check-out and test of loop and facilities, and characterization of oxygen meter.
Phase 2	Verification that a material of construction (Nickel 270) which suitably minimizes oxide-surface interactions has been chosen.
Phase 3	Study of Ni-O-Na ternary system.
Phase 4	Study of Fe-O-Na ternary system.

Additional studies on such ternary systems as Cr-O-Na, Zr-O-Na, and C-O-Na are anticipated. If the oxide-surface interactions are sufficiently small, other experiments such as an extension of the oxygen solubility curve may be performed.

A preliminary layout of the SCL has been completed, details were prepared on the surge tank and pump, and machining of parts for the inert atmosphere transfer system have been completed. All Ni-270 required for the loop has been ordered and a portion of it received. Vendors have been requested to bid on bellows-sealed valve assemblies to be used in the loop. The pump configuration has been tested relative to the magnetic field distribution within the pump, and no operational problems are anticipated. Preparation has started of the laboratory in which the loop will be operated.

C. SODIUM-CARBON SOLUBILITY STUDIES

Five carbon solubility experiments were completed using the methods and materials described in previous reports. The sodium used was from the most recently purified batch, and had an initial carbon content of about 6 ppm, as sampled directly from the extruder into evacuated glass collection vials. Table 1 shows the results of these experiments, all of which were run at 1000° for 6 hours in Hi-270 capsules.

TABLE 1

CARBON IN SODIUM SOLUBILITY EXPERIMENTS

Capsule Number	Solute	ppm C	Special Conditions
3-3	diamond	27	Na originally loaded into a separate capsule and gettered with Zr-Ti for 21 hrs at 1000°, then transferred to the solubility capsule in an argon-filled glove box.
4-4	none	22	
8-16	diamond	13	
9-9	diamond	23	
10-10	none	11	Zr-Ti getter added to capsule in place of solute

These experiments were designed to corroborate results previously obtained by J. B. Ott and also to serve as indicators of the problem areas in experimental and analytical procedures. The effect of oxygen contamination, which was observed in the transfer of the gettered sodium to capsule 3-3, may account for the high carbon content. This high result is in accord with the apparently greater carbon solubility in oxygen-contaminated sodium which has been observed at several other laboratories.

An increase in carbon content of the sodium in capsule 4-4 in the absence of a solute suggests that the capsule material itself may be a carbon source. Ni-270 has a specified carbon level of 100 to 200 ppm, which is as low as can

be obtained for commercially available nickel. The advantage of using a nickel capsule is illustrated by the instability of Ni_3C, which has a positive standard free energy of formation in the 700 to 1100°C temperature range. Ni-270 therefore seems to be the best choice for capsule material, but the observed interaction between the sodium and the capsule must be understood before the results with solute additions can be considered meaningful.

The low result for capsule 8-16 illustrates another problem area. The sampling procedure was observed to be somewhat different from that seen in other experiments. An attempt to standardize sampling procedures by redesign of the capsule configuration is now in progress. In addition, a series of experiments is being planned to study the entire analytical procedure in an attempt to isolate and solve other problems in the "dry combustion" technique.

The results for capsules 9-9 and 10-10 are in good agreement with those reported by Ott for similar experimental conditions. Once again, however, the key to their validity may depend on sampling procedures, analytical techniques and capsule interactions. As an additional aid to the study of these problem areas, the possibility of using ^{14}C techniques has been explored. It is expected that the use of such techniques will serve two purposes: first, to provide needed insight into the problem areas in the conventional technique, and second, to serve as an independent method for verifying solubility data. Until the present disparity between carbon solubilities based on chemical analysis, and those based on ^{14}C analysis, are resolved, both sets of numbers will remain in doubt.

D. METAL SOLUBILITY STUDIES

Table 2 shows the results of metal-in-sodium solubility experiments completed during the quarter. The two higher temperature iron points, No. 297 and No. 298, are on the curve for iron solubility reported in the previous quarterly report,

$$\log_{10} S_{Fe}(ppm) = 1.549 - 517/T.K \quad .$$

The other two iron points are just outside the 95% prediction interval calculated from the previous data. Further treatment of the data is required.

TABLE 2

METAL SOLUBILITY EXPERIMENTS

Run Number	Solute	Temperature (°C)	Time (hr)	Solute in Na (ppm)
294	Fe	1000	6	Ti collector ballooned, sample lost
295	Fe	500	6	26.8
296	Fe	650	6	25.0
297	Fe	700	6	9.9
298	Fe	800	6	14.6
299	Ni	700	6	3.0
300	Ni	800	6	4.0
501	Ni	900	6	4.9
503	Ni	180	0.25	7.5
288	Cr	700	6	3.3
289	Cr	800	6	3.2
290	Cr	900	6	2.1
291	Cr	1000	6	1.6
505	Mo	800	6	1.4
506	Mo	850	6	0.5
507	Mo	900	6	0.9
508	Mo	950	6	1.2
511	Mo	1005	6	1.3

The nickel data reported in the table show much lower apparent solubilities than reported on the basis of similar experiments. Continuing efforts to improve the measures to prevent contamination may be responsible. The fact that the very low temperature run, 180° for 15 minutes, showed more nickel than the others is confusing. It is not known at this time whether the failure to obtain consistent data arises from inadequate control in some step of the experimental procedure or in the analytical chemistry, or from some other source.

The chromium results reported in the table are the first obtained. Although no evaluation of the uncertainty of the analysis has yet been made, it does not seem unlikely that all of these results are within the experimental uncertainty. Qualitatively, it seems that the solubility of Cr in liquid Na is greater than that of Mo, but less than that of Cu, Fe, or Ni.

All ten experiments with molybdenum solute (five of which have been reported earlier) have given results less than 2 ppm. The 95% confidence interval for the analysis at this level is about ±0.5 ppm, based on the sample size used. The solubility of molybdenum in sodium is thus found to be less than 2 ppm at temperatures below 1000°, with no definable dependence on temperature in the 700 to 1000° range.

The lack of agreement between solubility studies in which wet chemical analytical methods were used and those in which radiochemical methods were used has been discussed for many years, based on the results of work at Mine Safety Appliances Research Corporation and the Naval Research Laboratories. Very recent experiments using both methods at BNL, combined with the AI wet chemistry results, further emphasize the discrepancy without providing any definitive answers. To help solve this problem of lack of agreement between results from wet chemical and radiochemical experiments, which has appeared in solubility studies of Fe, Ni, and C in sodium, crucibles of Fe and solute rods of Cr are currently being irradiated. It appears that experiments with irradiated solutes can be carried out in the present equipment without extensive shielding.

E. ANALYTICAL CHEMISTRY RESEARCH

1. The Determination of Niobium in Sodium

The reliability of the measurement of traces of niobium in sodium has been verified. Using 4-(2-pyridylazo) resorcinol (PAR) as the chromogenic agent, a spectrophotometric method for determining 0 to 10 μg Nb in the presence of 0.5g Na and up to 1 mg Ti has demonstrated a 2 σ uncertainty of ±0.65 μg.

Several series of up to seven calibration sets were prepared, varying the quantities of potential interfering species. Each set was analyzed statistically, then the 94 data points were pooled. No attempt was made to exclude data

points which appeared to be discrepant. Thus some unfavorable statistical weighing may have occurred. Of the seven calibration sets analyzed, only one failed to be enclosed by the 2 σ envelope. The data from this set were not excluded from the pooled data, however, and the statistical values given above are for all 94 data points.

In summary, the method involves treating the dissolved sample with tartaric acid, then adjusting to pH 6.0 with NH_4OH/HAc. EDTA is added to complex any foreign ions and boric acid is added to complex fluorides. After readjusting to pH 6.0, PAR and an NH_4Ac/HAc buffer are added and, after 1-hr, diluted to volume with water. Color is allowed to develop overnight and the solutions are read at 550 nm in 5-cm cells.

2. Spark Source Mass Spectrometer (SSMS)

A "standard sample" of sodium has been prepared having 20 to 25 ppm of six known metal impurities. Weighed amounts of each of the relatively soluble metals Ag, Au, Bi, In, Mg and Pb were added to about 370 g of sodium from the Systems Quality Sodium Loop. Three sealed samples for the SSMS were filled with this sodium by ladling from the solution at temperature while stirring.

A slight, but noticeable, deterioration in the focusing ability of the mass spectrometer has been corrected, partly by cleaning of surfaces adjacent to the ion beam path and partly by realignment of the SSMS to move the ion beam further from such surfaces. The phenomenon has been tentatively attributed to the buildup, during the past few months, of a coating of sodium which oxidized when air was let into the whole system, forming an insulating surface. During an analysis, this surface is subject to a charge buildup which can deflect the ion beam. Because the SSMS is seldom vented, this occurrence should not cause a significant operating problem.

A plate-measuring comparator and automatic data digitizing system for the SSMS has been ordered, with delivery scheduled for the end of June 1968. This system will digitize the density of the spectral lines on the mass spectrometer photoplate and will read the data onto a magnetic tape which is directly acceptable to the IBM-360 computer. Work has started on the adaptation and modification of existing data reduction codes. The program will obtain a

photoplate calibration curve, correct each spectral line for area and background, and then correlate the data by the Churchill-celidometer method. This equipment will reduce the time required for an analysis to less than one-fourth that is now needed and will markedly improve the accuracy by utilizing significantly more of the data on the plate than is now possible.

IV. EVALUATION OF EFFORT TO DATE

Progress toward the objectives of this project is satisfactory. The forthcoming re-direction of some of the solubility work to include irradiated solutes, and radiochemical analysis, will slow the rate of data accumulation, but will result in a better understanding of the solubility process for iron and chromium. The work on the carbon-sodium system has been given new impetus by the arrival of a new senior staff member. The foundation for significant work in the area of solute interactions in sodium has been laid by the design of the SCL.

V. NEXT REPORT PERIOD ACTIVITIES

Solubility experiments will continue with irradiated iron and chromium, and with nickel, niobium, and carbon. Especial effort will be given to the carbon-sodium system in an effort to determine whether or not the experiments being carried out are really giving representative results for the solubility of carbon. Fabrication of the SCL will begin. Analytical chemistry activity, particularly that related to the assessment of the SSMS as a tool for sodium analysis, will continue.

THIS PAGE

WAS INTENTIONALLY

LEFT BLANK

Program: HNPF
AEC Task: 13 — HNPF Retirement
Project Manager: J. E. Owens
Reporting Period: January-March, 1968
General Order: 7709 Subaccount: 11400 AEC Category: 46-01-00-00.0

Principal Investigator: B. F. Ureda

I. PROJECT OBJECTIVES

The project objective is the accomplishment of the AEC-designated tasks and the CPPD subcontractual tasks in the retirement of the HNPF. During the past quarter these tasks were as follows: (1) Provide engineering and quality assurance support for the manufacture, delivery, and checkout of two shipping casks for the shipment of irradiated HNPF fuel from the HNPF to the Savannah River fuel reprocessing plant. In addition, the casks are to have future utilization as multipurpose casks for shipment of unspecified radioactive material. (2) By further testing, analysis, and design, support the implementation of the discrete activities comprising the HNPF retirement. (3) Coordinate the disposal of HNPF excess property to other AEC users or to storage in accordance with AEC direction. (4) Prepare the definition of the HNPF building package for use by the AEC in determining the ultimate disposition of these buildings. (5) Assist CPPD in disposal of irradiated fuel. (6) Assist CPPD in writing detailed procedures for the design of a sodium reaction process system. (7) Obtain motion picture record of significant retirement operations. (8) Continue preparation of final report.

II. MAJOR ACCOMPLISHMENTS IN FISCAL YEAR 1968

Accomplishments to date during FY 1968 are: (1) completion of fabrication of the spent fuel shipping casks, (2) obtaining AEC approval of the HNPF Retirement Plan, (3) development of the 12 activity specifications, (4) removal and shipment off-site of excess property, (5) canistering of 72% of the irradiated fuel elements, (6) removal of bulk primary and secondary sodium from site, (7) shipment to Savannah River of 9 cask loads of irradiated fuel.

III. PROGRESS DURING REPORT PERIOD

A. SPENT FUEL SHIPPING CASK ENGINEERING FOLLOW ON AND QUALITY ASSURANCE

Fabrication of the two spent fuel shipping casks was completed on January 24, 1968, at which date they were shipped to the HNPF. After checkout of the casks with a dummy loaded basket, and after a few minor adjustments and corrections, an irradiated fuel basket was loaded into the cask and the initial shipment left the HNPF on February 1, 1968.

At the Savannah River Plant, an adjustment to the fit of the cask in the spreader base was necessary and was accomplished after a few hours delay.

The operations at HNPF and at SRP were witnessed by the Atomics International cask design engineer. As a result of these observations, cask handling procedure improvements were recommended and were implemented by CPPD as deemed practicable.

B. ACTIVITY SPECIFICATION DEVELOPMENT

Ten of the twelve Activity Specifications have been approved by the AEC. Activity Specification No. 7, "Disposition of Contaminated and Irradiated Materials," has been reviewed by the CPPD Safety Review Committee but requires further explanations of the hazards aspects of the long-time containment. The explanation by Atomics International has been submitted to CPPD. The CPPD Safety Review Committee is currently reviewing the explanation.

Activity Specification No. 10, "Securing of Isolation Structure," has also been submitted, but the question of final disposition of the buildings has not been answered; consequently, this specification will not be acted upon until the remaining interface between CPPD structures and the HNPF is defined and accepted by all interested parties. Atomics International has prepared a definition of this interface and of the remaining building contents. This definition may be modified by the AEC and CPPD to obtain mutual agreement. The final definition will provide the basis for requesting bids from demolition contractors. At that time, Activity Specification No. 10 should be approved by CPPD and submitted to the AEC for approval.

C. EXCESS PROPERTY DISPOSAL

Removal and shipment of excess property continues. In the past three months 169,200 lb of property were shipped off site. The steam generator components which were sent to Idaho Nuclear for storage constituted the bulk of the shipments.

Special permits for shipping components containing radioactive or non-radioactive sodium were requested and obtained from D. O. T. These requests of D. O. T. entailed detailed design of the containment and packaging.

A survey and inventory of AEC excess property at the HNPF was made. This list of items that are not designated for delivery, storage, or other AEC contractors has been included in the HNPF buildings definition package. This package will be distributed by the AEC to contractors interested in demolition of the buildings.

Dissemination of technical and costs information, requested by recipients of excess property, is a continuing activity at the site.

D. CPPD

The writing of detailed procedures which delineate the work outlined in the activity specifications is continuing. The main effort is in preparing the procedures for the residual sodium reaction process. Procedures for steaming the residual sodium in the reactor are completed and are being reviewed by the AEC. Procedures for steaming the coolant loops are being reviewed by CPPD.

Design of the sodium reaction process system is completed and assembled. The first use of this process system will be for steaming the reactor. The process system is connected to the reactor and final instrumentation, adjustment, and checkout is now in progress. Detailed drawings of the connection of this process system to the coolant loops have not been released by Atomics International. The drawings are 90% completed. The six intermediate heat exchangers (IHX) units have been isolated from the system and are ready for shipment to storage.

Special tools for handling problem fuel elements were designed and procured. A procedure for encapsulating fuel element MF-117 was prepared and submitted to the AEC for approval.

Canistering of the 100th element was completed. Shipment of 9 baskets of fuel was completed. The canistering operation is dependent upon the shipment. When a basket is returned with the cask, this basket is then refilled. If more storage space for loaded baskets were available, the canistering of fuel would be completed in a few weeks.

A motion picture record of significant steps in the retirement program has been made. Of particular significance were the motion pictures of the cask checkout and loading operations. The final report, which will summarize the important aspects of the entire program, is being compiled.

IV. EVALUATION OF EFFORT TO DATE

Fuel disposal and residual sodium are the two remaining critical operations in the HNPF Retirement Program. The fuel disposal, now that the casks are available, is progressing at a faster rate than first anticipated. Shipments are averaging about one per week, whereas it was earlier estimated that the rate would be one per one and one-half weeks.

Disposal of the residual sodium became a more complicated operation than expected. As all interested parties reviewed the design, each suggested improvements which increased the complexity of the system. The fabrication of this system is perhaps more permanent than need be, but the justification of less permanency on an activity oriented primarily by safety considerations would be difficult.

Progress on resolution of the HNPF buildings disposition problem is slow. Besides the economic considerations, CPPD requirements must be factored into the final solution.

The performance of the retirement activities is lagging, in some areas, from the plan as scheduled by CPPD on January 23, 1968, and is ahead in others. The fuel disposal is no longer the critical path in the scheduled sequence of events. Currently the reactor and loop steaming operations are on the critical path.

V. NEXT REPORT PERIOD ACTIVITIES

Approval of the remaining activity specifications will be obtained in the next report period.

The residual sodium reaction process system will be operated to react the sodium in the reactor and the coolant loops. After operation, the system will be dismantled and scrapped.

Fuel canistering will be completed and fuel shipment to SRP will be over 80% completed.

Excess property will be shipped off site as it is removed. Building demolition contractors will be contacted and selected by the AEC.

Motion picture records and final report completion will continue.

THIS PAGE

WAS INTENTIONALLY

LEFT BLANK

Program: Advanced Development Program
AEC Task: 15 — High Temperature Chemistry
Project Manager: S. J. Yosim
Reporting Period: January-March 1968
General Order: 7711 Subaccount: 53020 AEC Category: 05-05-01-00.0

Responsible Engineer: S. J. Yosim

I. PROJECT OBJECTIVES

The project is divided into two general areas: the study of fused salts and the study of metal-metal salt solutions. The objective of the study of fused salts is to achieve an understanding of ionic melts (halides, oxides, oxy-salts and glass systems) by (1) establishing the nature of the species existing in ionic melts, (2) determining the physico-chemical interactions between species, and (3) formulating systematic relationships between the physico-chemical properties of fused salt systems and the molecular parameters of the species.

The objectives of the metal-metal salt study are to determine phase diagrams for — and the nature of interactions between — metals and their salts at high temperatures, to determine the species in these solutions and, finally, to predict the solubilities in metal salt systems.

II. MAJOR ACCOMPLISHMENTS IN FISCAL YEAR

A. PUBLICATIONS

The following papers were published:

1) "Thermoelectric Properties of the Molten Bismuth-Bismuth Halide Oxidation-Reduction Thermocells," by J. D. Kellner, J. Phys. Chem., 71, 2434 (1967)

2) "Viscosity of Molten Bismuth-Bismuth Triiodide Solutions," by J. D. Kellner, J. Phys. Chem., 71, 3254 (1967)

3) "Electrical Conductivity of Liquid and Saturated Vapor of $BiCl_3$ and $HgCl_2$ to Their Critical Temperatures," by L. F. Grantham and S. J. Yosim, J. Phys. Chem., 72, 762 (1968)

The following papers are in press:

1) "Cell Assembly to Measure the Electrical Conductivities of Molten Salts to Their Critical Temperatures," by L. F. Grantham, E. B. Harrelson, P. H. Shaw, and C. M. Larsen, Rev. Sci. Instr.

2) "Phase Diagrams of the Bismuth Trihalides at High Pressure," by A. J. Darnell and W. A. McCollum, J. Phys. Chem.

3) "Fused Salts," by S. J. Yosim and H. Reiss, Ann. Rev. Phys. Chem.

4) "Viscosity of Molten Bi-Bi Halide Solutions," by Jordan D. Kellner, J. Phys. Chem.

The following paper was submitted for publication:

"Interatomic Distance and Polymorphism in the Alkali Halides," by A. J. Darnell and W. A. McCollum

B. TALKS

The following papers were presented:

1) An invited paper, "Electrical Conductivities of Supercritical $BiCl_3$ and $HgCl_2$," was presented at the Fused Salt Gordon Conference, August 1967, by L. F. Grantham

2) "Phase Diagrams of the Bismuth Halides at High Pressure," at the 154th National Meeting of the American Chemical Society, Chicago, Ill., September 1967

3) "Thermoelectric Properties of Metal-Metal Salt Thermocells," by J. D. Kellner at the 155th National Meeting of the American Chemical Society, San Francisco, April 1968

4) S. J. Yosim was Chairman of the Transport Session at the Fused Salt Gordon Conference.

C. TECHNICAL ACCOMPLISHMENTS

1) A study of the effect of pressure on the electrical conductivities of bismuth halides was completed. Pressure increased the conductivities.

2) A review, "Fused Salts," was completed for the Annual Review of Physical Chemistry.

3) The Soret measurements on metal-metal salt solutions has been completed.

4) A new rule which relates the transition pressure and transition volume to the interatomic distance has been discovered for the alkali halides.

III. PROGRESS DURING REPORT PERIOD

A. ELECTRICAL CONDUCTIVITY OF $CuCl$-$CuCl_2$ SOLUTIONS

The electrical conductivities of pure $CuCl_2$ and $CuCl$ solutions containing 5, 20, 30, 40, 50, and 60 mole % $CuCl_2$ have been measured from the liquidus temperature to above 700°C. Conductivity vs composition plots showed maxima at all temperatures. Both the magnitude of conduction and the "activation energy" for conduction are much larger in the intermediate concentration range than for either pure salt. This suggests that semiconduction is occurring at intermediate concentrations. As expected, the system is different from the Bi-BiX_3 in that the conductivity of the pure subhalide ($CuCl$) is much less than the conductivity of molten mixtures of the subhalide and pure salt. This is probably due to stability of the Cu_2Cl_2 dimer.

B. PHASE DIAGRAMS OF ALKALI HALIDES-ALUMINUM HALIDES

The consolute temperature was measured for 8 mole % $NaBr$-$AlBr_3$. Normal consolute behavior was observed in this system, in contrast with the previously measured KCl-$AlCl_3$ and $CsCl$-$AlCl_3$, systems where no consolute temperature was observed. A consolute temperature of 255 ± 2°C was observed as compared with a literature value of 232°C.

C. ELECTRICAL CONDUCTIVITIES OF PURE $AlCl_3$

The specific conductance of pure $AlCl_3$ was remeasured using the parallel-plate-electrode cell and the impedance bridge. The conductance was somewhat lower than that previously measured with the standard tungsten-wire-electrode cell. A maximum in the specific conductance vs temperature curve was again

observed near 300°C. The measurements were much less sensitive to frequency, perhaps due to the platinized electrodes.

D. ELECTRICAL CONDUCTIVITIES OF ALUMINUM HALIDE-ALKALI HALIDE MIXTURES

A study of the electrical conductivities of the $AlCl_3$-KCl system has been initiated. Solutions of KCl containing 15, 25, 33, 40, 50, 67, and 80 mole % $AlCl_3$ were examined. A maximum in the conductivity vs temperature curve was observed for 50 miles % $AlCl_3$-KCl near 1000°C. The conductivities exhibit negative deviation from additivity when plotted against composition. A well-defined minimum on the conductivity vs composition curve was found at a mole ratio of K:Al = 2. This may be due to a stable chloroaluminate anion with aluminum, having a coordination number greater than four.

E. COMPRESSIBILITIES AND VOLUMES OF FUSION OF MOLTEN $BiCl_3$ AND $AlCl_3$ AT ELEVATED PRESSURES

Measurements of the compressibilities of selected fused salts are being carried out to obtain P-V-T data so that electrical conductivity studies can be made on liquids maintained at constant volume. Preliminary compression measurements have been made on molten $BiCl_3$ and $AlCl_3$ up to 1500 bars. As might be expected from the difference in bonding in the liquid state of these two compounds, the initial compressibility of $AlCl_3$ is three to four times higher than that of $BiCl_3$. Preliminary volumes of fusion of these salts were also obtained as a function of pressure. The fractional volume of fusion ($\Delta V_{fusion}/V_{solid}$) decreased from 0.8 at 1 atm to 0.6 at 1,000 bars in the case of $AlCl_3$, whereas it changed only slightly in the case of $BiCl_3$. The relatively high change of the volume of fusion and compressibility, in the case of $AlCl_3$, may be due to an increase in salt-like behavior of $AlCl_3$ at high pressures.

F. POLYMORPHIC TRANSITIONS IN THE ALKALI HALIDES

The experimental work carried out last year on the polymorphic phase changes in the alkali halides has been analyzed. As a result of this work, an empirical rule was developed which relates the transition pressure and the transition volume to the first power of the interatomic distance in the group of alkali halides which have common anions. A paper describing these results has been submitted for publication.

G. THERMOELECTRIC PROPERTIES OF METAL-METAL SALT SYSTEMS

Earlier it was reported that the Soret effects (a partial demixing when a mixture is placed in a thermal gradient) were extremely large in bismuth-bismuth halide solutions. For example a solution of $BiBr_3$ containing 3 mole % Bi exhibited a steady state thermoelectric potential of about 16,000 μv/deg at 500°C. However, we have since found in a different program that these high potentials were not due to the Soret effect. The cells were therefore redesigned and the true Soret potentials of the Bi-$BiBr_3$ system were redetermined. The potentials were between -50 and +50 μv/deg. This completes the study of the Soret effect in metal-metal salt solutions. A paper describing the above results will be prepared.

IV. EVALUATION OF EFFORT TO DATE

The emphasis in the experimental approach continues on high-pressure transport experiments. Results of the high-pressure transport measurements indicate that these experiments will be very important in shedding light on fused salt theory. The same applies to the supercritical salt studies. The statistical mechanical approach for developing liquid theory so that the physico-chemical properties of pure liquids and solutions can be calculated from equations with no adjustable parameters has been very fruitful and will be resumed.

V. NEXT REPORT PERIOD

The CuCl-$CuCl_2$ conductivity measurements will be completed. The study of the compressibilities of $BiCl_3$ and $AlCl_3$ to 1.5 kbar will also be completed. The study of the effect of pressure on the electrical conductivity of $AlCl_3$ will be resumed. Conductivity measurements on KCl-$AlCl_3$ as a function of composition and temperature will be completed. Conductivity measurements will be initiated on the KBr-$AlBr_3$ system. The scaled particle theory will be extended to $BiCl_3$ solutions near the critical temperature, assuming that this salt is molecular, as reported by Cubicciotti.

THIS PAGE

WAS INTENTIONALLY

LEFT BLANK

Program: Advanced Development
AEC Task: 16, Radiation Chemistry
Project Manager: R. A. Holroyd
Reporting Period: January-March, 1968
General Order: 7712 Subaccount: 53050 AEC Category: 05-05-02-00.0

I. PROJECT OBJECTIVES

The objectives of this project are to delineate the fundamental physical-chemical processes occurring in the radiolysis of organic systems and to study these processes in separate experiments designed to increase our understanding of their nature and their role in radiolysis.

II. MAJOR ACCOMPLISHMENTS IN FISCAL YEAR 1968

A. THE FOLLOWING PAPERS HAVE BEEN PUBLISHED.

1. R. A. Holroyd, J. Y. Yang and F. M. Servedio, "Vacuum Ultraviolet Photolysis of Liquid Organic Mixtures - Energy Transfer from Neutral Excited Cyclohexane," J. Chem. Phys. 46, 4540 (1967)
2. G. T. Tiedeman and R. B. Ingalls, "An ESR Investigation of the Reactions of Hydrogen and Deuterium Atoms with Alkylstyrene Polymers," J. Phys. Chem. 71, 3092 (1967)
3. R. A. Holroyd, "The Reaction of Nitrous Oxide with Excited Molecules in the Radiolysis and Photolysis of Liquid Alkanes," J. Phys. Chem. 72, 759 (1968)
4. J. Y. Yang, F. M. Servedio and R. A. Holroyd, "Photolysis of Liquid Cyclohexane and Cyclohexane Solutions in the Vacuum Ultraviolet," J. Chem. Phys. (in press)

B. THE FOLLOWING PAPERS HAVE BEEN ACCEPTED FOR PUBLICATION

1. R. A. Holroyd, "Radical Yields in the Radiolysis of Hydrocarbons," a review to be published in Aspects of Hydrocarbon Radiolysis by Academic Press

2. R. A. Holroyd, "Radiolysis of Organic Liquids," a review to be published in Fundamental Processes in Radiation Chemistry by Wiley

3. R. A. Holroyd, "The Reaction of Nitrous Oxide with Excited Molecules in the Radiolysis and Photolysis of Liquid Alkanes," to be published in the Advances in Chemistry Series

C. THE FOLLOWING PAPER WAS PRESENTED

1. R. A. Holroyd, "The Reaction of Nitrous Oxide with Excited Molecules in the Radiolysis and Photolysis of Liquid Alkanes," Am. Chem. Soc. April, 1968

III. PROGRESS DURING REPORT PERIOD

A. PULSE RADIOLYSIS OF MOLTEN AROMATICS

The experimental phase of the Pulse radiolysis of liquid naphthalene, biphenyl, and benzophenone is underway. Intermediates are to be detected in these liquids on the nanosecond time scale. Aromatic ions as well as both singlet and triplet excited molecules will be detected. It is hoped that this study will establish the relative importance of intersystem crossing and ion recombination in the formation of triplet states.

B. REACTION OF HYDROGEN ATOMS WITH ORGANIC ACIDS

A study of the reactions of hydrogen atoms with amino acids and other organic acids has been initiated. Electron spin resonance is used to identify the radicals formed. The relative rates of reaction at various sites will be determined. The results show that hydrogen atoms abstract tertiary and secondary hydrogen atoms from the side chains in leucine, isoleucine, valine, arginnine, and lysine; and add to benzene rings in phenylalanine and tyrosine. The alpha hydrogen position in amino acids is unreactive; specifically, the rate constant for abstraction $< 6 \times 10^6\ M^{-1}\ sec^{-1}$.

An unusual result was obtained with leucine sample. This was shown to be a crystal structure effect. It was found that leucine exists in two crystalline

modifications and although the same radical is formed in both by H-atoms, the ESR spectra are different because of different molecular orientations in the two crystals.

C. RADIOLYSIS AND PHOTOLYSIS OF TETRAHYDROFURAN

The radiolysis of substituted tetrahydrofuran compounds is of biochemical interest since the backbone of DNA consists of alternating tetrahydrofuran rings and phosphate groups.

It has been shown that radiation ruptures the tetrahydrofuran ring and smaller molecules are formed; $G(C_3H_6) = 1.0$ and $G(C_2H_4) = 0.5$. The role of excited molecules in this radiolysis is being evaluated by studying the 1470 Å photolysis of the liquid. The following primary processes have been identified:

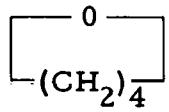

$$+ h\nu \rightarrow C_3H_6 + CH_2O \qquad \phi = 0.2$$

$$\rightarrow C_2H_4 + CH_3CHO \qquad \phi = 0.1$$

the same ring cleavage reactions occur in the photolysis and the ratio $(C_3H_6)/(C_2H_4)$ is 2 in both cases. Thus ring cleavage in radiolysis can be attributed to excitation.

IV. EVALUATION OF EFFORT TO DATE

The ESR studies have demonstrated the specificity of thermal hydrogen atom reactions and provided relative rate constant data. It has been shown that ring cleavage which is a major process in the radiolysis of tetrahydrofuran can be attributed to excitation processes. The high yield of this process is significant since it may contribute to backbone scission in DNA molecules.

V. NEXT REPORT PERIOD ACTIVITIES

Intermediates and products of the radiolysis of substituted tetrahydrofuran compounds will be determined. The reactions of thermal hydrogen atoms with various organic compounds will be investigated as a function of temperature. The pulse radiolysis of molten naphthalene, biphenyl, and benzophenone will be investigated.

Program: Physical Research Program
AEC Task: 17 — Electronic Structure of Metals and Alloys
Project Manager: R. G. Breckenridge
Reporting Period: January-March 1968
General Order: 7713 Subaccount: 54010 AEC Category: 05-06-02-00.0

Principal Scientists: R. G. Breckenridge, L. J. Barnes, H. J. Fink and W. J. Tomasch

I. PROJECT OBJECTIVES

The objective of this project is the acquisition of knowledge regarding the electronic structure of metals and alloys (configuration of electronic energy states in momentum space) and the role of this structure in determining electrical, thermal, magnetic, vibrational, and alloying characteristics. Detailed information on the shape of the Fermi surface is provided by de Haas-van Alphen studies in magnetic fields up to 200 kilogauss, and the density of electronic states at the Fermi level is deduced from low-temperature specific heat measurements. The latter also yield information on lattice vibrational modes and on the interactions involved in superconductivity and magnet ordering. Further characterization of magnetic interactions is accomplished by means of conventional magnetic susceptibility techniques. Considerable effort is devoted to the exploration of high-field superconductivity, with emphasis on thermodynamic and transport characteristics, and of the electron energy spectrum as deduced from thin-film electron-tunneling measurements. The results of these experimental investigations are correlated with current theory, and attempts are made to quantitatively characterize the relationship between superconductivity and the normal-state electronic structure.

II. MAJOR ACCOMPLISHMENTS IN FISCAL YEAR 1968

Publications were as follows:

1. W. J. Tomasch, "Geometrical Resonances in the Tunneling Characteristics of Thick Superconducting Films," Proceedings of the Advanced Study Institute on Tunneling Phenomena in Solids (Riso, Denmark, 1967).

2. W. J. Tomasch, "Calculation of Conductance Structure for Tunneling Between Superconductors," Bull. Am. Phys. Soc., 13, 475 (1968).

3. W. J. Tomasch, "Tunneling from In Films with Superconductive and Ferromagnetic Overlays," Phys. Letters, 1968.

III. PROGRESS DURING REPORT PERIOD

A. ELECTRONIC TUNNELING FROM SUPERCONDUCTORS - W. J. TOMASCH

A second computer program has been compiled for the purpose of synthesizing diode characteristics corresponding to tunneling between two superconductors, one of which has had a model perturbation added to the BCS density of states function. As indicated earlier, calculations with the first program were quite valuable in that they demonstrated the existence of an amplitude magnification effect and further suggested that the degree of magnification decreases significantly as thermal smearing is introduced, i.e., as the temperature is raised. Owing to the misbehavior of certain convolution integrals at several of the limits of integration, the simple approach of this program was not adequate to the task of more detailed computations. Furthermore, it tended to be relatively inefficient, increasing execution times and costs. For these reasons, a second program was compiled on the basis of a mathematically transformed representation of the original problem.

Subsequent experience has demonstrated that the new program is free from the aforementioned shortcomings. To begin with, computations with the new program reproduced the earlier results with regard to the magnification effect. In addition, two other general conclusions have emerged. First, the energy dependence governing the decay of the resonances in the density of states is faithfully mimicked by the voltage damping of the corresponding conductance structure, provided the structure is not too near the edge of the energy gap. Secondly, it would appear that a direct inversion of the detailed conductance data, to obtain corresponding detailed density of states information, is generally required for structure near the gap edge or when additional fine structure is present. These results, together with the general downward revision of the density of states amplitudes, constitute the major accomplishments of the machine calculations to date.

In a related program (T. Wolfram, NARC, Science Center) considerable headway has been made on the theory of quasiparticle interference in thick super conducting films.* Successful investigation has been made of the mechanisms which give rise to the oscillatory structure in the quasiparticle density of states of superconducting films with spatially varying electron-electron interaction. It has been shown that observed effects result from processes in which a quasiparticle is condensed into the sea of Cooper pairs, leaving behind a different (but energetically degenerate) quasiparticle. The tunneling density of states has been obtained for a composite, two-region superconductor. The nature of the density of states structure depends strongly upon the ratio of the energy gaps of the two regions. In the low-energy range, bound eigenstates characterized by the quantization of the difference of the momenta of the degenerate quasiparticles have been developed for the case of infinite mean free path. Beyond this, explicit results have been presented for the composite film systems (thick film plus thin overlayer film) In-Al and In-Pb for several values of the electronic mean free path.

Due to the mathematical complexity of Wolfram's analytical results, it is not fruitful to pursue the analytical decompositions required to employ the second program (in its present form) in order to examine the agreement between experiment and theory. A scheme has been devised whereby the existing program can be modified (generalized) to the extent that it can accept a relatively arbitrary density of states presented in tabular numerical form. Although such a modification is not a trivial task, the resultant updating of the second program would allow the desired comparison between experiment and Wolfram's theory.

Subassembly, development and construction activities have continued on the He-3 refrigerator. Final drawings are nearing completion, and will be followed by final systems assembly.

*T. Wolfram, "Tomasch Oscillations in the Density of States of Superconducting Films," to appear in the Phys. Rev. 1968.

B. FLUCTUATIONS IN SUPERCONDUCTORS - H. J. FINK

Attempts were made to theoretically correlate the observed depression of the transition temperature by Parks et al and Webb et al to a theory other than that of Langer and Ambegokar.

We assume that current fluctuations are responsible for this depression. In narrow channels the kinetic energy per unit volume is $\frac{1}{2}|\Psi|^2 \frac{p_x^2}{m}$. We believe that there is a restriction due to the boundary conditions on the momentum p_x, namely

$$p_x = p_o \pm \sum_n \frac{2\pi n}{L} \hbar \quad .$$

If the kinetic energy due to the fluctuation in the current is equated to the thermal energy (equipartition principle) the following relationship is obtained:

$$\frac{1}{2} kT_c = \frac{|\Psi|^2}{2m} (\Delta p)^2 \, V \quad .$$

This leads to:

$$\Delta T_c = \frac{1}{f^2} \left(\frac{1}{2\pi}\right)^2 \frac{1}{\sum_i n_i^2} \tau$$

where

$$\tau = \frac{\pi}{2} \frac{k T_c^2 L}{a^2 \sigma H_c^2(o) \xi^2(o)} \quad .$$

τ is the result which was originally obtained by Parks et al which, however, is one order of magnitude larger than the experimental results. When n is cut-off at 1/2, ΔT_c is approximately that observed experimentally. At this time it is

still uncertain where the cut-off of n should be, but it is certain that there should be a cut-off.

C. THE STABILITY LIMIT OF THE SUPERHEATED MEISSNER STATE – H. J. FINK

We have previously calculated the maximum critical field when the Meissner state is superheated magnetically. In these calculations the critical fluctuations, which always occur in nature, were disregarded. They, however, should give rise to a lowering of the superheating field, since the latter is strongly dependent on the material parameter . Theoretical investigations have been made of two-dimensional fluctuations in the order parameter and the vector potential, but machine calculations of these important critical field value have not been completed.

D. SUPERCONDUCTING POINT CONTACTS – L. J. BARNES

In continuing the study of superconducting point contacts, increasing attention is being given to the pure superconducting tunneling aspects that can be obtained with point contacts. The dc behavior of the point contacts is, in general, very complicated. In particular we have observed that, as the pressure on the contacts is increased, the behavior becomes increasingly more complicated. At the lightest contact pressures we often observe pure superconducting tunneling behavior. This situation is understood on the basis of present theory and can be used as a convenient starting point for study of the more complicated behavior attendant with more strongly coupled contacts.

The observation of superconducting tunneling behavior in point contacts is interesting from another viewpoint. In principle, measurement can be made of the energy gaps of any materials that can be fabricated into point contact junctions. Many of the alloy superconductors cannot be fabricated successfully into thin film superconducting tunnel diodes and in these cases the point contact will prove to be the best method of measuring the gaps. In the process of developing experimental techniques the energy gaps of Nb, Nb + 50% Ta, Ta, Nb + 5% Ti, Pb, and Pb-Tl alloys have been measured. The values are in good agreement where they can be compared with thin film data.

Within the last reporting period instrumentation for measurements of the dynamic (ac) resistance of our contacts was completed, considerably improved the sensitivity of the measurements. Also, considerable effort has been expended in discovering good anodizing techniques for transition metals and their alloys. This effort, which is necessary to obtain good tunneling behavior in the point contacts, has been reasonably successful.

IV. EVALUATION OF EFFORT TO DATE

This program has maintained a very active pace during the report period. The recent emphasis in the tunneling studies has been on an analysis of the experimental results obtained thus far. This work has been quite successful, and a much improved understanding of the resonance effects is being developed. The theoretical work continues to elucidate a number of problems in superconductivity. The work on superconducting point contacts is proving to be highly productive. The experimental problems are being solved and useful information is now being obtained. It is already apparent that this information will be a very valuable tool for superconductor studies.

V. NEXT REPORT PERIOD ACTIVITIES

The work on the present tasks will be continued with no important changes in emphasis. The assembly of the He^3 refrigerator will begin.

Program: Physical Research Program
AEC Task: 18 – Radiation Damage in Crystalline Solids
Project Manager: R. G. Breckenridge
Reporting Period: January-March 1968
General Order: 7714 Subaccount: 54040 AEC Category: 05-06-02-03.0

Principal Scientists: W. Bauer, D. W. Keefer, H. H. Neely, A. Sosin, K. H. Thommen and D. Vawter

I. PROJECT OBJECTIVES

The materials requirements of modern technology demand an increased understanding of the effects of lattice defects on the physical properties of crystalline solids and of their behavior when subjected to various kinds of radiation. Studies of radiation damage in solids not only directly yield information on the effects of radiation, but also provide a means of investigating defects in solids. It is the objective of this project to study the production of defects in crystalline solids by radiation; to attain an understanding of their structure, their interactions with each other and with impurities and dislocations; their effect on the physical properties of solids; and their recovery kinetics. Comprehension of these points should assist in the understanding of lattice defects produced in solids by other means, and help make possible the development of materials of superior properties as the ability to better control defect structure is developed. The materials chosen for study are metals, metal alloys, and semiconductors.

II. MAJOR ACCOMPLISHMENTS IN FISCAL YEAR 1968

Publications were as follows:

1. A. Sosin and W. Bauer, "Defect Production in Metals by Irradiation at Low Temperatures," Proceedings of the International Conference on Solid State Physics Research with Accelerators, Brookhaven National Laboratory Report BNL 50083, p. 204 (1968).

2. Walter Bauer, "Damage Rate Measurements in Platinum and Other Metals by Electron Irration," in Lattice Defects and Their Interactions, edited by R. R. Hasiguti, (Gordon Breach New York), p. 567 (1967).

3. A Sosin and W. Bauer, "Atomic Displacement Mechanisms in Metals and Semiconductors," to be published in "Studies in Radiation Effects in Solids," Vol. III, edited by G. J. Dienes (Gordon Breach, New York), manuscript approved by editor.

4. W. Bauer, A. Sosin and K. R. Garr, "Stage III Recovery of Electron Irradiated Aluminum," Bull Am. Phys. Soc., 13, 381 (1968).

5. H. H. Neely and D. W. Keefer, "Resistivity Studies of Electron Irradiated Iron," Phys. Stat. Sol. 24, 217 (1967).

6. H. H. Neely, "Recovery of Electron Irradiated Zirconium at Low Temperature," accepted for publication in Can J. Phys.

7. H. H. Neely, D. W. Keefer and A. Sosin, "Electron Irradiation and Recovery of Tungsten," submitted to Phys. Stat. Sol.

8. O. Buck, D. Keefer, J. Robinson, A. Sosin and H. Wiedersich, "Low Temperature Deformation of Electron Irradiated Aluminum," Acta Met. 16, 195 (1968).

9. K. Thommen, "Effects of Low Temperature Electron Irradiation on the Electrical Properties of Undoped GaSb," IEEE Transactions on Nuclear Science NS14, 40 (1967).

10. K. Thommen, "Energy and Orientation Dependence of Electron Irradiation Induced Damage in Undoped GaSb," Bull. Am. Phys. Soc. 13, 380, (1968).

III. PROGRESS DURING REPORT PERIOD

A. CONTINUOUS ANNEALING IN STAGE I – W. BAUER, H. H. NEELY AND A. SOSIN

The process of assembling equipment for a novel approach to continuous annealing is now essentially completed. This approach involves reading the difference in resistance, ΔV, between an irradiated specimen and a dummy specimen as a function of annealing temperature. If the specimen resistances have been suitably matched prior to the irradiation readings of ΔV represent essentially the radiation damage recovery and deviations from Mathiessen's Rule. The deviation from Mathiessen's Rule is a slowly varying function of

temperature in comparison to the recovery substages in Stage I. Therefore, the number and relative height of the substages can be identified, although the absolute neight and, therefore absolute amount of recovery, cannot. The number of recovery substages in Stage I recovery, especially of copper, is of immediate interest, due to the bearing on the recovery models.

The experimental approach to the measurement of ΔV as a function of time (temperature at constant heat-up rate) involves an entirely electronic display-digital voltmeter coupled to a punched tape. The system, which is now assembled allows several readings per second. This speed, in combination with an optimized heat-up rate, results in a resistance reading every 0.05°K temperature annealing interval. This is approximately five times better than can be achieved by conventional isochronal methods.

The cryostat to be used for the continuous annealing experiments is the same one currently used for the aluminum experiments. The latter experiments should be completed within a few months, allowing starting the continuous annealing experiments.

B. RESISTIVITY RECOVERY IN ALUMINUM NEAR ROOM TEMPERATURE (STAGE III - IV) — W. BAUER, A. SOSIN AND K. GARR

As has been reported in the last quarterly report, experiments are being conducted to resolve the difference in interpretation in the Stage III region in aluminum. Some of the results of these experiments were reported at the Berkeley meeting of the APS. The abstract is included here:

"We measured the resistivity recovery of a pair of 99.9999% pure ($\rho_o \sim 4 \times 10^{-9}$ Ω-cm) aluminum foils (~0.001 in. thick). One specimen was prequenched; both were irradiated near 10°K and annealed simultaneously. The resistivity increments due to prequenching and irradiation were matched in the Stage III region ($\Delta\rho \sim 5 \times 10^{-10}$ Ω-cm). The unquenched specimen exhibited one recovery peak centered at 255°K (Stage III) and the prequenched specimen exhibited two peaks; at 255°K and 320°K (Stage IV). These results are in good agreement with work by Budin and Lucasson. The data can best be explained by primarily random migration of interstitials in Stage III and vacancy migration in Stage IV. Calculations indicate that the Stage IV recovery can be accounted for by vacancy

diffusion to dislocations ($\sim 10^7$ - 10^8 lines/cm^2), whereas to attribute the Stage III recovery, as well, to vacancy migration requires unreasonably high vacancy concentrations or sink concentrations."

During the last few months we have analyzed the data in considerably more detail:

1) The activation energy, E, of the 255°K peak by the Meechan-Brinkman method is 0.60 ± 0.10 ev. This is in good agreement with the results of Koehler and Lucasson et al. Using only the isochronal data and second order kinetics a value of E = 0.45 ev was deduced, in good agreement with previous work of Sosin. This value of E is considered low, primarily as a result of the inappropriateness of the assumptions in the second order analysis. For example it is assumed that the same defect (interstitial) migrates up to temperatures where the isochronal recovery reaches its asymptotic value. The recent data is in contradiction to this assumption. Moving the asymptote to lower temperature results in a higher value of the activation energy.

Although there now seems to be general agreement in the activation energy area, the central problem still remains of why there are two peaks with nearly equal activation energies but separated by 70°K. Data is being analyzed in detail for kinetics, and further experiments are being conducted.

C. DISPLACEMENT PROCESSES IN IRON WHISKERS — W. BAUER AND W. F. GOEPPINGER

Damage rate measurements as a function of energy and orientation are continuing. For several reasons; this work has been more time consuming than originally anticipated: (1) The irradiation times are very long due to the requirement of a scattering foil in the electron beam. (2) Background magnetoresistance effects necessitated novel measuring procedures heretofore not required. Measurements obtained up to the present point toward no gross anisotropy in the threshold energy surface of iron. However, considerable experimental work remains to be done before detailed conclusions can be made.

D. MODULUS CHANGES AT LOW TEMPERATURES – D. W. KEEFER AND J. C. ROBINSON

1. Dislocation Pinning in Copper

A detailed examination of the effect of temperature on dislocation pinning in copper during irradiation is continuing. A previous report described how irradiation at temperatures between about 100 and 150°K leads to a significantly enhanced pinning rate during a subsequent irradiation at 77°K. In each case, measurement of the pinning rate was made at 77°K. We have recently found that this effect is intimately related to the exhibition of an 80°K Bordoni internal friction peak by the sample. A well-annealed sample having a greatly reduced Bordoni peak shows no enhancement of the pinning rate at any point in the irradiation and annealing procedure. If the sample is then cold-worked at room temperature, so that a relatively large Bordoni peak is present at 80°K, irradiation at, say, 150°K enhances the pinning rate observed during the next 77°K irradiation. Further, at-temperature measurements show that this pinning rate enhancement is observable at measuring temperatures between about 40 and 150°K. No enhancement is ever observed for measuring temperatures below 40°K. The temperature range between 40 and 150°K is precisely that over which the observed Bordoni peak extends. Analysis of these most unusual results in terms of the point defects (interstitials) involved and the dislocation relaxation mechanism for the Bordoni peak is presently underway.

2. Dislocation Pinning in Silver

A study has recently been initiated of dislocation pinning in electron irradiated silver. A sample has been irradiated at 4.2°K with 1.5 Mev electrons to a dose of 1.125×10^{16} e/cm^2. A detailed isochronal annealing study between 4.2 and 680°K has revealed the presence of several pinning stages. The first of these begins at 30°K and is complete by 50°K. This is followed by a temperature interval of some 150°K over which three contiguous stages occur. Between 200 and 340°K, a slight amount of unpinning occurs. This is followed by the final pinning stage between 340 and 410°K. The wide temperature interval between this stage and its predecessors is an unusual result and will allow study of the stage in some detail. The final release of pinning points from dislocations occurs between 420 and 680°K. These preliminary results are most encouraging, and a thorough study is anticipated.

E. RECOVERY OF ELECTRON IRRADIATED ZIRCONIUM – H. H. NEELY

The preliminary study of electron irradiated zirconium is completed and the manuscript is written. The manuscript has been accepted for publication in the Canadian Journal of Physics, following is the abstract.

"The low-temperature recovery of the electrical resistivity of polycrystalline zirconium was measured after electron irradiation below 8°K. The material used in this irradiation was the same low oxygen material (0.015 at. %) used by Swanson to study recovery after deformation at 4.2°K. Substage I_B was found to be only of the order of 4% of the irradiation-induced resistivity change, compared to ~6% observed by Swanson after deformation. Stage I (4.2 to 160°K) in Zr contains six substages while Stage II (160 to 310°K) contains only one substage after electron irradiation. While no study of kinetics was made, it seems likely that close pair annihilation processes are responsible for the recovery spectrum below 118°K and that longer range defect migration occurs in the neighborhood of 140°K.

F. RECOVERY OF IRRADIATED TUNGSTEN – H. H. NEELY, D. W. KEEFER AND A. SOSIN

The preliminary investigation of electron-irradiated tungsten is completed and the manuscript has been written. The manuscript has been submitted to Physica Status Solidi for publication, following is the abstract:

"Electron Irradiation and Recovery of Tungsten - Damage rates and recovery of 99.99% pure tungsten have been investigated after electron irradiation near 4°K by means of electrical resistivity. The damage rate data though not corrected tend to a value of T_o = 38 to 42 ev. The recovery of the residual electrical resistivity shows three major stages; Stage I from 4.2 to 100°K; Stage II from 100 to 500°K, Stage III from 500 to 1000°K. Stage I is dominated by only one major peak at 70°K; this peak was analyzed assuming first and second order kinetics. The first order process did not fit a straight line in the activation energy analysis. The second order plot fit a straight for over two decades of data, yielding an energy of 0.17 ev. This data is convincing evidence that the 70° peak is due to a process in which considerable interstitial migration is involved. Since only ~26% recovery is seen in Stage I we propose

that the suppression is due to interstitial trapping with impurities. Other models were investigated. Stage II seems to be due to release from impurity traps as seen in other materials. Stage III accounts for about 40% of the induced resistivity recovery and has a center temperature of 760°K. The stage was analyzed assuming second order kinetics, this analysis gave an energy of 1.1 ev."

G. SEMICONDUCTOR IRRADIATIONS: GaSb – K. H. THOMMEN AND D. VAWTER

Measurement of the energy and orientation dependence of the defect production by electron irradiation of undoped GaSb have been completed. Study of the dependence of the production rates of the defects associated with the four major annealing stages on the energy of the bombarding electrons yielded the following threshold electron energies: Stage I: 0.34 Mev, Stage II: 0.17 Mev; Stage III: 0.33 Mev, Stage IV: 0.34 Mev. When a monocrystalline sample is irradiated with a collimated electron beam, Stage I defect production is higher when the electron beam is aligned with the [111] direction than when it is aligned with the [$\bar{1}\bar{1}\bar{1}$] direction. The opposite is the case for Stage II, III and IV defects. The observed anisotropies of the defect production rates are very small and are clearly outside the experimental error only for irradiation energies near the threshold energies. The results of the orientation dependence measurements lead to the conclusion that Stage I defects are related to the displacement of Sb atoms, whereas Stage II, III and IV involve displacement of Ga atoms. From the threshold energies of the Stage I and Stage II defects, the displacement energies of Sb and Ga atoms can be evaluated as 8.0 and 6.2 ev, respectively. It is very likely that the Stage I and Stage II defects are close-pair Sb-Frenkel defects and close-pair Ga-Frenkel defects, respectively. The configurations of the Stage III and IV defects are not quite as clear. Comparison of the energy dependence of the Stage III and IV defect production rates with the Stage II defect production rate suggests that each of the Stage III and IV defects involves the displacement of atoms (most probably two) in a so-called "multiple displacement process" in which the primary knock-on atom has sufficient energy to displace another lattice atom.

On the basis of a Kinchin-Pease type model, calculations were made of the ratio of the production rate for defects created by multiple displacements to the production rate for isolated Ga-Frenkel defects for irradiation energies between 0.4 and 1.0 Mev. The results of this calculation were compared with the experimental values for $(\eta_3 + \eta_4)/\eta_2$, where η_1 is the production rate for stage I defects. Calculated and experimental values were in excellent agreement with respect to both their absolute magnitude and their energy dependence.

A paper on this work is being prepared.

H. SEMICONDUCTOR IRRADIATIONS: GaAs – K. THOMMEN AND D. VAWTER

Annealing experiments after irradiation at 4.2°K were performed with "pure" n-type GaAs (room temperature mobility $\approx$6000 cm^2 $volt\text{-}sec^{-1}$). Since previous measurements with less pure material had indicated that, in the temperature range 4 to 60°K, thermally activated emptying of traps occurred, the cryostat was modified so that it became possible to shine light on the sample during the annealing studies. Illumination with white light creates electrons and holes and therefore provides a convenient way to refill thermally emptied traps. Most of the light is absorbed in a region near the exposed surface and only a small fraction with wavelengths near the band edge penetrates into the bulk of the sample. Despite this, the experimental observations indicated that most, if not all, of the emptied traps can be refilled by white light illumination.

It was found that even the unirradiated sample contained traps which could be emptied by annealing the sample at temperatures near 30°K and refilled by white light illumination at 4°K. Annealing studies of a 1 Mev electron irradiated sample included isochronal pulse annealing in the range 4 to 75°K with the sample either in the dark or illuminated with white light during the temperature pulses. In neither case was there recovery observed, which would indicate reorientation or annihilation of radiation-produced atomic defects in this temperature range. There was, however, a very small gradual change of the resistivity, measured at 4.2°K, which is most probably the result of some electronic redistribution process, but the details are not understood at the present time. Investigation of the recovery at temperatures above 77°K with and without simultaneous illumination are in progress.

IV. EVALUATION OF EFFORT TO DATE

This program has made progress in several aspects of radiation effects in solids. The apparatus for the continuous annealing is now being tested and will shortly be in operation. There is every indication that the new equipment will be most productive. The continuing work on resistivity recovery in aluminum is gradually clarifying the nature of the Stage III and IV processes, and it is anticipated that a reasonably complete picture of the recovery processes will soon be available. The extension of this type of measurements to the more complicated case of bcc metals, namely Fe and W, is now under way and some studies have been made of zirconium, whose structure is hcp. The work in GaSb is making excellent progress and a number of details of the defect production are now being revealed. It has been possible to clearly establish the directional dependence of the defect production and to measure the threshold displacement energy for Ga and Sb. Similar work has been initiated on GaAs. The intercomparisons possible in the III-V compounds should aid in interpreting many details of the observations.

V. NEXT REPORT PERIOD ACTIVITIES

The continuous annealing apparatus will be applied to a restudy of copper, the classic case, and should elucidate the fine structure in Stage I recovery. Resistivity studies will continue on the Fe, W and Zr. Mechanical effect studies will continue on Ag. The semiconductor studies will continue on GaAs, and some measurements will be made on doped GaSb.

THIS PAGE

WAS INTENTIONALLY

LEFT BLANK

Program: Advanced Development
AEC Task: 22, Radiation Chemistry of Chromosomes
Project Manager: R. A. Holroyd
Reporting Period: January-March 1968
General Order: 7724 Subaccount: 17001 AEC Category: 06-04-00-00.0

Principal Scientist: R. A. Holroyd

I. PROJECT OBJECTIVES

The long range objective of this study is to obtain information which will correlate molecular alterations with biological damage. The immediate objective is a better understanding of the radiation chemistry of chromosomes and their main constituents: DNA and proteins.

II. MAJOR ACCOMPLISHMENTS IN FISCAL YEAR 1968

A. The following paper has been published.

1. D. E. Holmes, R. B. Ingalls, and L. S. Myers, Jr., "An ESR Study of Free Radicals Formed by Reaction of Nucleotides and Their Constituents with Hydrogen Atoms," International J. Rad. Biol. 12, 415 (1967)

B. The following paper has been accepted for publication.

2. D. E. Holmes, R. B. Ingalls, and L. S. Myers, Jr., "ESR Spectra of Free Radicals Induced in Pyrimidines, Purines and Related Analogs by Exposure to Hydrogen Atoms." International J. Rad. Biol. (in press)

C. The following papers are in preparation.

1. R. A. Holroyd and J. W. Glass, "Reaction of Hydrogen Atoms with DNA and Nucleoproteins" (to be presented at the 16th Annual meeting of the Radiation Research Society, Houston, April 1968)

2. R. A. Holroyd and J. W. Glass, "The Reaction of Electrons with Thymine, Thymidine and TMP"

D. The following presentation was made

1. L.S. Myers, Jr., R.B. Ingalls, et al., "Effects of Gamma Rays, H-Atoms, and OH Free Radicals on Nucleic Acids and their Constituents," at the 155th meeting of the American Chemical Society, April, 1968

III. PROGRESS DURING REPORT PERIOD

A. REACTIONS OF DNA WITH HYDROGEN ATOMS

During this quarter, the radicals formed by reaction of hydrogen atoms with DNA were identified by comparing the ESR spectrum obtained with DNA to that obtained by reacting hydrogen atoms with each of the four nucleotides in DNA (see Section III-C). The ESR spectrum of radicals induced by H-atoms in DNA at 25°C was shown to be almost identical to the spectrum obtained with thymidine-5'-phosphate (TMP); thus, most of the reaction occurs with this nucleotide. The reaction was shown to be predominately addition by reacting D-atoms with DNA. The resulting ESR spectrum was narrower demonstrating that hydrogen atoms add to DNA and are adjacent to the free spin on the radical.

More quantitative information was obtained by utilizing an existing computer program to analyze the ESR spectra. In the case of the reaction of hydrogen atoms with TMP, it was found that 60% of the radicals result from H-atom addition to thymine and 40% from abstraction from the deoxyribose. This result was surprising since thymine is more reactive than deoxyribose and in a one-to-one mixture of these, only thymyl radicals are formed. The reactivity of the sugar is enhanced in the nucleotide and in DNA.

This study also showed that at -90°C hydrogen atoms react mainly with deoxycytidine-5'-phosphate in DNA.

B. REACTION OF HYDROGEN ATOMS WITH PROTEINS

It was suggested earlier (last quarterly) that the presence of histones in DNA samples can prevent reaction with the DNA; therefore, analyses of the DNA samples for protein content were made. The sample of DNA which gave the most highly resolved ESR spectrum and in which reaction with the DNA

bases was shown to occur, contained less than 0.5% protein. The calf-thymus sample which gave less well resolved spectra but some indication of base attack contained 2% protein. A nucleohistone sample which contained 59% protein showed attack of hydrogen atoms only on the histone. Samples of DNA containing intermediate amounts of histone will be investigated to elucidate this effect.

C. REACTION OF ELECTRONS

Earlier work had indicated that electrons attach to thymine and thymidine and that proton transfer to the anion formed occurs readily, Reaction 1

$$T^- + H_2O \rightarrow TH\cdot + OH^- \qquad \ldots (1)$$

As a test of this mechanism, the reaction was studied in a D_2O-NaOH matrix. In this case, the radical formed would be TD· and its ESR spectrum would be predictably different from TH·. When electrons were reacted with thymidine in this matrix at -90°C, both TH· and TD· were formed. At higher temperatures where the radicals are decaying, the signal of the TH· radical disappeared, leaving that of TD·. This allowed a pure spectrum of the TD· radical to be recorded. It consists of 18 lines spread over 111 gauss.

These results demonstrate that the TH· radical which is observed in the radiolysis of thymine as well as in DNA could be formed as a result of electron attachment followed by proton transfer to the anion in aqueous media. Since electrons are known intermediates in the radiolysis of organic systems, this mechanism of radiation damage in DNA is quite reasonable; however, radicals have not as yet been observed to be formed on reaction of photolytically produced electrons with samples of DNA and meta-phase chromosomes in this study.

D. REACTION OF HYDROGEN ATOMS WITH CONSTITUENTS OF DNA

The reaction of hydrogen atoms with deoxyribose, nucleosides, and nucleotides has been restudied, since recent results disagreed with those of Holmes et al., (1967). The samples for this study are in the form of a porous powder rather than a fluff, and the reaction is being studied as a function of temperature.

Deoxyribose gives a spectrum containing five resolved hyperfine lines spread over 42 gauss (contrary to earlier findings by Holmes et al). This spectrum is very characteristic; and, thus attack on deoxyribose is evident if it occurs in mixtures of deoxyribose with DNA bases or in nucleotides. For example, in a 10:1 mixture of sugar and thymine, ~50% of the radicals are on the pentose.

The computer program GLAD was used to synthesize the ESR spectra of the radicals formed by H-atom attack on deoxyribose and on each base of DNA. The percentage of base and sugar radicals induced by H-atom attack on the nucleotides could then be determined. In the case of H-atom attack on TMP, it was found that 60% of the radicals are on thymine and 40% on the sugar. In the case of dGMP, even more sugar attack occurred and only 40% of the radicals formed are on guanine.

IV. EVALUATION OF EFFORT TO DATE

The reactions of hydrogen atoms with DNA, metaphase chromosomes, histones, and the components of DNA have been investigated. At low temperatures, hydrogen atoms react with metaphase chromosomes and the radical formed is not on DNA but very likely on a phenyl group in the protein component. At 25°C, hydrogen atoms react selectively with DNA by addition to thymine base groups and by abstraction from deoxyribose. At -90°C, hydrogen atoms add mainly to cytosine base groups in DNA. A variation in reactivity of DNA has been observed and attributed to the amount of histone present. The reaction of electrons with pyrimidine bases have been investigated. Electron attachment to thymine is followed very rapidly by proton transfer from surrounding water molecules. The radical thus formed is identical to that observed in the radiolysis of DNA and other thymine containing compounds; thus, a mechanism of radical formation which could occur in DNA and chromosomes has been identified.

V. NEXT REPORT PERIOD ACTIVITIES

Samples of chromosomes will be reacted with hydrogen atoms at 25°C for comparison to the low temperature results. The ESR spectrum obtained at low temperatures indicated hydrogen atoms add to phynyl groups in the histone. The computer program will be utilized to analyze this spectrum and verify this assignment. Studies of electron reactions will continue. Mixtures of purine and pyrimidine nucleotides will be investigated to determine their relative reactivities.

THIS PAGE

WAS INTENTIONALLY

LEFT BLANK

Program:	LMFBR Analysis Implementation
AEC Task:	25 — Noise Analysis Instrumentation
Project Manager:	C. W. Wheelock
Reporting Period:	January-March 1968
General Order: 7757	Subaccount: 53100 AEC Category: 04-01-61-03.4

Principal Investigator: R. L. Randall

I. PROGRAM OBJECTIVES

The overall objective of the Noise Analysis Instrumentation program is the application of basic noise analysis techniques to the measurement of liquid metal flow rate and other operating parameters. This type of measurement is necessary and desirable in the operation of liquid metal facilities and fast reactors.

The immediate phase of this program is oriented toward the development of an out-of-core flow calibration instrument that can be used in the Sodium Pump Test Facility (SPTF), the Fast Flux Test Facility (FFTF), and future Liquid Metal Fast Breeder Reactors (LMFBR's).

The first phase of the development program will be the experimental demonstration of the conductivity cell cross-correlation method in a 50 gpm water loop. The objective of this phase is to establish the accuracy of the method in cylindrical flow sections and to determine variations of uncertainty with flow rate, fluid density, viscosity and channel size.

The second phase of the program will be the extension of the knowledge gained in the first phase to the measurement of waterflow rates in cylindrical sections, using thermocouples. The objective of this phase is to provide the knowledge required to extend the technique to use in liquid metal.

The third and fourth phases, which are extensions of Phases 1 and 2, are concerned with the application of the techniques developed in Phase 1 and 2 to a liquid metal system.

II. MAJOR ACCOMPLISHMENTS IN FISCAL YEAR 1968

The authorization to initiate work on this project was received in January 1968. Initial studies and test planning were started immediately, and work has been progressing towards initial loop testing. All study efforts and loop fabrication activities required to accomplish Phase 1 and 2 objects are well underway.

III. PROGRESS DURING REPORT PERIOD

Techniques for measuring and comparing thermocouple time responses were investigated. An apparatus for measuring and comparing thermocouple time responses was assembled and checked out. Preliminary testing indicated the system was capable of resolving thermocouple time response differences of about 1-msec. The system was successfully used in attempts to match the time response of two 20-mil sheathed thermocouples. The matching technique involved: measuring the relative response time of two TC's; filing a few mils of sheath material from the junction end of the slower TC, and repeating the response comparison. The second filing attempt brought the response difference to less than 1-msec. This test verified the feasibility of production-line matching of TC time response. The apparatus was returned to the data reduction lab for modifications designed to simplify operation and improve measurement stability. A lamp and solar cell were added to provide a standard reference signal for checking operation of the apparatus, a suitable signal for the tachometer, and a phase reference signal with negligible delay (response time the order of 10 microseconds) for comparison with thermocouple signals.

The apparatus for measuring and comparing thermocouple time response was returned and set up in the thermocouple laboratory. In the first phase of testing, the phase response of each of the forty 20-mil grounded junction, sheathed chromel alumel thermocouples will be compared against the light source and a solar cell. Phase comparison will be made at 10 and 20 cps. The TC that has the fastest response will then be used as the reference TC, and attempts will be made to reduce the response time of all the other TC's by a filing procedure.

Work began on the conceptual design of thermocouple mounting fins for use in the test sections, in water and liquid metal. Dummy fins using wire to simulate TC's are being constructed to develop assembly techniques. Present plans call for test sections to be designed in three basic sizes, each with multiple experiments. Test sections built with TC's will be designed for later use in sodium or NaK. Major design effort will be directed to development of in-stream mounting structure or fins for supporting TC's, to permit measurement of velocity profiles and assure high position and spacing accuracy and stability with minimum flow perturbation, and ease of installation. The first dummy fin structure was machined from a strip 2-1/2 inches by 1/2 inch by 60 mils. The side was hollowed out and 13 holes were drilled in the leading edge for the protruding 20 mil TC's. Wires will be inserted to simulate TC's and the side of the fin will be filled using a furnace brazing technique.

The size, material, insulation and electrode configuration to be used in the conductivity sensor test sections were studied. The sensitivity, reaching distance, and field linearity of various electrode configurations were compared using Teledeltos paper. Results indicated that flush-mounted wall electrodes, while suitable for very small channels, are not suitable for large channels unless the ratio of electrode diameter, insulator diameter, and channel diameter remains constant. To achieve a moderately linear field gradient with wall electrodes in a 3-in. diameter pipe would require electrode diameters in excess of 1-in. and insulator diameters in excess of 2-in. Comparison of various in-stream electrode configurations led to selection of two basic types for use in the first test section. The first electrode is simply a thin metal rod extending across the pipe diameter. It will be installed using glass seal headers for insulators. This type of electrode has excellent field linearity and is applicable to essentially any pipe size. The second electrode design uses two rods, one directly behind the other. The latter configuration has a shorter feeling distance and should have a sharper response to passing eddies. Glass seal headers suitable for use as electrode insulators have been obtained. These headers will be used to support 40-mil electrodes. The electrodes are to be made from 40-mil stainless steel welding rods.

Work began on preparation of the water loop for the test program. Various conceptual designs of a water dump system for accurate flow measurement were

studied. Designs for modifications to the water loop were completed. Lists were prepared of specific parts, fittings, tanks, and pipe to be ordered. Steel drums to be used as storage and dump tanks were ordered, along with fast-action solenoid valves to transfer flow from the storage tanks to the dump tanks for accurate volumetric flow determination. Except for the storage tank heaters, all components to be used for the preparations and modification of the water loop have been obtained or ordered. At the present time, external, clamp-on, heaters are under consideration.

IV. EVALUATION OF EFFORT TO DATE

The planning, sensor studies, and loop fabrication work initiated since the authorization to begin work have progressed well. The initial studies performed with thermocouples have shown that the required time response matching can be readily achieved. Conductivity cell studies have resulted in several possible designs for use in large pipes.

V. NEXT REPORT PERIOD ACTIVITIES

During the fourth quarter of GFY 1968, a test plan for water loop operation will be completed. Modifications to the water loop will be finished, and flowrate measurements using conductivity cells will be initiated. Also, thermocouple parameter studies will be completed and flow measurements will be initiated using thermocouples in water.